Whole Transcriptomic profile of canine oral melanoma and its human analogy

The United Graduate School of Veterinary Science

YAMAGUCHI UNIVERSITY

Md Mahfuzur Rahman

March 2020

Whole Transcriptomic profile of canine oral melanoma and its human analogy

Academic Dissertation

Submitted to

The United Graduate School of Veterinary Science

Yamaguchi University, Japan

By

Md Mahfuzur Rahman

Department of Veterinary Medicine

Joint Faculty of Veterinary medicine

Kagoshima University, Japan

In partial fulfillment of requirements of the degree of

Doctor of Philosophy

In

Veterinary Medicine

March, 2020

Major Supervisor

Professor Dr. Naoki Miura

Department of Veterinary Medicine

Joint Faculty of Veterinary medicine

Kagoshima University, Japan

Co-Supervisors

Professor Dr. Fujiki Makoto

Department of Veterinary Medicine

Joint Faculty of Veterinary medicine

Kagoshima University

Professor Dr. Okamoto Yoshiharu

Department of Veterinary Medicine

Joint Faculty of Veterinary medicine

Tottori University

Professor Dr. Osamu Yamato

Department of Veterinary Medicine

Joint Faculty of Veterinary medicine

Kagoshima University

Associate Professor Dr. Takahashi Masashi

Department of Veterinary Medicine

Joint Faculty of Veterinary medicine

Kagoshima University

DEDICATION

The thesis is dedicated to my beloved father and mother who are the pioneer of my life and to my little daughter Mehroosa Muntaha and my spouse Al Asmaul Husna who are the inspiration of my study.

Table of Contents

List of Tables

List of Figures

Overview

Genomic instability is a hallmark of cancer. Cancer does/results due to numerous genetic events. A few are drivers, but others accumulate as passive progression. Critical identification of specific cancer causative drivers should be more useful for the development of therapeutic strategies. A study with the model organism facilitates better understanding of the drivers. The term “spontaneous cancer model” revealed to be a better identifying and understanding the drivers. Dog’s oral melanoma considered as a spontaneous cancer model for human melanoma. However, melanoma transcriptome and its analogy between the two species has been entirely undetermined yet. Moreover, to be a useful therapeutic preclinical model knowing the melanoma transcriptome between humans and dogs is important. Gene expression monitoring by analyzing the transcriptome helps in investigation of the cancer drivers. Moreover, in human 80% of the genome is biologically active however, proteins translated from coding RNA occupy less than 2% of the genomic information. It reveals that a considerable portion of the DNA is transcribed into non-coding RNA (ncRNA) including functional RNA molecules. Studies have been shown that ncRNAs are not a junk transcriptional sequences, but active, functional regulatory

molecules. So, cancer transciptomic study I include both coding and non-coding RNA analysis.

In this study I represent the systematic analysis of the whole canine oral melanoma (COM) transcriptome including the non-coding and coding RNAs by next generation sequencing. I present my transcriptome study in three parts based on the RNA species. First microRNA (miRNA/miR)-a well studied non-coding RNA, second other non-coding RNAs (snoRNA, snRNAs, and tRNA fragments, and also the piRNAs) and finally the mRNA profile in COM. In each section I also compare their analogy with human melanoma. In the miRNA section along with tumor suppressor, I report several oncogenic miRNAs in COM without previous implication. Gene regulatory function of oncogenic miRNAs was also investigated in reference to human study. Thus I established a comprehensive miRNA study profile. In the other non-coding RNAs section I find several non-coding RNAs like snoRNA, snRNAs, tRNA derived fragments and also piRNAs are aberrantly expressed in our next generation sequencing analysis. I confirmed their expression in the tissue, cell line and plasma by qPCR. I also found that snRNA and snoRNA have similar expression pattern in human melanoma cell line. In my final mRNA transcriptome analysis several differentially expressed annotated and novel genes are identified. Known and novel transcription factors

binding site for the up-regulated genes are reported. Finally, driver signature genes for melanoma are listed by the cross species analysis.

General Introduction

Dogs are, no doubt, man's best friend. There is an old joke that, after a while human begins look like their pets. But unfortunately, the similarities also extend to cancer. Dogs develop many of the same types of cancer as humans, such as brain, lung, bone and skin cancer like melanoma. For dog, to be a useful therapeutic preclinical model, knowing the cancer transcriptome and its analogy with human is important. Canine oral melanoma (COM) considered a natural spontaneous model for human melanoma. However, until now the transcriptome alterations of COM and its analogy with human melanoma still unrevealed. So, the objectives of this thesis are to comprehensive study of COM transcriptome by high-throughput sequencing technology and find out its analogy with human melanoma.

Initially, I will introduce the aspects and backgrounds about the history of studying dog for the benefit of human diseases, the term "comparative oncology" canine model of human cancer, and significance of transcriptome analysis of a model organism. Later, I will introduce my study in detail. I present the transcriptome analysis broadly into two parts; non-coding RNA and mRNA. In the first part of non-coding RNA transcriptome analysis, I will introduce the microRNA (miRNA) transcriptome profile in COM in the first chapter

and the profile of small RNA other than miRNA (snoRNA, snRNA, tRNA fragments and piRNA) will be presented in the second chapter. Later, I will introduce the mRNA profile of COM and its human analogy in the third chapter.

G.1 Animal model for human study

Animals were used to study human physiology and anatomy in the second century AD as documented by a Greek physician and philosopher, Galen (1). However, in 2011 medical journal "Animal testing and medicine" author Rachel Hajar examines the earliest known use of animals dates back during great Greek philosophers, Aristotle, (384 – 322 BC) and Erasistratus, (304 – 258 BC) (2). From then till now, the trending for the use of animal as diseases model varies from non-human primates to rodents. Until now many lives changing breakthroughs were achieved through the animal model study. Research on cow helped to develop world's first vaccine which ends smallpox (Figure G.1). Monkeys, dogs, and mice led to opining the polio vaccine.

a

b

Figure G.1 Development of the smallpox vaccine. (a). This file comes from welcome images, a website operated by welcome trust, a global charitable foundation based in the united kingdom. (b)The vial is containing the 1902 smallpox vaccine sample.

Also, animal models require for any drug development. In 1937, an American pharmaceutical company created sulfanilamide preparation without animal testing. The preparation led to causing death for more than hundred people. In 1938 the several similar disasters led to pass the Federal Food, Drug, and Cosmetic Act requiring safety testing of drugs on animals before human medication (2). As a result drugs used to combat cancer, HIV/AIDS, malaria, hepatitis, Alzheimer's would not be developed without animal experiments. More interestingly, from 1901 two-third of the most prestigious award "Nobel prizes" in medicine was awarded to the researcher for their achievement on the animal model. More recently, from 2003-2015 seven out of ten and even the most recent Nobel prize of 2018 in medicine were animal based breakthroughs (1). So, the use of animals as a

study model for human diseases is recognized as an imperative understanding of the causes, biology, and prevention of diseases. Now a day's researchers study animal models almost any diseases like eye diseases, diabetes, cardiovascular, obesity, metabolic, kidney, liver, hereditary disorder and most promisingly in cancer (3). Previously, larger animals like chimpanzees were used as experimental models because they seem to be closer to humans. However, large animals have increasingly difficult to handle and maintain; besides they are costly in nature. The other disturbing fact is most human diseases could not be induced or replicated to them. As a result, scientists started to develop simpler and effective (humanized) model especially transgenic mice (4). Therefore, during the selection or development of an induced animal model researchers adopt different criteria like homology, analogy, and fidelity of the model animal with humans (5). In this case homology refers to the genetic similarity; analogy is the quality of resemblance or similarity in function or appearance, but not of origin or development and fidelity refers to resemblance of model with the human for the condition being investigated. Human diseases are typically artificially induced in animals. These enormous efforts of reproducing complex human diseases in animals limit their usefulness(6). However, discordance exists in the translation of induced model's experimental outcome to human clinical trial even if the design and conduct of animal experiment are sound and standardized (6–9). For

example, in cancer less than 8% successful translation from animal experiments is being considered for human clinical trials (7). So a considerable number of experimental animal efforts seem to be useless. Therefore these limitations intend the researcher to look for the more natural model so that the achievements of the animal experiment can be translated to human therapy successfully. Hence the term "spontaneous model" revealed (5,10). Because as the term "spontaneous" implies, this model requires appearing the diseases naturally in the population. Scientist those are interested in the hereditary and cancer, focusing more on the spontaneous natural model. Also, several examples exist in the hereditary, inflammation and cancer (5). For example, NOD strain of mouse exhibits a heritable susceptibility to diabetes comparing to most mice strains. Therefore it has been used as a spontaneous model for type 1 diabetes (11). N-IF mouse is spontaneous model for chronic liver inflammation (12). Dog appears as one of the most common spontaneous models of several human diseases (13,14).

G.2 Dog model for human diseases

The time frame for dog domestication varies from 12,000-40,000 years ago (15–18). Whenever is the time of dog domestication, they are trusted friend of human. Unfortunately their friendship also exists in case of diseases. The domestic dog, *Canis familiaris* bears

over 450 diseases, among them approximately 360 of which are reported analogous to human diseases (19–21). Because of strong anatomical and physiological similarities especially with respect to the cardiovascular, urogenital, nervous and musculoskeletal systems they are in early interest and efforts for the scientist and researcher. Dogs provide an excellent system for the identification and study diseases loci as a spontaneous model for many heritable diseases (19,20,22). A well known disorder is congenital stationary night blindness described in Briards breed. Leber amaurosis in children is the counter-part of this disease in children. On the other hand, Duchenne muscular dystrophy has its canine counter-parts in the Golden retriever, Beagle and German short-haired pointer (23). Alport syndrome (AS) is a form of hereditary nephropathy (HN) in human caused by the defects in the glomerular basement membrane. Spontaneous AS has been identified in several canine families. X-linked HN (XLHN) was identified first in the Samoyed breed which also later found in the mixed-breed family (24). Co-relation was found among the amyloid-β (Aβ) plaque deposition between the dog cognitive dysfunction (CCD) and Alzheimer's disease (AD) in humans. This finding supports the senescent dog with spontaneous CCD is a valuable non-transgenic model for the investigation of the neurodegenerative process associated with the aging and early stage AD (25). Numerous studies also exist which

support the dog as a model for human cancer. In the following section I will gather the studies that reported the dog as a valuable spontaneous model for various human cancers.

G.3 Comparative study of dog and human cancer

The canine model has long been used in cancer drug discovery and development research because of its similarities to human anatomy and physiology (Figure G.2). NIH proposes spontaneous animal tumor registries to study comparative oncology. The high level of veterinary health care, available data and as a most common companion animal species make the dog as one of the suitable spontaneous model candidates for human cancer (26–28).

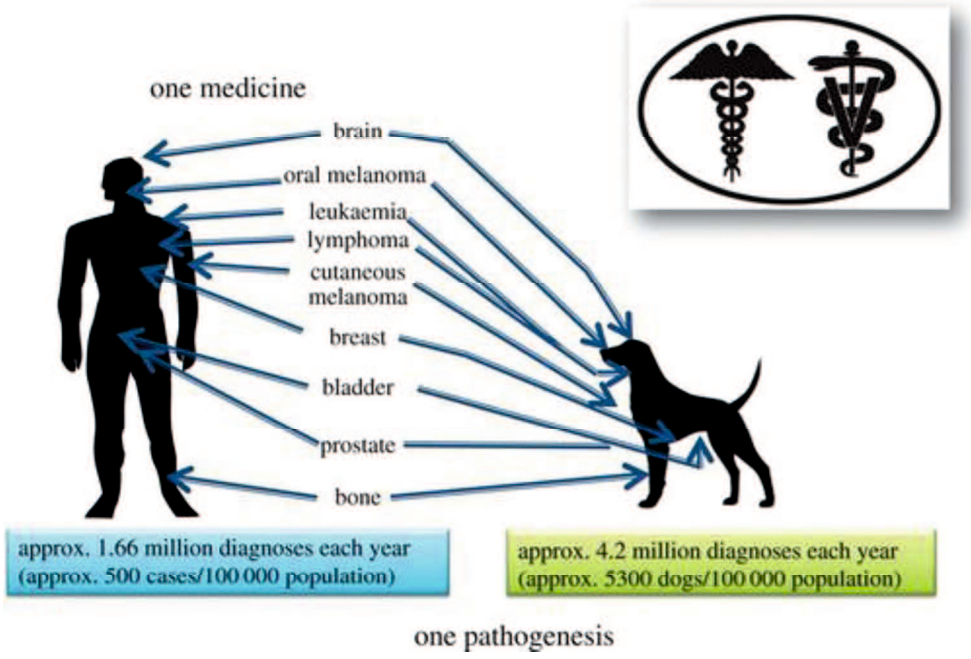

Figure G.2 The remarkable similarity in cancers shared by human and dog. The cancers shown are found in both human and canine populations, and several ongoing studies are highlighting the similarities at the genomic level. The incidence of cancers in both species is shown, highlighting the more than 2.5×number of cancers diagnosed in pet doges each year. Comparative oncology is a growing trans-disciplinary field that harnesses these data, adding evidence to support a shared pathogenesis.(29)

Human and dog share common environmental factors. These give the benefit to study the environmental factors inducing in human cancers. Dog's age length is five to seven times shorter than human and lives till old age. So disease progression is more rapid which permits the assessment of a novel treatment faster (e.g., 1-2 years than 5-10 years) and also promptly. On the other hand, high coverage genome sequencing has shown stronger similarities between the canine and human genomes as compared with mouse genomes

(30). Moreover, canine cancers are described as in the same language as their human counterparts. For example, histological and clinical staging systems used in human cancers classifications (National Cancer Institute Working Formulation, World Health Organization histopathological classification system) (31,32). A Cancer registry is one of the important features of the epidemiological study of comparative oncology. Cancer registry for human has been established in 1940s, while for dog it becomes available from 1960s (33,34). Also cancers in dog face key feature like surgery, chemotherapy and radiation therapy as like to human. For example, CHOP (Cyclophosphamide, Hydroxydaunorubicin, Oncovin, Prednisone) based chemotherapy protocol is the mainstay both for human and dog lymphoma treatment. Additionally, the incidence of certain cancer is higher in dogs than human. For example, less than 1,000 people have osteosarcoma (OSA) in a year, while dog OSA is at least 10 times more prevalent (35). These cancers assist in providing significant larger study population to develop and evaluate new therapeutic strategies for rare and common human cancer. Advancement of the recent comparative studies between the species highlights the future scope to study the human counterpart of the dog cancer more specifically.

G.3.1 Dog mammary gland tumor and human breast cancer

The mammary tumor is the most common neoplasm identified in female dog. About 70% of tumors in dog European cancer registries are mammary gland tumors (36). In human mammary cancer (breast cancer) is also the most common and leading cause of cancer associated death among women in the world. According to the biennial update from American cancer society 2019, more than 4 women will die per hour due to breast cancer in the US. Clinical stage and tumor grade are the two most consistently reported prognostic factors in both dog and human mammary cancer (32,37). Although, other risk factors like breed, age, hormonal exposure, and possibly obesity were also reported for the development of mammary tumor (32). Specific molecular markers not only classified human breast cancer but also lead to successful cancer therapies that improve patient survival. There is estrogen receptor (ER)-positive subtypes; Luminal A and Luminal B. On the other hand ER negative subtypes are HER2 over-expressing, normal breast like and basal-like subtypes that are characterized by the lack of estrogen, progesterone, and HER2 receptor expression(38,39). In dog stromal cell MMP9 and tumor cell Ki-67 expression considered independent molecular markers for canine mammary tumors (40). Breast cancer in human is recently now characterized by the gene expression profiles targeting specific molecular markers (41). The correlation was found among three histological subtypes of

canine MGC (ductal, simple, and complex) and four molecular subtypes of human BC (HER2+, ER+, ER&HER2+, and TNBC) when analyzing the differential expressed genes obtained by the transcriptome analysis. BRCA, a candidate gene for human breast cancer was investigated in the English springer spaniel; a breed frequently develops mammary tumors. The study found germline mutation of BRCA1 and BRCA2 has significant association of mammary cancer in that breed (42). Moreover, comparative pathway expression analysis of orthologous dog/human genes demonstrates that cancer-related pathways were similar in mammary or breast cancer in both species (43). Thus identification of molecular drivers in the pathogenesis of the mammary or breast cancer led to the development successful cancer therapy. For example, HER2 expression is now used as biomarker to identify patients those can be treated with the trastuzumab (Herceptin®), a monoclonal antibody targeting HER2. In canine mammary carcinomas loss of HER2 expression associated with poor prognosis is also reported. 20-29.7% canine malignant tumors over expressed HER2 mirroring the incidence of human breast cancer (44–46).

G.3.2 Soft tissue sarcoma

Soft tissue sarcomas (STS) are heterogeneous groups of mesenchymal tumors clinically present on both human and dog. The annual incidence in dog is 35 per 10,0000

(32), whereas 1% people diagnosed STS among all types of cancer (47). A recurrent chromosomal aberration has been identified both in human and dog (48–50). Loss or chromosomal rearrangements of *CDKN2A/CDKN2B* have been identified both in the human and dog in where human *CDKN2* loss associated with worse prognosis (51,52). Molecular subtypes of gastrointestinal stromal tumors (GIST) have been classified by the KIT mutation in both species (32,53). In human mutation rate is around 80%, whereas in dog it's 35.5% and the location of mutation in both species are in exon 11 (53,54). Local control is a crucial strategy for successful treatment for the both species including surgery with or without radiation therapy (32,55).

G.3.3 Osteosarcoma (OSA)

OSA is significantly prevalent in dog and human with a reported incidence of 13.9 in dog and 1.02 in human per 100,000 individuals (35). The incidence is higher in older dog (median age is 7 years), whereas in human its more common in the adolescence group (10 to 14 years old age group) (35). Fundamental genes and signaling-pathways related to OSA pathogenesis are conserved between human and dog. Similar mutation or alteration of oncogenes implicated in the etiopathogenesis of OSA is also reported between the species. For example, mutations of the tumor suppressor genes like *p53, RB1, PTEN* and alteration

of the *MET* and *MYC* were reported in both species (35). The mutation rate of the *p53* in OSA is near to be similar (23-47% human and 15-30% dogs) between these two species (35,56–61). Dog and human OSA represent 29-61.5% and 30-75% genomic alteration of RB1 respectively (62,63). *IL8* and *SCL1A3* are over-expressed in canine OSA which is also associated with an aggressive clinical course and poor outcome in human OSA (64). Similar to the other tumors constitutive activation of the STAT3 was found in the human and canine OSA and cell lines (65–67). This evidence bring the consideration of canine OSA into comparative cancer and translational cancer research which indicates the potentiality to share and novel therapeutic targets ultimately care the advancements in both species.

G.3.4 Lymphoma

Both human and dog have increased similarities non-Hodgkin lymphoma, one of the most common lymphomas in both species. The incidence is around 15-30 per 100,000 individuals in both species (68,69). B-cell lymphoma is more prevalent than T-cell, and diffuse large B-cell lymphoma (DLBCL) is the most common subtype in both species (68,69). Several shared incidence of molecular signaling and pathologic features are also reported (68). For example, *MYC* associated dysregulation and cytogenic abnormalities are

conserved between human and dog (70,71). Significant overlap exists in case of altered FLT3, NF-κB and B-cell receptor pathway signaling (72–75). Mutation in the immunoglobulin heavy chain in canine DLBCL also co-relates with the human DLBCL (73). TRAF3 inactivating mutation was first identified in canine DLBCL and then in the human (76). These reports provide strong support for the utility of dog as a model for human lymphoma study.

G.3.5 Leukemias

Chronic lymphocytic leukemias represent the most common forms of adult leukemia in people where the incidence is far more common in the dogs (77,78). Conserved genetic alteration of RB1 gene locus exists in both species. A region CFA22 homologous to the human HSA13q4 which is related to the RB1 gene expression was reported to be deleted in both species in leukemias (70). These indicate that the disease may have molecular similarities with respect to RB1 signaling. Chromosomal rearrangement or translocation (Raleigh chromosome in dog equivalent to Philadelphia chromosome in human) was found both in the human and dog in case of chronic myelogenous leukemia (CML) (70,79). In case of acute lymphocytic leukemia (ALL) FTL3 tandem duplication is

also present in human and dog with a variable percentage which supports the notion that the biology of the ALL and FTL3 are conserved between the species (80,81).

G.3.6 Transitional cell carcinoma (TCC)

TCC in the urinary bladder of dogs shares many biological, clinical histological and molecular similarities with high grade invasive TCC in human (82). For example, the COX2 over-expression is reported both human and canine invasive TCC (83,84). More importantly, treatment with COX inhibitor produces similar biologic effects (85). Additionally, telomerase activity and altered expression or activation of several other proteins like survivin, androgen receptor, urine basic fibroblast growth factor is observed (83,84).

G.4 Study of Transcriptome

Most of the previous studies were the single or multiple gene approach to investigate the similarities in the comparative oncology. However, with the advancement of the sequencing technologies it's becoming the far better choice to study the comparative oncology at the whole transcriptomic level. Cancer transcriptome study in veterinary research is scarce. However the trend of transcriptome study is increasing recently. On the other hand, after the first revealing of the partial transcriptome from human brain the

transcriptome study in cancer is increasing year by year. For example, only the breast cancer transcriptome study increases more than 200 times within 2006-2014 (Figure G.3) which shows the necessity to study the canine mammary gland tumor transcriptome in the field of comparative oncology.

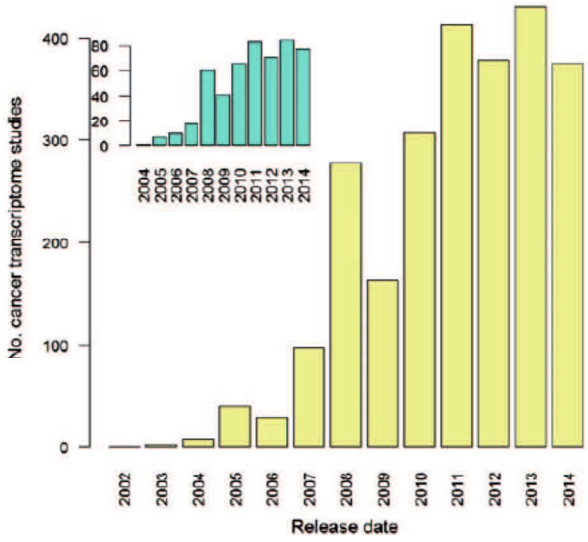

Figure G.3 The increase in the number of cancer transcriptome profiling studies. ArrayExpress was queried for human cancer data sets acquired from at least 30 samples by RNA microarray or sequencing assays. Main bar plot data sets acquired from any cancer type; insert plot: data sets from breast cancer studies only(86).

The transcriptome is the study of all RNA molecules in cell. More specifically, transcriptome study refers to the complete set of mRNA and non-coding RNA transcripts produced by cells from the genome under specific circumstances. The study of the transcriptome of different circumstances allows the identification of genes or transcripts

that are changed (differentially expressed) due to the condition. Some of them are driver, and others are changed due to the secondary effect. So the comparison of the transcriptome in various diseases or experimental conditions reveals the differential as well as the driver genes or transcripts.

G.4.1 Short history of Transcriptome study

Transcriptomics study has been characterized by the advancement of new technologies. The first attempt to report the transcriptome was human brain, which was published in 1991. They reported 609 mRNA sequences from the brain (87). The first cancer portrait of transcriptome was published from human breast cancer in 2000 (39). They identified the variation in messenger RNA levels related to the specific feature of diseases. From 2003, new sequencing technologies; next generation sequencing (NGS) has increased the speed and reduced the cost of sequencing. This technology advanced our understanding of cancer subtypes through several national and international large-scale transcriptome studies. The International network for cancer genome projects was established in 2010. This network deal with the systematic studies of over 25,000 cancer genomes at the genomic, epigenomic, and transcriptomic levels (88). From 2011, clinicians

have begun to translate genome and transcriptomic approaches for patients with cancer in the clinic (89).

G.4.2 Common strategies for transcriptome analysis

The contemporary technique for whole transcriptome analysis is microarrays and RNA-Seq. Microarrays measures a defined set of transcripts via their hybridization to an array. This technology allowed the assay of thousands of transcripts simultaneously at a greatly reduced cost per gene. To perform microarray analysis, RNA molecules are converted to complementary DNA (cDNA), and each sample group is labeled with a fluorescent probe with a specific color. Then the sample group mixed together and allowed to hybridization. Following hybridization the microarray slide is scanned to measure the expression of each gene depending on the fluorescent intensity.

An RNA-seq method totally depends on sequencing technologies. It refers to the sequencing of the transcript cDNAs. Therefore the technique heavily depends on the development of high-throughput sequencing technologies. Massively parallel signature sequencing (MPSS) was an early example of generating 16-20 bp sequences via a series of hybridization (90). Four hundred fifty four technologies are the pioneer as the earliest RNA-seq work, published in 2006 (91). This technology allows 10^5 transcripts sequence.

RNA-seq gains more popularity when new Solexa/Illumina technologies (San Diego, CA) allowed 10^9 transcript sequences to be recorded in 2008 (92–95).

G.4.3 Significance of transcriptome analysis

In multicellular organism, nearly every cell contains the same genome and thus capable of encoding the same genes. However, in every cell all genes are not transcriptionally active. Different cells show different patterns of gene expression. The variations underlie due to the wide range of physiological and pathological conditions under different mechanisms. Thus comparing different types of cell's or tissue's transcriptomes, we can gain deeper access how the transcriptional activity changes reflect or contribute to disease or physiological condition. For example, transcript study of the stem cells reveals their unique property of plasticity or continues growth in the cell culture. Also gene expression associated with cancer progression can be examined. Moreover, proteins are interacting dynamic molecules. The changeability of the proteins makes the proteomic snapshots study difficult. Also there are many technical challenges in characterizing the molecules. One example is a gene can produce variant of mRNA because of alternative splicing, RNA editing, or alternative transcription initiation and termination sites. Moreover, non-coding RNAs like microRNA (miRNA), piRNA, snoRNAs or other

RNAs also contribute to the fine tuning of the proteome. Thus transcriptome study is able to capture a level of complexity which is not visible only with the simple genome or proteome analysis. Therefore measuring the intermediate step of the genes and proteins (transcripts of messenger RNA) researcher able to understand the modification during the transformation process. Also the transcriptome study of different cells and tissues facilitates to develop the complex gene expression databases (96–98). These databases are useful to understand the complex transcripts aberration under different diseases and physiological state. Thus it helps to distinguish "driver" from "passenger" genomic events. Transcriptome study revolutionized our understanding how genomes are expressed in a functional way and the modifications that are taken place during the process of a functional state.

G.4.4 Review of transcriptome study in comparative oncology

Cross species comparison of genomes, transcriptome and gene regulation are the key features for the study of spontaneous cancer in the field of comparative oncology. During the study researcher try to find out the comparative similarities and dissimilarities regarding the diseases between the species. Insights have been gained in case of conservation between human and the other model animals at the level of not only gene expression, but also in the epigenetics and other inter-individual variation. The comparative

transcriptome of the three distant species (human, worm and fly) have been studied to identify conserved biological principles (99). They found co-expression modules shared across animals, many of which are developmental genes. Moreover, non-canonical, non-coding transcription is similar in between the organism. After these early study comparative transcriptomics between human and mouse "a well known cancer model" was reported (100). With the advancement of time comparative study of the cancer transcriptome between human and its spontaneous counterpart are in continuous investigations. Transcriptome study of the Canine Mammary Gland Tumors and its comparison with human breast cancer showed the co-relation between the subtypes (101). Another study showed the conserved stromal reprogramming during mammary carcinoma development (102). Conserved intertumor transcriptional variation was present in tumor sets when osteosarcoma from human, dog, and mice were compared in the transcriptomic level (103). Metastasis associated gene signature was reported in osteosarcoma by the cross species analysis of the genes between the human and dog. Genetic similarities of osteosarcoma also identified between children and dog (61). RNA-seq of the invasive urothelial bladder carcinoma in dog showed similar ERBB2 and TP53 pathway aberration (104,105). Another cross species analysis of the canine and human bladder cancer transcriptome revealed that gene functions are remarkably similar in the functional and pathway levels (106).

G.5 Author's perspective in the experimental topics

Since 2003, The National cancer institute (NCI) has been using the "comparative oncology" terms as a field of studies of canine cancer to help and guide the studies of human cancer and vice versa. Human and pet dogs share similar living spaces, so they are exposed to some of the same environmental factors related to cancer. Moreover, cancers in both species take several years to develop, and in many cases it's often driven by similar genetic mutations. And not only that cancer spread, or metastasizes, from one body part to another usually spreads to the same organs such as the lungs, liver, and brain. Furthermore, the immune system which can help and or prevent cancer growth works a lot like dog's do. No one model can perfect for understanding cancer. However, comparative oncology studies offer a different perspective than studies of artificially created cancers in lab animals such as mice and rats. Because the cancers developed in an immunocompetent animal model. Considering these important similarities, studying pet dogs with naturally occurring cancers provide researchers valuable clues about human cancer therapy.

Since the 1960s, attempts have been conducted and reported to answer the questions about cancer therapy using canine model (107–112). However, at that time we didn't know how many genomic similarities exist between these two species. Thanks to the high-throughput sequencing technology which revealed the mystery of whole genome sequence

both human and dog. Genome sequencing reveals that dogs share much of their ancestral DNA with humans (30). This study encourages us for the comparative transcriptomics study of COM. I characterize the global transcriptome profile, both small and mRNA of COM by using the high-throughput sequencing technology to understand the alteration in the non-coding and coding components and further validation by the quantitative real-time PCR (qPCR). Molecular pathways and common gene signature impacts by the altered transcriptome are investigated. Furthermore, the shared transcriptomic analogy between COM and human melanoma are also reported.

Chapter 1
Micro RNA Transcriptome Profile in Canine Oral melanoma.

(Rahman, M *et al*., 2019 *Int J Mol Sci.* Sep 28;20(19). pii: E4832)

1.1 Abstract

MicroRNAs (miRNAs) dysregulation contribute the cancer pathogenesis. However, the miRNA profile of canine oral melanoma (COM), one of the frequent malignant melanoma in dogs is still unrevealed. This study aims to reveal the miRNA profile in canine oral melanoma. MiRNAs profile of oral tissues from normal healthy dogs and COM patients were compared by next-generation sequencing. Along with tumor suppressor miRNAs, I report 30 oncogenic miRNAs in COM. The expressions of miRNAs were further confirmed by quantitative real-time PCR (qPCR). Pathway analysis showed that deregulated miRNAs impact on cancer and signaling pathways. Three oncogenic miRNAs targets (miR-450b, 301a, and 223) from human study also were down-regulated in COM and had a significant negative correlation with their respective miRNA. Furthermore, I found that miR-450b expression is higher in metastatic cells and regulated *MMP9* expression through a PAX9-BMP4-MMP9 axis. In silico analysis indicated that miR-126, miR-20b, and miR-106a regulated the highest numbers of differentially expressed transcription factors with respect to human melanoma. Chromosomal enrichment analysis revealed the X chromosome was enriched with oncogenic miRNAs. I comprehensively

analyzed the miRNA's profile in COM, which will be a useful resource for developing therapeutic interventions in both species.

1.2 Introduction

The Neoplastic proliferation of melanocytes results the melanoma development. One person dies every hour from melanomas; new melanoma cases have increased by 53% in the US (113), and the WHO reported that 132,000 new melanoma cases are diagnosed every year in the world. These reports clearly confirm the importance of melanoma studies. In human, melanoma arises from cutaneous, uvea of the eye, and within mucous membrane. Molecular studies have enriched the definition of melanoma sub-types (114,115). The continuous investigation makes the scenario more diverse. In human cutaneous melanoma is more common, which characterize by the mutation in BRAF, N/H/K/-RAS, or NFI mutation (116–118). Alongside the triple wild-type (TWT) subtype bears the features that underlie non-cutaneous melanoma, including mucosal melanoma (115,119). Human mucosal melanoma is more aggressive with less favorable prognosis than other subtypes.

Engineered mice and zebrafish models were used in melanoma. In this model system different strategies including BRAFV600E or NRASQ61R/K defined mutation to CDKN2A, or PTEN inactivation were adopted to study the molecular process in cutaneous melanoma (120–122). Previous studies suggested dog melanoma as a natural model for

human melanoma (123,124). Malignant melanoma is frequent in dog, and the majorities are in the oral mucosa. Oral melanoma in dogs is considered a typical model for non-UV or TWT melanoma in human (114,115). Dog melanoma genes have the same mutations or aberrant expression as human melanoma genes, *BRAF*^{V600E}, *NRAS* (Q61) (125), *PTEN* (123), and *KIT* (126). Besides the protein-coding RNAs, non-coding RNAs (ncRNAs) also have important roles in gene regulation. Among them, small non-coding RNAs have widespread regulatory functions in human diseases, and microRNAs (miRNAs) are now in phase I trials to treat human hepatitis, diabetes, lymphoma, scleroderma, and lung cancer (127). Next-generation sequencing (NGS) has been used widely to study miRNA, including their role in human melanoma. For dogs to be a useful therapeutic preclinical model, knowing the miRNA profile in dog melanoma is important. There are few reports of tumor suppressor miRNAs in canine oral melanoma (COM) (128,129), and studies of miRNA profiles of human TWT or mucosal melanoma are scarce. Moreover, the global deregulated miRNAs expression profile of COM is still unrevealed. So I aimed to use next-generation sequencing to study global aberration of miRNAs in COM bearing following three objectives: (1) Comprehensively profile miRNA expression pattern in COM, (2) Validation of findings in the COM tissue samples by using qPCR, and (3) Investigate the gene-regulatory function and molecular pathways of differentially expressed miRNAs. In my

study, I obtained the miRNA profile of eight COM tissue samples by NGS which were further validated by qPCR. I found several miRNAs were differentially expressed. I also explored a new function of miR-450b. The impact of global changes in the miRNA profile was shown by Kyoto Encyclopedia of Genes and Genomes (KEGG) pathway analysis. Finally, a common miRNA and transcription factor (TF) network was constructed and analyzed to find the most important miRNAs for the regulation of TFs expression between dog and human melanoma.

1.3 Result

1.3.1 Small RNA Profile of Canine Oral Melanoma

To investigate the miRNA profile in COM, RNA from three normal oral tissue samples from healthy dogs (hereafter referred to as ‘‘normal’’) and eight samples from dogs with COM was sequenced (Appendix 1-1A). After adapter trimming and quality check, I obtained 51 and 142 million clean reads from normal and melanoma libraries, respectively (Appendix 1-1B). Sequences were submitted to the SRA database (PRJNA516252). Length distribution analysis showed 90% and 82% of clean reads in the normal and melanoma libraries, respectively, were 20–24-nt long, indicating an alteration in the small RNA profile (Appendix 1-2A). I annotated the reads using miRBase or Ensembl dog and human ncRNAs (see methods), witch 92.5% and 84.23% of the reads in normal and melanoma, respectively, were annotated (Appendix 1-2B). Among the annotated reads miRNAs were the most abundant small RNAs. Interestingly, the percentage of other ncRNAs reads (Mt-rRNA, Mt-tRNA, linc-RNA, sno-RNA, snRNA, misc-RNA, rRNA, other miR) was two times more in the melanoma group (Figure 1-4A). SnRNA, snoRNA, and mitochondrial tRNA-derived small RNA fragments were the most

altered between the two groups. As miRNAs were the most abundant I analyzed the miRNAs further.

I found significant differences in the chromosome distribution of the annotated miRNAs mapped reads between the normal and melanoma groups (Figure 1-4B), implying altered global miRNA profiles in the melanoma group. I annotated 542 miRNAs in both groups, among them, 64 miRNAs were differentially expressed (Figure 1-4C). The top 20 highly expressed miRNAs made up >70% of the total reads that were annotated to miRBase (Figure 1-4D). Among them, 12 miRNAs were common between the groups. I selected the rank of the miRNAs on the basis of their expression. The rank orders of miRNA's were different in melanoma than normal (Figure 1-4D). Four of the top 10 highly expressed miRNAs in melanoma were not in the top 10 of the normal group. Importantly, miR-21, which is a well-characterized miRNA oncogene frequently found to be over-expressed in various malignancies, was ranked one in melanoma and 12 in normal. Also, miR-22, miR-148a, and miR-186, all of which have been reported to be oncogenic, but not statistically significant in my study, changed their rank within top 10 in melanoma (130–132). However, the ranks of some known anti-oncogenic miRNAs were much lower in melanoma than in normal. For example, miR-203 and miR-205, which were reported to be anti-oncogenic in melanoma (128) were ranked 6 and 7 in normal, were outside the top 20

in melanoma. So, melanoma reduced expression of anti-oncogenic miRNAs while taking favor of others highly expressed miRNAs by remodeling their expression position according to their target functionality.

1.3.2 Global miRNAs Expression in Canine Oral Melanoma

Unsupervised hierarchical clustering and principal component analysis were performed for all the differentially expressed miRNAs (FC > 1, without considering the FDR and mean read count) to evaluate similarities between the studied samples at the global level (Figure 1-5A, and Appendix 1-2C,D). After applying stringent filtering criteria (Fold change >2, FDR <0.05, and miRNA mean read counts in either normal or melanoma >50), I obtained 30 up- and 34 down-regulated miRNAs (Figure 1-5B, Appendix 1-3). The heatmap and clustering tree revealed a distinct miRNA expression pattern between the groups. The principal component analysis and clustering tree showed that the differentially expressed miRNA was enough to distinguish the two groups, and heatmap showed the miRNA expression patterns were similar within a group. Data showed there were significant changes in the miRNA profile in COM.

1.3.3 Validation of miRNA Expression

I selected 20 differentially expressed miRNAs for validation by qPCR by 12 normal oral and 17 melanoma tissue samples (Figure 1-5C, D, and Appendix 1-4). I selected these 20 miRNAs on the basis of three different criteria: (1) miRNAs those were not reported or validated previously (miR-450b, 301a, 140, 542, 223, 190, 429, 96, 375,183, 200b, 141), (2) miRNAs those were reported or validated previously (miR-21, miR-122, 383 and 143) (133), (3) miRNAs those were beyond (numerically close) to the stringent filtering criteria (miR-122, miR-34a, miR-338, miR-182, and miR-1). Among the up-regulated miRNAs, miR-450b, miR-223, miR-140, miR-542, and miR-383 showed >10-fold change, and miR-301a, miR-21, and miR-190 showed >5 fold-change (Figure 1-5C and Appendix 1-4A–C). Among the down-regulated miRNAs, miR-429, miR-200b, miR-141, and miR-375 showed <−10-fold change, miR-96 showed <−3 fold-change, and miR-183 and miR-143 showed <−2-fold change (Figure 1-5D and Appendix 1-4D). There was significant positive correlation of fold differences between the NGS and qPCR results (Figure 1-5E), and the expression levels of miR-122, miR-34a, miR-338, miR-182, and miR-1 (Figure 1-5C,d and Appendix 1-4) which were beyond my stringent filtering criteria, showed similar trends between NGS and qPCR indicates the strength of my filtering criteria. These results

confirm the expression of several oncogenic and tumor suppressor miRNAs in COM revealed by NGS and validated by qPCR.

1.3.4 Gene Regulatory Function of Oncogenic miRNAs

MiRNAs do their function by negatively regulating the gene expression in the mRNA and protein levels. To know the differentially expressed miRNAs function, I need to focus on the expression of their respective target genes. However, it is unfeasible to explore all the differentially expressed miRNAs targets in a single study. So, I selected three miRNAs (miR-450b, miR-301a, and miR-223) to know their gene regulatory function because, to my knowledge, miR-450b has no report in melanoma and other two miRNAs are less studied in human melanoma and no report in COM. I selected *PAX9*, *NDRG2*, and *ACVR2A* as targets of miR-450b, miR-301a, and miR-223, respectively, from previous studies where they validated miRNA-mRNA binding experimentally (134–136). The binding sites in the 3′ un-translated regions of these genes predicted by TargetScan 7.2 were conserved between human and dog (Appendix 1-5). So, I hypothesized that similar phenomenon (miRNA-mRNA binding) might exist in the canine oral melanoma. As in my experiment, miR-450b, 301a, and 223 were up-regulated so if my hypothesis is true the target genes must be down-regulated, and they should have a strong negative correlation

with the respective pairs. My qPCR results showed significant down-regulation of *PAX9*, *NDRG2*, and *ACVR2a* in melanoma compared with normal, and the relative expression of the respective miRNA–mRNA pairs showed significant negative correlation (Figure 1-6A, B). This inverse relationship indicates the miRNAs may bind the respective mRNA targets like previous human studies and suppress their expression in melanoma. In addition, study reported that PAX9 down-regulation decreases BMP4 expression which can increase *MMP9* expression (137,138). So I investigated the PAX9-BMP4-MMP9 axis in my study. My qPCR results showed that *BMP4* was down-regulated and *MMP9* was up-regulated in melanoma tissue samples (Figure 1-6C). MMP9 is required for the degradation of the extracellular matrix, which is a prerequisite for tumor invasion and positively correlates with tumor metastasis. So I expected high MMP9 expression in metastatic cells along with miR-450b. Therefore, I further investigated the relative expressions of miR-450b, *PAX9*, *BMP4*, and *MMP9* in two COM cell lines: KMEC established from primary oral melanoma and LMEC from metastatic mandibular lymph node of oral melanoma (139). qPCR analysis showed that miR-450b was up-regulated and *PAX9* and *BMP4* were significantly down-regulated in LMEC compared with KMEC. Conversely, as expected, *MMP9* was significantly up-regulated in LMEC compared with KMEC, as shown in Figure 1-6D. So, I

concluded that up-regulation of miR-450b and down-regulation of *PAX9* and *BMP4* were interconnected with the high *MMP9* expression in metastatic melanoma cells (Figure 1-6E).

1.3.5 Gene Ontology and KEGG Pathway Analysis of the Differentially Expressed miRNAs

To determine the global function of the differentially expressed miRNAs, I predicted their target genes by overlaying the results obtained using TargetScan and miRDB. I detected 2555 and 2464 target genes of the down- and up-regulated miRNAs, respectively. I functionally annotated the target genes by assigning gene ontology (GO) terms and KEGG pathways. Target genes of the down-regulated miRNAs were analyzed against cancer and other databases (Appendix 1-6). I found oncogenic genes related terms were enriched, which indicates these genes have an oncogenic function. From GO analysis I found protein modification (e.g., phosphorylation, transcription, or repression from DNA), extracellular matrix, and receptor signaling GO terms were assigned for the target genes of down-regulated miRNAs. It indicates down-regulated miRNAs inhibit their target genes from maintaining target genes terms related function in normal condition which was disrupted in melanoma due to the miRNA down-regulation. Target genes of the up-regulated miRNAs were involved mainly in the protein ubiquitination system because

ubiquitin-dependent protein catabolic process and ubiquitin-protein ligase activity terms were enriched in GO (Table 1-1). Ubiquitylation is long known for driving cell cycle transition, and ubiquitin ligase has relation to the cell cycle control. This indicates that up-regulated miRNAs may be involved in cell cycle control by ubiquitination system.

The KEGG pathway analysis of the target genes revealed that the down-regulated miRNAs were involved in tuning of several signaling pathways that are known to be disrupted in diseases, and the up-regulated miRNAs were related to remodeling of extracellular matrix organization, packaging, circadian entrainment, recycling and modification of receptors, proteins, chemokines and enzymes in favor of disease progression (Table 1-2).

1.3.6 miRNA–Transcription Factor Interaction Network between Dog and Human Melanoma

Previous human melanoma studies indicate that several differentially expressed miRNAs have a similar trend of expression with COM (140–144). Transcription factors like MITF can play a critical role in melanoma (145,146). So, I was interested in finding a common miRNA–TFs co-regulatory network in human and dog for melanoma. Moreover, miRNAs that can target maximum number of TFs will be considered to be important for

melanoma-related TFs regulation. I considered the same seed sequences miRNAs between human and dog from my study and the miRNAs target (genes) orthologues TFs that were differentially expressed in human melanoma (GSE31909) were selected for network construction. A total of 34 up-regulated and 33 down-regulated TFs were obtained from GSE31909 (Appendix 1-7). I constructed two networks, one using down-regulated miRNAs and up-regulated TFs, and the other using up-regulated miRNAs and down-regulated TFs (Figure 1-7A, B). See methods for details. I measured the degree and betweenness centrality of the networks to detect the key miRNAs that can regulate maximum TFs in both groups. Nodes that had higher centrality values than average were considered to influence the network biologically.

In the down-regulated miRNA–TF regulatory network (Figure 1-7A), the miR-126, miR-183, and miR-200 families, let-7 family members had higher degree centralities than average. Among them, miR-126 had the highest centrality (Appendix 1-8A).

In the up-regulated miRNA–TF regulatory network (Figure 1-7B), miR-130 family, and miR-9, miR-20b, miR-371, miR-106a, miR-450b, miR-21, and miR-424, had higher degree centrality than average. Among the miRNAs, miR-20b and miR-106a had the highest centralities (Appendix 1-8B). So it indicates that among the differentially expressed

miRNAs, miR-126, miR-20b, and miR-106a are the most potent to regulate the maximum number of TFs in melanoma.

1.3.7 Differential miRNA Chromosomal Enrichments

Studies reported that more than 50% of miRNA genes are encoded in the cancer-associated regions or fragile sites or chromosomal breakpoints which are frequently absent, amplified or rearranged in tumour specimens(147,148). Thereby, the dysregulation of miRNA expression occurred in tumor. For example, miR-15a/16-1 is located in genomic locus containing tumor suppressor that is frequently deleted in leukaemia (149). So to investigate the melanoma-associated regions or fragile sites it's important to understand in which chromosome the differential miRNAs reside. I analyzed the chromosomal locations of all 542 annotated miRNAs from miRBase. Stem-loop or mature sequences were mapped against the dog genome to obtain locations for the hsa-miRs (miRNAs that were annotated by the human sequence). Among the 542 miRNAs, 70 (12.84%) were in the X chromosome, and 14 (2.57%) and 24 (4.40%) were in chromosomes 4 and 5, respectively. Three chromosomes were focused because most of differentially expressed miRNAs were encoded in these chromosomes (Figure 1-8A, B). Out of 30 up-regulated miRNAs, 11 (34.4%) were in X, an about 2.8-fold significant enrichment ($p = 5.6\times 10^{-4}$). Among the

down-regulated miRNAs, four in chromosome 4 (p = 0.008, enrichment = 4.55-fold) and six in chromosome 5 (p = 0.001, enrichment = 4.55-fold) were enriched.

Among the 11 up-regulated miRNAs in Chromosome X, nine miRNAs encode from two clusters: mir-106a/18b/20b/19b-2/92a-2/363 and mir-424/503/542/450a-2/450a-1/450b. Other members in the clusters (miR-19b-2, miR-92a-2, and miR-503) are not listed among the up-regulated miRNA list because they did not meet my stringent criteria, but the changes in their expression were similar to other members of the clusters, except miR-92a-2. Two miRNAs, miR-223 and miR-421, are encoded separately as single genes.

Among the four miRNAs in Chromosome 4 two from miR-143/145 cluster, and rest miR-1271 and miR-1260a encode as a single gene. Rest six down-regulated miRNAs from chromosome 5 encode from two clusters, the miR-200 family and miR-99a-2/let-7a-2, and miR-101 as a single gene. All the family miRNAs had similar expression patterns.

These results are consistent with that study, found clustered miRNAs stay and act together (150). It also indicates that in chromosome X, 4, and 5 most of the differentially expressed miRNAs were from clusters and their other cluster members also have a similar trend of expression. This may recognize COM specific chromosomal fragile sites.

1.4 Discussion

Despite dogs being considered as a preclinical model for human melanoma (124), until now, the global miRNA profile was not fully revealed. In this study, I comprehensively analyzed the miRNA profile in COM. The expression levels of miRNAs studied previously (128,129) and my recently reported oncogenic miRNA (133) expression were consistent with those of the present study. Moreover, I detected several differentially expressed miRNAs that have not been reported previously (Appendix 1-3).

Some of the differentially expressed miRNAs (up-regulated miR-301a, 130, 383, 21, 454, 335, 132, 423,424, 146b, 9, 20b and down-regulated let-7a, 7b miR-126, 125a, 183, 26b, 29c, 152, 31, 145, 141, 205, 203, 200, 101) were reported in human melanoma (140–144). The expression trends of these miRNAs correlated well between human melanoma and COM. This indicates an overlap of miRNomes between the species and can be used as a model for human miRNA therapeutics development. It also affirms that dogs share much of their ancestral DNA with humans (30). To further understand the functions of the miRNAs compared to humans, the targets of miR-450b (*PAX9*), miR-301a (*NDRG2*), and miR-223 (*ACVR2A*) which were reported previously (134–136) in human were analyzed. I found, *PAX9* and *NDRG2*, which were down-regulated in human and

mouse melanoma, also were down-regulated in COM (151,152). The expression of the miR-450b–*PAX9* and miR-301a–*NDRG2* pairs was significantly negatively correlated, which supports two studies that reported miR-450b and miR-301a could bind and suppress PAX9 and NDRG2 activity, respectively (134,135). *ACVR2A* is reported here for the first time in melanoma with significant negative correlation with miR-223. These results suggest that the tumor suppressive function of PAX9, NDRG2, and ACVR2a were disrupted by miR-450b, miR-301a, and miR-223, respectively, to maintain oncogenic characteristics in COM as like the human studies. Moreover, as previous study reported that PAX9 is down-regulated and miR-301a, 223 is up-regulated in human melanoma (140,152,153). It also indicates that there are similarities between human and canine melanoma in respect of PAX9, miR-301a, and 223 expressions.

The predicted binding site of miR-450b-PAX9 is conserved between human and dog (Appendix 1-5A). BMP4, a downstream of PAX9, was suppressed when miR-450b degraded the function of PAX9, resulting in an increase of MMP9. Previous studies also showed that suppression of PAX9 decreased BMP4 expression and subsequently increased MMP9 (137,154). My study revealed that, in COM, this axis is also maintained and interconnected with high expression of miR-450b. Additionally, high MMP9 expression in metastatic melanoma cells may be maintained by this axis.

Axon guidance, endocytosis, and regulation of actin cytoskeleton and pathways in cancer are common pathways between human and dog melanoma regulated by miRNAs (144). With canine cutaneous melanoma, only PI3K-Akt signaling, focal adhesion, and ECM-receptor interaction pathways are common (155). This is not surprising because there are molecular differences between cutaneous and mucosal melanomas, so different pathways are likely to be affected (114,115).

TFs can regulate single or multiple gene expressions, so investigation of miRNAs that influence TFs could be more meaningful. MiR-126 has maximum influence over eight TFs that were up-regulated in melanoma. Although, low miR-126 expression was found to have poor prognostic value in several cancers (156), up-regulated miR-20b and miR-106a influenced 11 and 10 TFs, respectively. The miR-20b seed sequence is similar to that of human miR-17-5p, and miR-106a belongs to the miR-17-92 family. Over-expression of hsa-miR-17 and miR-106a is a good predictor of poor overall survival in several human cancers (157), indicating these miRNAs may be a prognostic marker and also a good therapeutic option in both species.

Chromosomal enrichment showed that the X chromosome harbored up-regulated miRNAs. In human melanoma, X-linked miRNAs are also enriched. Women have consistent advantageous prognosis in melanoma compared with men (158). However, in

mucosal melanoma, the incidence is higher in females (159). Also, breast cancer has X chromosome-linked differential miRNA enriched in women (160). To my knowledge, until now, the correlation between X-linked miRNA and poor survival has not been explained. However, in humans, a high number of miRNAs related to cancer located in X chromosome compared to Y(161). Also study shows 52.5% of human miRNA genes are encoded in the cancer-associated regions or fragile sites or chromosomal breakpoints (148). As a result miRNAs are frequently absent, amplified or rearranged in tumor specimens (148,149). So, the speculation that miRNA clusters or family members are co-regulated with melanoma-related genes to achieve a regulatory net outcome on a cell or environment is a reasonable explanation of the enrichment of X chromosome-linked differentially expressed miRNAs. On the other hand, down-regulated miRNAs enriched in chromosomes 4 and 5. Previous studies showed that miR-15a/16-1 is down-regulated in leukaemia, due to the deletion of genomic locus containing a putative tumor suppressor-containing region, (149). Also let-7g/mir-135-1 deletion is reported in varies human malignancies(148). So, further study regarding the down-regulation of two cluster miR-143/145 and 200 families may be interesting to find putative region in the respective chromosomes.

One drawback of my experiment might be the use of less normal samples in NGS screening. However, I overcome the issue by the qPCR validation of 20 differentially

expressed miRNAs within 12 normal and 17 melanoma samples. Moreover, all the normal samples were from healthy laboratory beagle dogs, which minimize the limitation of diversity regarding normal samples.

My study comprehensively established a miRNA profile of COM that has not been previously implicated. I have also shown the significance of miR-450b over-expression in metastatic melanoma cells, and future studies are necessary to evaluate the others. Furthermore, I am able to report some melanoma-related miRNAs that are also important in human. Besides, as dog oral melanoma is considered as a typical model for non-UV or TWT melanoma in human my findings will give an insight into the miRNA expression of TWT and mucosal melanoma.

1.5 Materials and Methods

1.5.1 Clinical Samples and Canine Melanoma Cell Lines

COM tissue specimens were acquired from tumors excised from dogs that had undergone surgery at the Veterinary Teaching Hospital of Kagoshima University. Informed consents were obtained from dog owners. COM patient's information is presented in Appendix 1-1a. Normal oral tissues were collected from healthy laboratory beagle dogs (age range 8–10 years) at Kagoshima University. Experimental conditions and design were approved by Kagoshima University and Veterinary Teaching Hospital ethics committee (KV004; 18.04.2011). All experimental methods were carried out in accordance with the approved guidelines and regulations.

Tissue samples were collected immediately after excision from dogs that had undergone surgery. The diagnosis was confirmed histopathologically by the hospital. The tissue specimens were placed in RNA*later* (AM7021, Invitrogen, Carlsbad, CA, USA) immediately after isolation and stored at −80 °C after overnight incubation at 4 °C.

Dog melanoma cell lines KMEC and LMEC were stored in freezing medium (039-23511, CultureSure, Fujifilm Wako Pure Chemical Corporation, Osaka, Japan). Cell lines were

cultured according to the procedure described previously (139). Cells were grown until confluence and then RNA was extracted for evaluation.

1.5.2 RNA Extraction and Sequencing

A mirVana RNA Isolation kit (AM1560, Thermo Fisher Scientific, Waltham, MA, USA) was used for RNA isolation according to the Manufacture's standard protocol. The total RNA concentration was measured using a NanoDrop 200c spectrophotometer (ND2000C, Thermo Fisher Scientific). The RNA quality and integrity were assessed with an Agilent 2100 Bioanalyzer (G2939BA, Agilent Technologies, Santa Clara, CA, USA). The RNA Integrity Number (RIN) mean value was 8.8 (range 7–10) for tissue samples and 9.9 (range 9.6–10) for the KMEC and LMEC cell lines.

Following RNA isolation and quality measurement, samples were sequenced by the Hokkaido System Sciences Company (Hokkaido, Japan). Briefly, small RNA (sRNA) libraries were constructed using 1 μg of total RNA with the TruSeq Small RNA Library Preparation kit (Illumina, San Diego, CA) following the manufacturer's protocol. After obtaining the sRNAs (18–30 nt) from the total RNA, 5′ and 3′ adaptors were ligated to the sRNAs. Then, reverse transcription followed by amplification was performed to create cDNA constructs. A gel purification step was applied to purify the amplified cDNA

constructs for cluster generation and Illumina/Hiseq2500 sequencing analysis by the Hokkaido System Science Co., Ltd. (Hokkaido, Japan). The high-quality cleaned reads that I obtained from the company are shown in Appendix 1-1B (Phred score > 34). The raw sequences have been submitted to NCBI sequence read archive (SRA) database under accession number PRJNA516252

1.5.3 Bioinformatics Analysis of Small RNA Reads

The RNA sequencing data were imported into the CLC Genomics Workbench (CLC Bio, Qiagen, Germany) as recommended in the manufacturer's manual (http://resources.qiagenbioinformatics.com). Normalization of reads, quality, ambiguity, and adapter trimming as well as quality control was performed using the CLC Genomics Workbench (versions 9 and 10). Briefly, the sequencing generated about 103 and 266 million reads from the normal and melanoma libraries, respectively, with single-end reads (Appendix 1-1B). I performed a two-step trimming process to remove adapters and other contaminants. In step one, I aimed to remove low quality, ambiguous nucleotides, 3′ adapters, and short (>15 nt) and long reads (>29 nt). In step two, I removed contaminated sequences, 5′ adapters, and the Illumina stop oligo sequence (5′-GAATTCCACCACGTTCCCGTGG-3′). Finally, I obtained about 51 and 142 million reads

from the normal and melanoma libraries, respectively, for further analysis of the small RNA reads (Appendix 1-1B). Clean reads were analyzed according to the small RNA analysis guideline of the CLC Genomics Workbench. Briefly, the CLC Genomics Workbench was used to extract and count the small RNA from the clean reads and then compare them to databases of miRNAs and other small RNA databases for annotation. Sequence/fragment counts were used as the expression values for the miRNAs/small RNAs in the libraries.

To annotate the small RNA other than miRNA, CLC bio uses two other reference databases (Canis_familiris.canfam3.1.ncrna and Homo_sapiens.GRCh37.ncrna) from ensemble to annotate sequences that had no matches in miRBase (162). Differential expression between the two groups was followed the EDGE (empirical analysis of differential gene expression) analysis within the CLC bio.

1.5.4 Edge Analysis

EDGE follows the exact test developed by Robinson and Smyth for two-group comparisons (163). The exact test counts data that follow a negative binomial distribution and compares the counts in one set of count samples against the counts in another set of count samples. The variability of each group also is taken into account. The original count

data are used because the algorithm assumes that the counts on which it operates are negative binomially distributed. I used the default parameters throughout the analysis. Fold change was calculated from the estimated average count per million (cpm) from each group. The estimated average cpm is derived internally in the exact test of the algorithm. Fold change indicates the difference in average cpm values between the groups. The FDR is based on the p-value of the exact test.

1.5.5 Expression Analysis by qPCR

To measure the expressions of miRNAs and mRNAs by qPCR I used TaqMan microRNA and gene expression assays (Thermo Fisher Scientific). Total RNA (2 ng) was reverse transcribed to cDNA using a TaqMan MicroRNA Reverse Transcription kit (4366597, Thermo Fisher Scientific) according to the manufacturer's protocol. qPCR was performed using a TaqMan First Advanced Master Mix kit and a one-step plus real-time PCR system (Thermo Fisher Scientific). Thermal cycling was performed according to the manufacturer's instructions. All experiments were performed in duplicate. The Cq values of RNU6B in the normal and melanoma samples were consistent between the groups, so RNU6B was used as an internal control to calculate miRNA expression. ΔCq was calculated by subtracting the Cq values of RNU6B from the Cq value of the target miRNA.

ΔΔCq was calculated by subtracting the mean target miRNA ΔCq value from the ΔCq value of the normal and melanoma samples. The expression level was evaluated using the $2^{-\Delta\Delta Cq}$ method (164). qPCR reactions of undetermined Cq were assigned Cq = 36 cycle. TaqMan MicroRNA assays were used in this study can quantitate mature miRNAs. MiRNA primer IDs were as follows: RNU6B (ID: 001093), miR-450b (ID: 006407), miR-301a (ID: 000528), miR-140 (ID: 007661), miR-383 (ID: 000573), miR-542 (ID: 001284), miR-223 (ID: 000526), miR-190 (ID: 000489), miR-21 (ID: 000397), miR-122 (ID: 002245), miR-34a (ID: 000426), miR-338 (ID: 000548), miR-429 (ID: 001077), miR-96 (ID: 000186), miR-375 (ID: 000564), miR-183 (ID: 002269), miR-182 (ID: 002334), miR-1 (ID: 000385), miR-143 (ID: 002249), miR-200b (ID: 002251), and miR-141 (ID: 000463).

For the target gene mRNAs, 250 ng RNA was reverse transcribed to cDNA using ReverTra Ace qPCR RT master mix with gDNA Remover (FSQ-301, Toyobo, Osaka, Osaka Prefecture, Japan). The qPCR procedure was the same as that used for the miRNA experiments. The $2^{-\Delta\Delta Cq}$ method also was used to calculate the expression. *GAPDH* was used as an internal control. The TaqMan gene expression assay was used in the experiments. The gene IDs were as follows: *GAPDH* (ID: Cf04419463_gH), *PAX9* (ID:

Cf02705737_m1), *MMP9* (ID: Cf02621845_m1), *BMP4* (ID: Cf01041266), *NDRG2* (ID: Cf02631635_m1), and *ACVR2A* (ID: Cf02664427_m1).

1.5.6 Gene Ontology, Pathway Analysis and Network Construction

Gene Ontology and pathway analysis of miRNA target genes were done using the Database for Annotation, Visualization, and Integrated Discovery (DAVID) (165). A common miRNA–TF interaction network was constructed between human and dog by analyzing the differentially expressed TFs from GSE31909. Briefly, I used TargetScan 7.2 (166) and miRDB (167) to predict miRNA targets. The common target genes between the two predictions were considered as targets for the respective miRNAs. A low FDR was considered to indicate a strong relationship between the annotation and the gene.

To construct a common miRNA–mRNA interaction network between humans and dogs I analyzed the BioProject GSE31909 datasets using the GEO2R tool (https://www.ncbi.nlm.nih.gov/geo/info/geo2r.html#background) to get the differentially expressed genes in human melanoma. I picked the target genes of the differentially expressed miRNAs from the differentially expressed genes in GSE31909. From the differentially expressed target genes, I only considered the TFs for network construction. I also considered the miRNAs that had the same seed sequences as the orthologous human

miRNA sequences. The MSigDb gene families (http://software.broadinstitute.org/gsea/msigdb/index.jsp) were used to select the transcription factors (TFs) from the miRNA target genes. Since the expression of miRNAs and their targets are inversed, I built miRNA–TF co-regulatory networks with the inversely expressed TFs using Cytoscape v3.5 (http://www.cytoscape.org/) (168). That means I built two networks, one with down-regulated miRNAs and up-regulated TFs and the other with up-regulated miRNAs and down-regulated TFs. Since TFs can regulate each other, I also performed a STRING v.10.5 (confidence score 0.700) (http://string-db.org/) (169) network analysis within each group of TFs. The final miRNA–TF regulatory network was obtained after merging the STRING TFs network with the respective miRNA–TF regulatory network in Cytoscape. The degree and betweenness of the network were measured using CentiScaPe 2.2 (170).

1.5.7 Statistical Analysis

I used GraphPad Prism 7 (www.graphpad.com) for the statistical analysis. Hierarchical clustering analysis was performed using the $\log_{10}$ value that was converted from the expression value of every miRNA from each sample. Unsupervised hierarchical clustering was done with Euclidean distance metric and complete linkage. A Comparison of

the qPCR data was done using Mann-Whitney test followed by Tukey's test where appropriate. *P* values < 0.05 were considered significant. Correlation analysis was performed using Spearman's correlation coefficient. For the miRNA chromosomal enrichment analysis, I used hyper-geometric test.

Table 1- 3. Gene ontology (GO) functional analysis of the target genes of differentially expressed miRNAs.

Down-Regulated miRNA's Target Genes Ontology		
Biological Process		
Terms	FE [1]	FDR [2]
GO:0018105~peptidyl-serine phosphorylation	2.323	0.001
GO:0045944~positive regulation of transcription from RNA polymerase II promoter	1.461	0.025
Cellular Component		
GO:0005634~nucleus	1.277	1.65×10^{-6}
GO:0005654~nucleoplasm	1.374	2.49×10^{-5}
GO:0005737~cytoplasm	1.232	1.09×10^{-4}
GO:0005911~cell-cell junction	2.11	0.068146
Molecular Function		
GO:0004702~receptor signaling protein serine/threonine kinase activity	2.932	9.98×10^{-4}
GO:0005201~extracellular matrix structural constituent	3.373	0.002697
GO:0003682~chromatin binding	1.709	0.002892
GO:0003714~transcription corepressor activity	2.104	0.057312
Up-Regulated miRNA's Target Genes Ontology		
Biological Process		
Terms	FE [1]	FDR [2]
GO:0042787~protein ubiquitination involved in ubiquitin-dependent protein catabolic process	2.208	0.004
Cellular Component		
GO:0005654~nucleoplasm	1.441	1.35×10^{-7}
GO:0005737~cytoplasm	1.228	2.87×10^{-4}
GO:0005794~Golgi apparatus	1.590	8.03×10^{-4}
GO:0005634~nucleus	1.228	0.001041
Molecular Function		
GO:0061630~ubiquitin protein ligase activity	2.027	0.012
GO:0044212~transcription regulatory region DNA binding	2.127	0.019

[1] Fold enrichment, [2] False discovery rate.

Table 1- 4. KEGG pathway analysis of the target genes of the differentially expressed miRNAs.

Down-Regulated miRNAs Target Genes Pathway		
Terms	FE [1]	FDR [2]
cfa05206:MicroRNAs in cancer	2.522	6.72×10^{-7}
cfa04010:MAPK signaling pathway	1.917	1.20×10^{-4}
cfa04151:PI3K-Akt signaling pathway	1.762	1.65×10^{-4}
cfa04360:Axon guidance	2.307	4.96×10^{-4}
cfa05205:Proteoglycans in cancer	1.981	8.64×10^{-4}
cfa04910:Insulin signaling pathway	2.209	8.88×10^{-4}
cfa04152:AMPK signaling pathway	2.230	0.003
cfa04510:Focal adhesion	1.901	0.003
cfa04722:Neurotrophin signaling pathway	2.164	0.010
cfa04012:ErbB signaling pathway	2.384	0.013
cfa04512:ECM-receptor interaction	2.384	0.013
Up-regulated miRNAs target genes pathway		
Terms	FE [1]	FDR [2]
cfa04144:Endocytosis	2.424	1.31×10^{-11}
cfa04810:Regulation of actin cytoskeleton	2.273	2.78×10^{-7}
cfa05200:Pathways in cancer	1.604	0.010
cfa04710:Circadian rhythm	3.536	0.060
cfa05410:Hypertrophic cardiomyopathy (HCM)	2.398	0.063
cfa05414:Dilated cardiomyopathy	2.346	0.065
cfa04713:Circadian entrainment	2.210	0.098

[1] Fold enrichment. [2] False discovery rate.

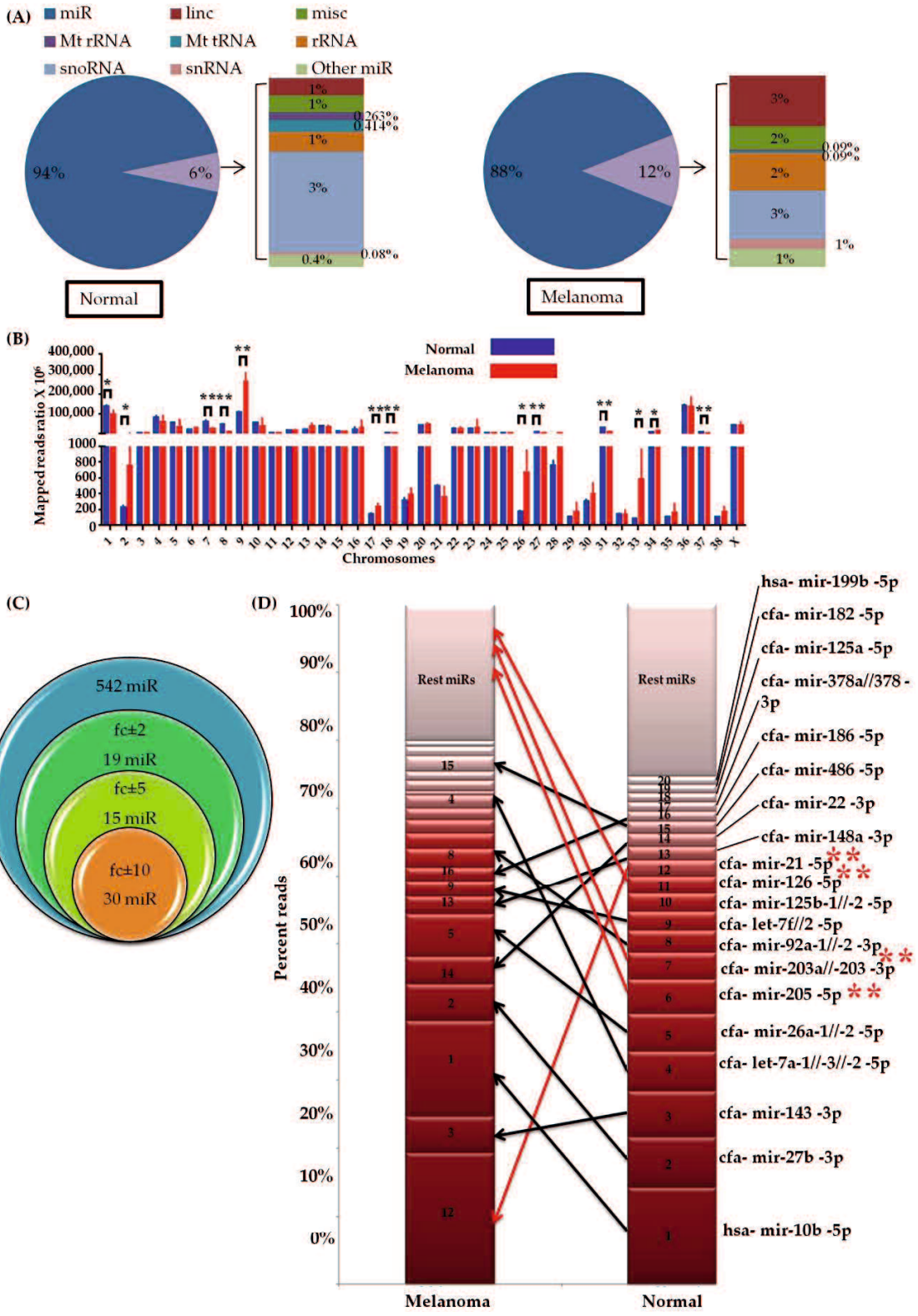
(A)
miR
linc
misc
Mt rRNA
Mt tRNA
rRNA
snoRNA
snRNA
Other miR
94%
6%
1%
1%
0.263%
0.414%
1%
3%
0.4%
0.08%
Normal
88%
12%
3%
2%
0.09%
0.09%
2%
3%
1%
1%
Melanoma
(B)
Normal
Melanoma
Mapped reads ratio X 10^6
400,000
300,000
200,000
100,000
1000
800
600
400
200
0
1 2 3 4 5 6 7 8 9 10 11 12 13 14 15 16 17 18 19 20 21 22 23 24 25 26 27 28 29 30 31 32 33 34 35 36 37 38 X
Chromosomes
(C)
542 miR
fc±2
19 miR
fc±5
15 miR
fc±10
30 miR
(D)
Percent reads
100%
90%
80%
70%
60%
50%
40%
30%
20%
10%
0%
Rest miRs
Rest miRs
Melanoma
Normal
hsa- mir-199b -5p
cfa- mir-182 -5p
cfa- mir-125a -5p
cfa- mir-378a//378 -3p
cfa- mir-186 -5p
cfa- mir-486 -5p
cfa- mir-22 -3p
cfa- mir-148a -3p
cfa- mir-21 -5p
cfa- mir-126 -5p
cfa- mir-125b-1//-2 -5p
cfa- let-7f//2 -5p
cfa- mir-92a-1//-2 -3p
cfa- mir-203a//-203 -3p
cfa- mir-205 -5p
cfa- mir-26a-1//-2 -5p
cfa- let-7a-1//-3//-2 -5p
cfa- mir-143 -3p
cfa- mir-27b -3p
hsa- mir-10b -5p

Figure 1-4. Profile of small RNA reads in canine oral melanoma by next-generation sequencing: (A) Percentages of the clean reads annotated under the different small RNA categories. Normal (n = 3), Melanoma (n = 8), (B) The miRNA reads were mapped to the canine genome (Canfam3.1) and the mapped reads ratio distributed in each chromosome was analyzed. Multiple t-test (many t-tests at once-one per row), *P < 0.05, **P < 0.01, (C) Venn diagram showing the total numbers of identified and differentially expressed miRNAs in melanoma. First Venn (blue) indicates the total number of miRNAs identified in both groups. Other three Venn indicates the number of differentially expressed miRNAs (up (+) and down-regulated (−)). fc, fold change, (D) Top 20 highly expressed miRNAs in the normal and melanoma. Twelve miRNAs were common between the groups and rests eight were left blank in melanoma. In the bar graph, the number in each cell represents the rank of the miRNA with respect to the normal group. Arrows represent the changed position of miRNAs in melanoma group, Red arrows indicate the positions of significant deferentially expressed miRs. miRNA/s (miR/s), *statistically significant differentially expressed miRs between normal and melanoma.

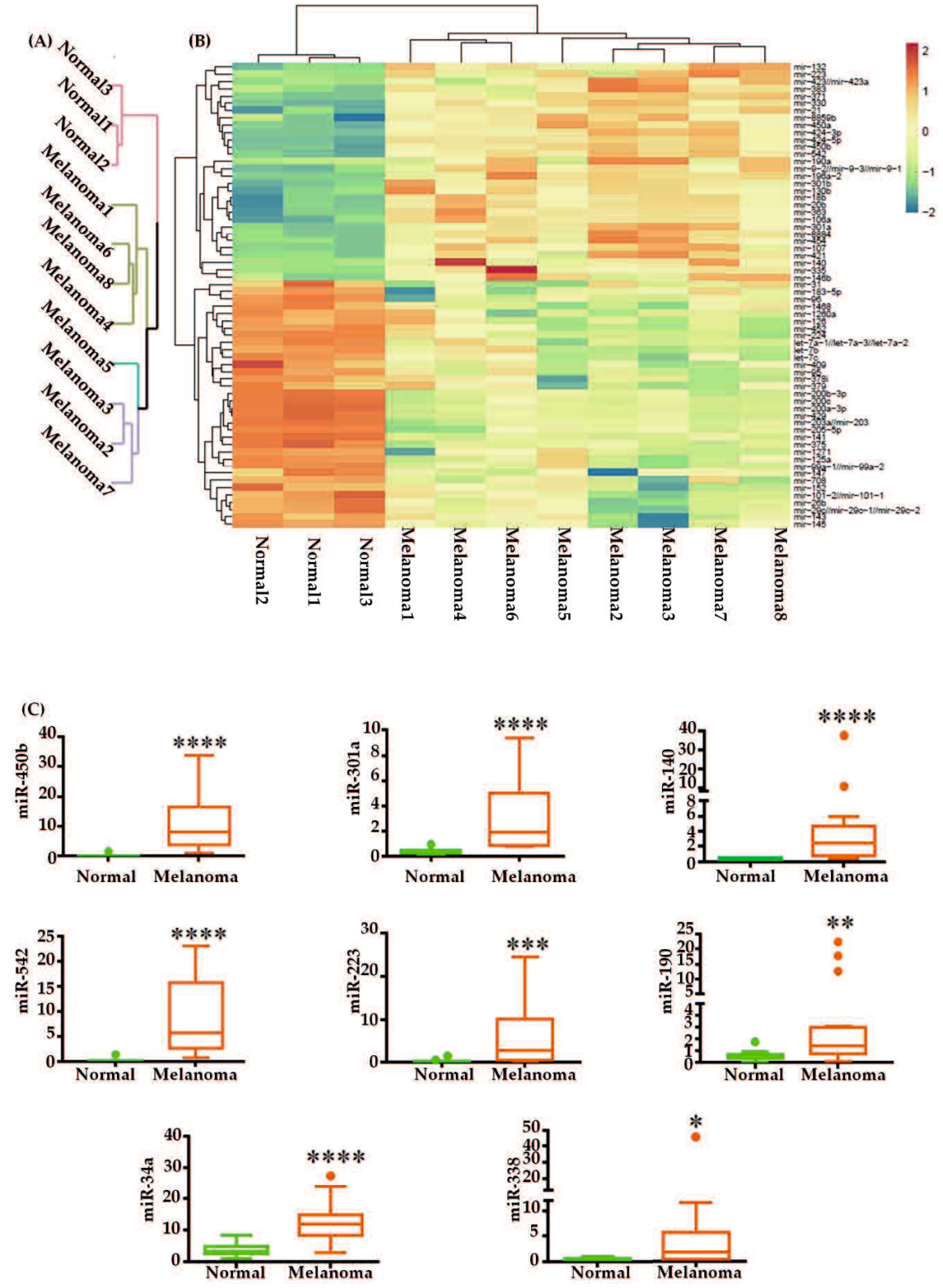
(A)
Normal3
Normal1
Normal2
Melanoma1
Melanoma6
Melanoma8
Melanoma4
Melanoma5
Melanoma3
Melanoma2
Melanoma7
(B)
Normal2
Normal1
Normal3
Melanoma1
Melanoma4
Melanoma6
Melanoma5
Melanoma2
Melanoma3
Melanoma7
Melanoma8
(C)
miR-450b
miR-301a
miR-140
miR-542
miR-223
miR-190
miR-34a
miR-338
Normal
Melanoma

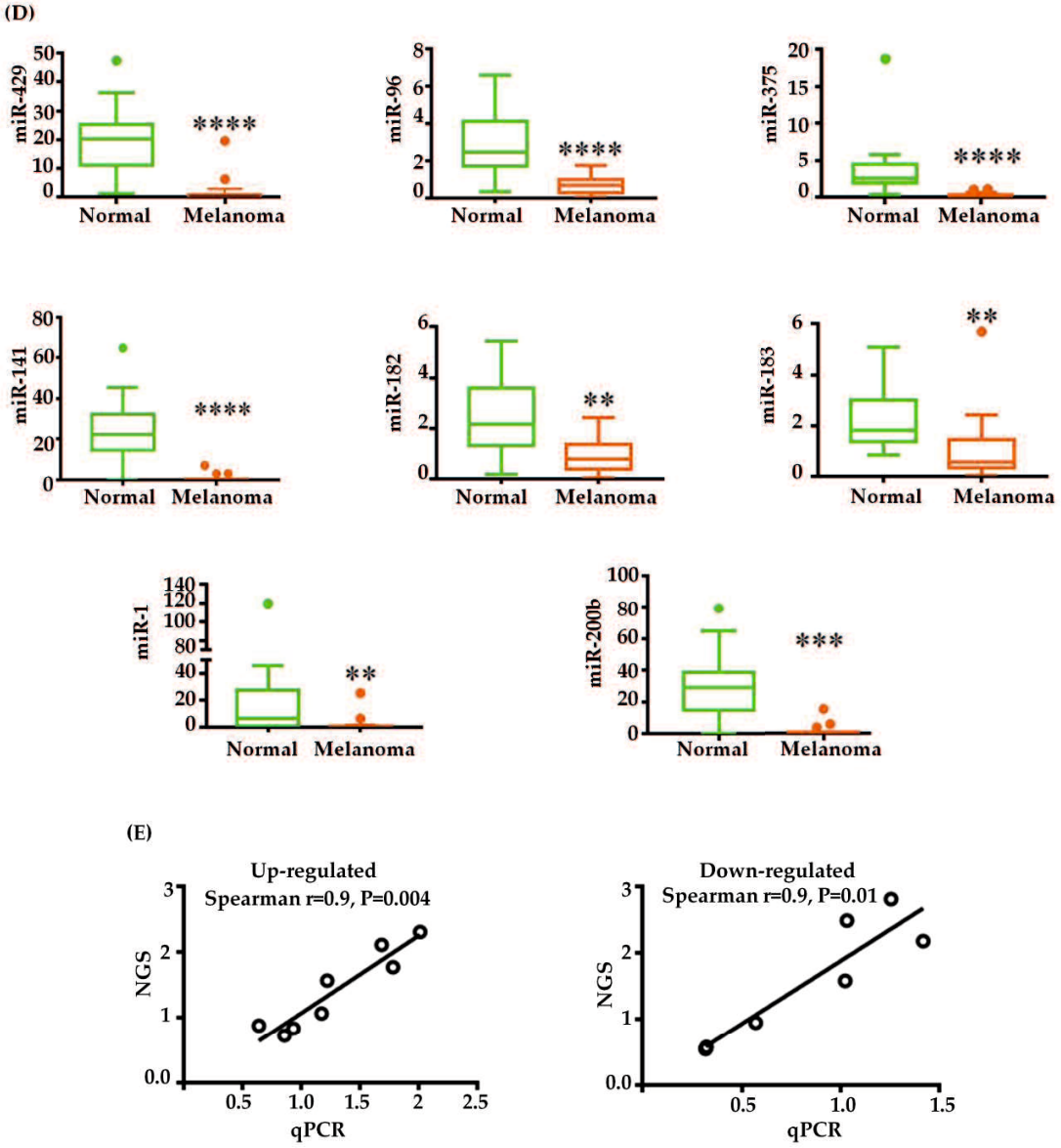
(D)
miR-429
miR-96
miR-375
miR-141
miR-182
miR-183
miR-1
miR-200b
Normal
Melanoma
****
**
***
(E)
Up-regulated
Spearman r=0.9, P=0.004
Down-regulated
Spearman r=0.9, P=0.01
NGS
qPCR

Figure 1-5. Differential miRNA expression in COM: (A) Unsupervised euclidean hierarchical clustering by the miRNA normalized expression values in the normal and melanoma libraries, (B) Heatmap visualizes the expression of statistically significant differentially expressed miRNAs in the normal and melanoma libraries. The color scale (upper right) indicates the expression values. Up- and down-regulated miRNAs are shown in red to green, respectively. Colour saturation indicates the deviation from the median, (C) Relative expression of oncogenic miRNAs and (D) tumor suppressor miRNAs selected from the next-generation sequencing confirmed by qPCR. The Y-axes indicates the relative miRNA expression levels normalized against RNU6B (normal $n = 12$, melanoma $n = 17$, Mann-Whitney test followed by Tukey's test, $*P < 0.05$, $**P < 0.01$, $***P < 0.001$, $****P < 0.0001$), (E) Correlation of fold change between next-generation sequencing (NGS) and qPCR of the up- and down-regulated miRNAs. Each black circle in the graph represents a miRNA.

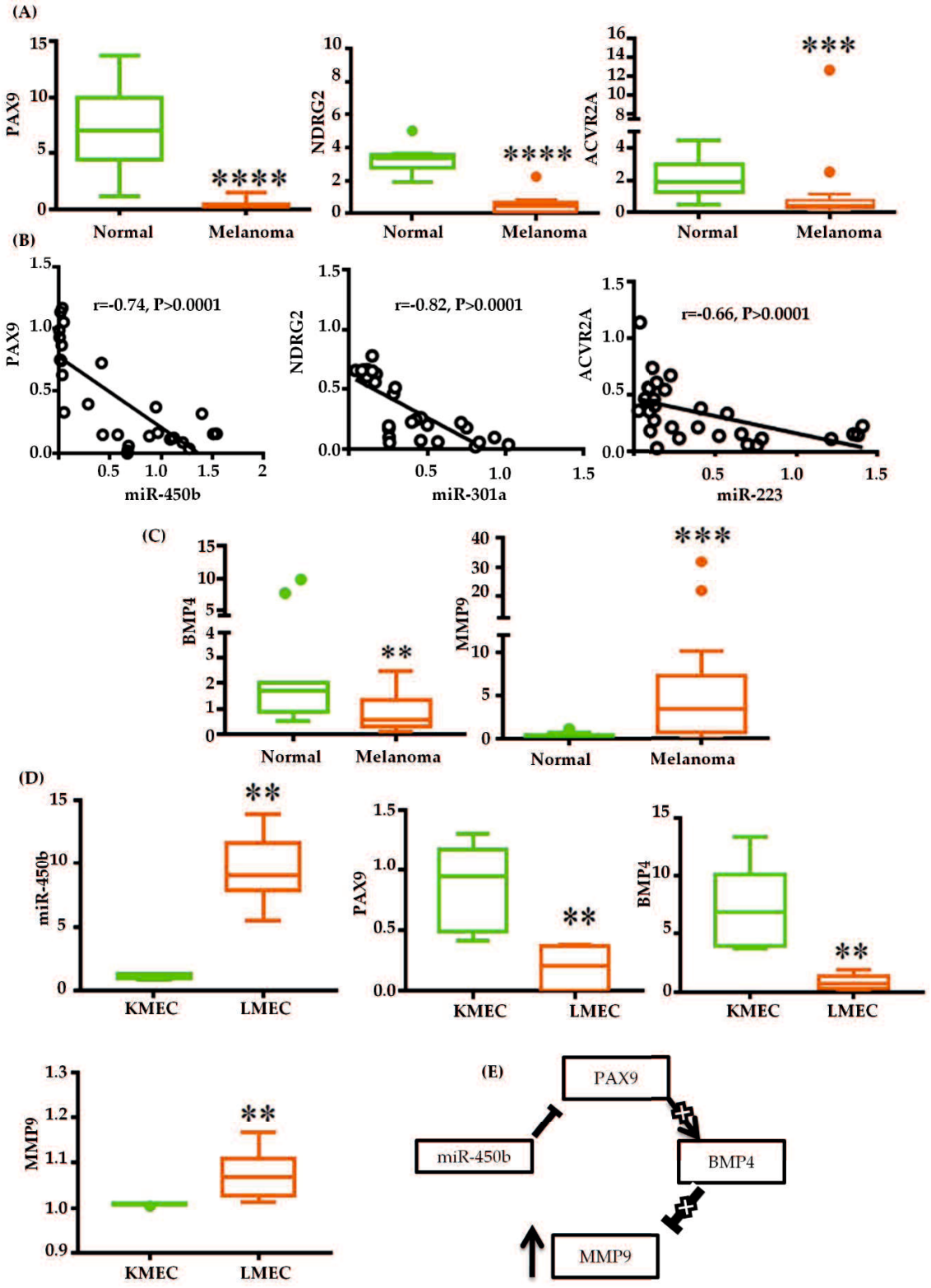
(A)
PAX9
Normal
Melanoma
****
NDRG2
****
ACVR2A
***
(B)
PAX9
r=-0.74, P>0.0001
miR-450b
NDRG2
r=-0.82, P>0.0001
miR-301a
ACVR2A
r=-0.66, P>0.0001
miR-223
(C)
BMP4
**
MMP9
***
(D)
miR-450b
KMEC
LMEC
PAX9
BMP4
MMP9
(E)
PAX9
miR-450b
BMP4
MMP9

Figure 1-6. Gene regulatory function of miR-450b, miR-301a, and miR-223: (A) Relative expression of the target genes *PAX9*, *NDRG2*, and *ACVR2A*. Y-axes indicates the relative mRNA expression normalized against *GAPDH*, (B) Spearman correlation of the expression of the miR-450b-*PAX9*, miR-301a-*NDRG2*, and miR-223-*ACVR2A* pairs, (**C**) Relative expression of *BMP4* and *MMP9* in melanoma tissue samples, (D) Relative expression of miR-450b, *PAX9*, *BMP4*, and *MMP9* in the canine melanoma cell lines KMEC and LMEC. Mann-Whitney test followed by Tukey's test, $*P < 0.05$, $**P < 0.01$, $***P < 0.001$, $****P < 0.0001$. (E) Schematic representation of the miR-450b regulatory function. MiR-450b inhibits *PAX9* and, as a result, BMP4-MMP9 regulation is disrupted (↑:–up-regulation, T:-Inhibition).

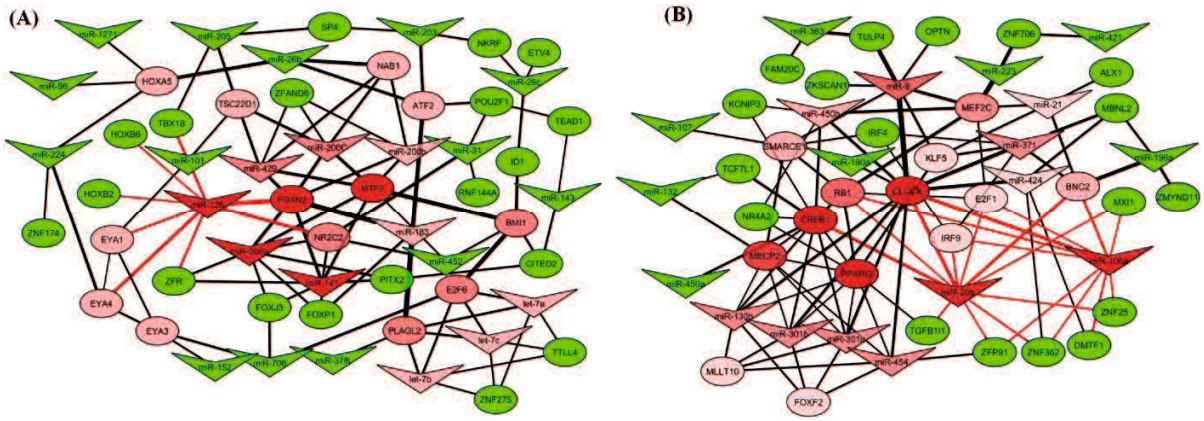

Figure 1-7. Common miRNA–transcription factor (TF) regulatory network between human and dog: (A) Regulatory network for down-regulated miRNAs and its up-regulated target TFs. MiR-126 influences eight TFs and has the highest centrality, (B) Regulatory network for up-regulated miRNAs and its down-regulated target TFs. MiR-20b and miR-106a have the highest centralities. A miRNA (V-shaped) or TF (oval-shaped) is considered a node and line between nodes considered edge. Green and red indicate degree scores less and above than average and saturation shows deviation. The colour gradient of the nodes (miRNAs/mRNAs) indicates the strength of network regulation. Edge width represents edge betweenness. Node's Edges with highest degree scores are in red.

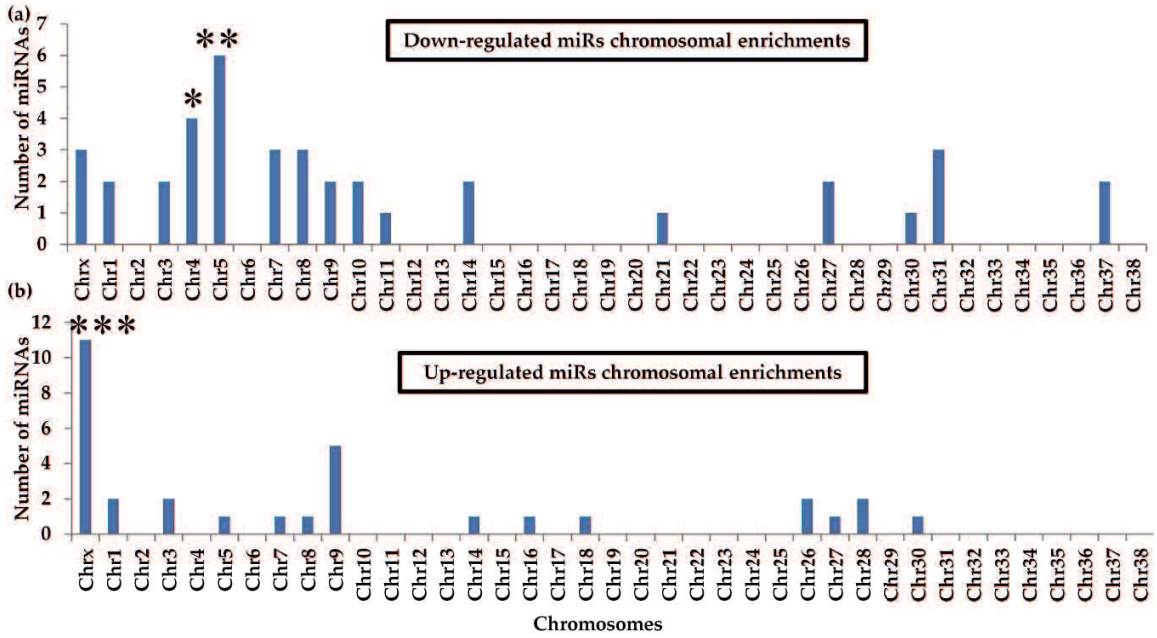

Figure 1-8. Chromosomal enrichment of differentially expressed miRNAs (miRs): (A) Chromosome enrichment of the down-regulated miRNAs, (B) Chromosome enrichment of the up-regulated miRNAs. Hypergeometric test, $*P < 0.05$, $**P < 0.01$, $***P < 0.001$.

Chapter 2
Aberrantly expressed snoRNA, snRNA, piRNA and tRFs in canine melanoma.

(Rahman, M *et al*., 2019 *Vet. Comp. Oncol).*

2.1 Abstract

Among small non-coding RNAs (sncRNAs/sRNAs), the functional regulation of microRNAs (miRNAs) has been studied in canine oral melanoma (COM). However, the expression level of other sncRNAs, like small nucleolar RNAs (snoRNAs), small nuclear RNAs (snRNAs), transfer RNA-derived fragments (tRFs) and PIWI-interacting RNAs (piRNAs), in COM is unknown. This study aimed to investigate sncRNAs other than miRNAs in COM from my small RNA sequencing project (PRJNA516252). I found that several snRNAs and piRNAs were upregulated, whereas tRFs and snoRNAs were downregulated in COM. Upregulation of U1 snRNA and piR-972, and downregulation of tRNA-*ser*(1) and snoRA24 was confirmed in dog melanoma tissue and cell lines by quantitative reverse transcription PCR (qRT-PCR). Consistently, the expression of tRNA-*ser*(1) and snoRA24 in plasma of COM cases was also decreased. Finally, I found a similar expression trend of U1 and snoRA24 in the human cutaneous melanoma cell line, MEWO, compared with human epidermal melanocyte cells (HEMa-Lp). In my study, snRNA, snoRNA, tRFs, and piRNA were dysregulated during melanoma progression. Moreover, the melanoma-associated expression of U1 and snoRA24 was similar in human and dog melanoma.

2.2 Introduction

The Human Encyclopedia of DNA Elements (ENCODE) is a public research project aiming to identify the functional DNA elements of the human genome. Previously, except the coding part much of which was considered as a junk. From their primary investigation it has been reported that 80% of the genome is biologically active (171). However, proteins translated from coding RNA occupy less than 2% of the genomic information(172). So, A large part of the DNA is transcribed into non-coding RNA (ncRNA) including functional RNA molecules. In the last decade, it has been shown that ncRNAs are not a junk transcriptional sequences, but rather active, functional regulatory molecules.

Sequencing technologies become advances very recently which enabled studying highly conserved small ncRNAs like microRNAs (miRNAs), small nucleolar RNAs (snoRNAs), small nuclear RNAs (snRNAs), transfer RNA-derived fragments (tRFs) and PIWI-interacting RNAs (piRNAs). Among these, miRNAs is one of the extensively studied groups of small non-coding RNA. Advancements of their investigation lead to human trials for cancer therapy(127). For example, miR-34 reaches phase- I and antimiR targeting miR-122 phase-2 clinical trial for cancer therapy. Other small non-coding RNAs like snoRNAs, snRNAs, tRFs and piRNAs are under continuous investigation to identify their expression

level and function in different diseases including cancer. In recent years, several snoRNAs like snoRA24, snoRA54, snoRD27 and snoRD93 were studied in human lymphoma, breast cancer, melanoma and myeloma (173–178). Among the snRNAs, U2 has been studied in ovarian, colorectal, lymphoma and lung cancers and in melanoma (179–182). Additionally, it has been reported that specific cleavage of pre and mature tRNAs generate tRFs during cancer and stress(183). Furthermore, evidence of dysregulation and pathogenic involvement of tRFs in several human cancers has accumulated in recent years(183–191). Finally, 30,000 piRNAs have been reported in humans(192), of which a subset regulates cancer regulatory genes via DNA-methylation (193). Recently, a serum piRNA biomarker for colorectal cancer has been reported (194,195) and aberrant expression was observed in human gastric cancer (196).

MiRNAs in canine oral melanoma (COM) have been studied by our group and others (128,129,133). Our current small RNA (sRNA) sequencing project (PRJNA516252) revealed more details about miRNAs in COM. However, even though COM is one of the frequent cancers in dogs and is considered a good natural model for human melanoma (123,124), until now no investigation of snoRNA, snRNA, piRNA, and tRFs has been reported. I think it is worthwhile investigating other sRNAs that are also derived from long genomic parental transcripts like miRNAs. In this study, I analyzed sRNA reads other than

miRNAs from our sRNA sequencing project. I found that various snoRNAs, snRNAs, tRFs and piRNAs were aberrantly expressed in COM. Finally, I confirmed their expression in patient tissues and plasma and in canine and human melanoma cell lines by quantitative real-time PCR (qRT-PCR).

2.3 Results

2.3.1 Aberrantly expressed sRNAs in canine oral melanoma

Out of our sRNA sequencing project submitted in the SRA database (PRJNA516252), I analyzed the reads other than miRNA. 6% of the reads in control and 12% in melanoma samples were annotated by the Ensembl dog and human ncRNA database. I found eight types of sRNAs (Figure 2-9). Among the sRNAs, snRNA, mitochondrial (mt)-tRNA, and snoRNA were significantly differentially expressed between the control and melanoma samples.

U1, U2, U5, and U11 snRNA were significantly upregulated in COM (Table 2-3). Abundant sequence fragments of snRNAs were different in length or nucleotides between the control and melanoma samples, except for U2 (Appendix 2-9). Three mt-tRNAs, two tRNA-*ser* and one tRNA-*trp*, were downregulated (Table 2-3). The length distribution of the tRNA fragments clearly showed that fragments with specific lengths were highly abundant in the control samples and significantly less abundant in melanoma samples (Appendix 2-10A), indicating the aberration of tRNA fragments in melanoma. The secondary structures of the tRNAs showed that the fragments were 5′ tRNA half (tRH) or 5′tRF (Appendix 2-10B).

Four C/D box (snoRD27, snoRD39, snoRD79 and snoRD93) and three H/ACA box (snoRA24, snoRA32, and snoRA54) snoRNAs were downregulated in melanoma (Table 2-3). The fragments of these snoRNAs mapped to the 5′ or 3′ end of the full length snoRNAs (Appendix 2-11). Except for snoRA24 and snoRD79, all of them mapped to the same end in the control and melanoma samples (Appendix 2-11).

Two piRNA sequences were annotated by RNAcentral among the rest unannotated reads (see methods). These sequences, which are conserved in mouse, *Drosophila melanogaster*, chicken and *Xenopus tropicalis*, were upregulated in melanoma (Table 2-4).

2.3.2 qRT-PCR validation of U1 snRNA, snoRA24, mt-tRNA, and piR-972 in COM

Expression in COM clinical tissue samples

To confirm the differential expression, the expression of sRNAs, U1 snRNA, snoRA24, mt-tRNA-*ser*(1), and piR-972 was measured by qRT-PCR with custom-made primers. The expression in 12 healthy control and 17 melanoma tissue samples was measured. The expression of snoRA24 and mt-tRNA-*ser*(1) fragments was downregulated in melanoma samples (Figure 2-10A and B) by 2.08-fold (P = 0.0380) and 2.51-fold (P = 0.0043), respectively, compared with the control samples. The relative expression of U1 snRNA was upregulated in melanoma by 5.06-fold ($P < 0.0001$) compared with the control samples (Figure 2-10C). The relative expression of piR-972 was upregulated by 2.76-fold (P = 0.0009) in melanoma compared with control samples (Figure 2-10D).

Expression in canine oral and skin melanoma cell lines

The differentially expressed sRNAs were further investigated in canine melanoma cell lines. Two oral (KMEC and LMEC) and one skin (CMEC1) melanoma cell lines were investigated. KMEC and LMEC were established from a primary site and from a metastatic mandibular lymph node of oral melanoma, respectively. CMEC1 is from primary skin melanoma. Consistent with the melanoma tissue expression results, the snoRA24 and mt-tRNA-*ser*(1) fragments were downregulated in all three cell lines (Figure 2-11A and B). However, the fold difference in snoRA24 (62.67-fold) and mt-tRNA (72.20-fold) expression was significantly higher in LMEC cells than in KMEC cells (snoRA24: 44.85-fold; mt-tRNA: 6.70-fold) and CMEC1 cells (snoRA24: 7.68-fold; mt-tRNA: 43.80-fold), compared with the control samples. Furthermore, piR-972 and U1 snRNA expression were upregulated in all three cell lines, which is consistent with the tissue expression findings (Figure 2-11C and D).

Expression in the plasma

As the expression of snoRA24, mt-tRNA, U1 and piR-972 in the tissue samples and cell lines was consistent, and I further investigated their expression in the plasma. I measured their expression in plasma samples from six healthy controls and seven oral

melanoma patients. Interestingly, consistent with the tissue and cell line expression, snoRA24 and mt-tRNA expression was significantly downregulated in the plasma of melanoma patients (Figure 2-12A and B). However, the expression of piR-972 and U1 was not significantly different between the groups (Figure 2-12C and D).

2.3.3 Expression of snoRA24 and U1 snRNA in human cutaneous melanoma

As dog is considered a natural model of human melanoma, I examined the expression of these sRNAs in human melanoma. I did a Blast search of my custom primer sequences using the ensembl blast search (https://www.ensembl.org) against the human GRCh38 genomic sequence. Among my custom primer sequences, U1 and snoRA24 snRNA were perfectly matched with the human U1 and snoRA24 (Appendix 2-12), suggesting I could measure the human snoRA24 and U1 snRNA expression using my custom sequences. I measured the expression of snoRA24 and U1 snRNA in HEMa-Lp cells and in MEWO cell line using my custom primer sequences. Consistent with the dog melanoma expression, U1 snRNA (2.35-fold, $P = 0.0022$) was upregulated and snoRA24 (3.67-fold, $P = 0.0152$) was downregulated in the MEWO cell line compared with the HEMa-Lp cells (Figure 2-13A and B).

2.4 Discussion

Non-coding RNAs are deregulated during cancer development in human and dog (197,198). In my study, I found that four sRNA species (snoRNA, tRNA, snRNA and piRNA) were differentially expressed in canine oral melanoma, using sRNA sequencing. I confirmed that snoRA24, mt-tRNA-*ser*(1), U1 snRNA, and piR-972 are aberrantly expressed in canine oral and skin melanoma. To the best of my knowledge, this is the first study showing that snRNA, snoRNAs, tRNA fragments and piRNA are aberrantly expressed in canine melanoma. Moreover, there are no reports of aberrant expression of U1 snRNA and snoRA24 in human melanoma.

The expression differences in snoRA24, mt-tRNA-*ser*(1), U1, and piR-972 were consistent between my sequencing and qRT-PCR results. The expression differences in snoRA24 and mt-tRNA-*ser*(1) were consistent among the tissue, cell lines and plasma samples. However, I did not find consistent expression differences in U1 and piR-972 in plasma samples compared with the tissue samples and cell lines. The U1 and piR-972 upregulation may not be up to the physiological threshold that affects the plasma levels.

In snoRNAs, the H/ACA box and the C/D box are associated with pseudouridylation and methylation, respectively. SnoRA24, snoRA54, and snoRA32 modify uridines into pseudouridines in *18S* and or *28S* rRNA (199,200). Pseudouridines provide structural

stability to the modified RNA, which is required for ribosomal biogenesis (201,202). Critically functional pseudouridine positions have been reported (203,204). These findings indicate that snoRNA-guided pseudouridine formation is involved in cancer (205,206). In my study, snoRA24 and snoRA54 were downregulated. Downregulation of snoRA24 has also been reported in human acute myeloblastic, acute and chronic lymphoblastic and peripheral T-cell lymphoma (173,174). Moreover, downregulation of snoRA54 was studied in human breast cancer (175). Among the C/D box snoRNAs, snoRD27 has been reported to be involved in alternative splicing of the cell cycle repressor, transcription factor E2F7 (207). In human uveal melanoma, a negative correlation was found between snoRD93 expression and the methylation level (176). Moreover, snoRD27 and snoRD93 overexpression were demonstrated in myeloma and breast cancer patients, respectively (177,178). These findings indicate that snoRNAs are not only involved in RNA modifications, but they also have disease-specific functions.

In my study, mt-tRNAs were downregulated. Recent studies have shown that tRNA (nuclear and mitochondrial)-derived sRNAs are aberrantly expressed in many cancers including skin cancers (183–187). In human lung cancer, a mt-tRNA-*ser* mutation and downregulation were found (188–190). In breast cancer, $tRNA^{Glu}$, $tRNA^{Asp}$, $tRNA^{Gly}$, and $tRNA^{Tyr}$ induction reduces the stability of several oncogenic transcripts (191). Another

study has shown that three tRNA-derived sRNAs (*ts-53*, *ts-46* and *ts-47*) are downregulated in leukemia and lung cancer and inhibit colony formation in lung cancer cell lines (186). They also showed that certain tRNA-derived sRNAs are strongly downregulated in aggressive late stage breast cancer cell lines. These results are similar to my results showing that mt-tRNA-*ser*(1) is strongly downregulated (72.20-fold) in the metastatic LMEC cell line compared with the control and other cell lines.

In my study, I found that U1, U2, U5 and U11 were upregulated, and I confirmed the U1 expression by qRT-PCR in a human melanoma cell line and in dog melanoma tissue and cell lines. A previous study has shown that U1 overexpression regulates several cancer-related genes and that it has profound effects on mRNA script modulation (208,209). U2 has also been reported as a circulating biomarker of ovarian, colorectal, lymphoma and lung cancers and of melanoma (179–182). SnRNAs are the most important among the splicing regulatory elements. Defective or faulty alternatively spliced pre-mRNA was reported in cancer (210). Alteration in the splicing regulatory elements results tumor associated RNA splicing which was reported in human cancer (210,211). Along with the upregulation of snRNAs I also found the abundant sequence fragments of U1, U5 and U11 are different between control and melanoma. This may indicate unique strategies that produce the snRNA fragments in melanoma that are different from the control group.

Moreover, I found that two piRNA, which is conserved in mouse and other species, were significantly upregulated in melanoma. Recently, Wenhao *et al*. have described the oncogenic properties of piR-1245 (195). Unlike miRNA, piRNA can regulate cancer-related genes by targeting the mRNA and through epigenetics (193,212,213). To my knowledge, this is the first report of piR-972 and piR-1086 in melanoma.

Herein, I identified new classes of aberrantly expressed sRNAs in canine and human melanoma. Recent studies have shown that these sRNAs (snoRNA, Mt-tRNA, snRNA and piRNA) play important roles in cellular processes including differentiation, proliferation, migration, apoptosis, metabolism, and defense. Further detailed studies are necessary to reveal the cellular pathways regulated by sRNAs that are involved in melanoma development.

2.5 Materials and Methods

2.5.1 Tissue and plasma samples (healthy and COM) and melanoma cell lines

Healthy oral tissues (considered as control(128)) and plasma were obtained from dogs from the Kagoshima University experimental animal sheds. COM tissue specimens were obtained from tumors excised from patients. Whole blood was obtained for plasma collection. Informed consent was obtained from the patient's owners. Data characterizing the melanoma patients are presented in Appendix 1-1A. The experimental design and conditions were approved by the Kagoshima University and Veterinary Teaching Hospital and animal care ethics committee.

Tissue samples were collected immediately after surgery, placed in RNA*later* (Invitrogen, Carlsbad, CA, USA) and stored at −80°C after overnight incubation at 4°C. Melanoma was confirmed by the hospital pathologist.

Whole blood was collected in 4.5-mL Terumo Venoject® tubes (Terumo Corporation, Tokyo, Japan) containing 3.2% sodium citrate. The whole blood samples were centrifuged at, 3000 × *g* for 10 min. Then, the plasma samples were transferred to another sterile, DNAse and RNAse-free tube, and centrifuged at 16,000 × *g* at 4°C for 10 min. Supernatants were placed in Eppendorf tubes and stored –80°C.

Three canine melanoma cell lines (KMEC from primary oral melanoma; LMEC from the metastatic mandibular lymph node of oral melanoma and CMEC1 from primary skin melanoma) were stored in freezing medium (CultureSure; Fujifilm Wako Pure Chemical Corporation, Osaka, Japan) in liquid nitrogen. Human epidermal melanocytes (HEMa-Lp) and a human skin melanoma cell line (MEWO) were obtained from Thermo Fisher Scientific (Waltham, MA, USA). The canine melanoma cell lines were cultured as described previously (139). The human cells were cultured according to the supplier's guidelines.

2.5.2 RNA extraction and sequencing

For isolation of total RNA from tissue and cell lines, a mirVana™ RNA Isolation kit (Thermo Fisher Scientific) was used. A mirVana™ PARIS™ Kit (Thermo Fisher Scientific) was used to isolate RNA from 300 µL of plasma according to the manufacturer's protocol. Briefly, recommended volume of homogenate additive (mirVana™) or 2X Denaturing Solution (PARIS™) was added with each sample and mixed by vortexing. Then the solution was incubated in the ice. An equal volume of acid/phenol/chloroform (Ambion) was added to each aliquot, mixed by vortexing for 1 min and centrifuged in a TOMY MX105 mciro-centrifuged according to the guidelines. The

resulting aqueous solutions were separated and mix thoroughly with 1.25 volume of 100% molecular-grade ethanol. Then solutions were passed through a *mir*Vana or PARIS column. The manufacturer's guidelines were followed to wash the column. Finally, total RNA was eluted in 100 µL of elution solution preheated to 95°C. After total RNA isolation, the concentration was measured using a NanoDrop 200c spectrophotometer (Thermo Fisher Scientific). The RNA quality and integrity were assessed with an Agilent 2100 Bioanalyzer (Agilent Technologies, Santa Clara, CA, USA). For tissue samples, the RNA Integrity Number (RIN) mean value was 8.8 (range 7–10), and for cell lines it was 9.9 (range 8.5–10).

After RNA isolation and quality measurement, the tissue total RNA was sent to Hokkaido System Sciences Company (Hokkaido, Japan) for sRNA sequencing. Briefly, 1 µg of total RNA was used for construction of sRNA libraries with the TruSeq Small RNA Library Preparation kit (Illumina, San Diego, CA, USA) following the manufacturer's protocol. 5′ and 3′ adaptors were ligated to the sRNAs (18-30 nt) obtained from the total RNA. cDNA was constructed by reverse transcription. Amplified cDNA was purified by a gel purification system for cluster generation. Illumina Hiseq2500 was used for sequencing.

2.5.3 Bioinformatics analysis of sRNA reads

Sequencing reads were imported to the CLC Genomics Workbench (Qiagen, Hilden, Germany) according to the manufacturer's manual (http://resources.qiagenbioinformatics.com). After normalization, ambiguity and adapter trimming and quality control, reads were analyzed according to the sRNA analysis guidelines of CLC. The miRBase-21.0 (162), Canis_familiris.canfam3.1.ncrna and Homo_sapiens.GRCh37.ncrna databases were used to annotate the reads. Reads annotated by the miRBase were not considered for further analysis. EDGE (empirical analysis of differential gene expression) analysis was used for statistical comparison between groups (163). Reads that were not annotated by the databases were pooled and subjected to EDGE analysis for differential expression. Reads with a significant false discovery ratio (FDR) < 0.05 were searched on the RNAcentral database manually for annotation (https://www.rnacentral.org/).

2.5.4 qRT-PCR

sRNA expression was determined by the custom TaqMan® gene expression assays (Thermo Fisher Scientific). For tissues and cell lines 2 ng, and for plasma equal volume of total RNA (1.25 µL) was reverse transcribed into cDNA using the TaqMan MicroRNA

Reverse Transcription kit (Thermo Fisher Scientific) according to the manufacturer's protocol. TaqMan® First Advanced Master Mix kit and a one-step plus real-time PCR system (Thermo Fisher Scientific) were used for qRT-PCR. The manufacturer's instructions were followed for thermal cycling. Experiments were performed in duplicate. Expression was measured by the $2^{-\Delta\Delta CT}$ method. To measure the relative expression, *RNU6b* was used as a housekeeping gene for tissue and cell line samples, and miR-16 was used as a housekeeping gene for plasma samples. The following custom-made TaqMan® primer sequences were used for the respective sRNA species: 5′-GAAAAAGUACUGCAAGAACU -3′ tRNA fragment, 5′-ACUCGACUGCAUAAUUUGUGGUAGUGGGG-3′ U1 fragment, 5′-UCCGGUGAGCUCUCGCUGGCCC-3′ piRNA and 5′-CUCCAUGUGUCUUUGGGACCUGUCAGCU-3′ snoRNA24.

2.5.5 Statistical analysis

GraphPad prism 7 (www.graphpad.com) was used for statistical analysis. qRT-PCR data were compared using the Mann–Whitney test followed by Tukey's test where appropriate. $P < 0.05$ was considered statistically significant.

Table 2-3. Differentially expressed non-coding RNAs

Small RNA Name	RNA type	FC	FDR
ENSCAFT00000040257.1	U1	16.3016	0.01224
ENSCAFT00000035074.1	U1	14.3686	0.04437
ENSCAFT00000033683.1	U1	7.44548	0.02864
ENSCAFT00000033602.1	U5	6.16182	0.04021
ENSCAFT00000040756.1	U11	4.85008	0.04548
ENSCAFT00000033276.1	U2	6.34498	0.02171
ENSCAFT00000033229.1	U2	7.37383	0.01136
ENSCAFT00000032993.1	U2	8.1348	0.00806
ENSCAFT00000032824.1	U2	9.68805	0.0053
ENSCAFT00000040145.1	U2	8.29074	0.00952
ENSCAFT00000040312.1	U2	10.0209	0.00419
ENSCAFT00000040041.1	U2	10.3585	0.00155
ENSCAFT00000034844.1	Mt tRNA	-14.173	7.2E-09
ENSCAFT00000034825.1	Mt tRNA	-4.0729	0.02088
ENSCAFT00000034831.1	Mt tRNA	-3.6345	0.01574
ENSCAFT00000040199.1	SNORD27	-5.8948	0.02171
ENSCAFT00000040426.1	SNORA54	-4.9391	0.01721
ENSCAFT00000034811.1	SNORA24	-12.925	5.7E-05
ENSCAFT00000040668.1	SNORD79	-3.9816	0.0063
ENSCAFT00000044574.1	SNORD39	-3.1984	0.04021
ENSCAFT00000040903.1	SNORD93	-16.031	5.3E-07
ENSCAFT00000033394.1	SNORA32	-6.4712	0.00164

FC, Fold Change
FDR, False discovery ratio

Table 2-4. piRNAs that are upregulated in melanoma and sequence homology between species

Sequence	Sequence homology	RNA central Id	Genome blast (Dog) E value < 6e-04	FC	FDR
TCCGGTG AGCTCTC GCTGGCC C	piR-mmu-39430051 piR-xtr-1795185	URS000008244F (piRNA-972)	chr2:10124813 to 10124834; chr7:80967838 to 80967859; chr8:41567784 to 41567805; chr20:34173439 to 34173460	28.336	0.007
CGGCGG CGTCCGG TGAGCTC TCGCTGG CC	piR-mmu-29920 piR-dme-5255895 piR-gga-20883 piR-xtr-5660309	URS00001D3FDE (piRNA-1086)	chr2:10124814 to 10124842; chr7:80967839 to 80967867; chr8:41567785 to 41567813;	39.618	0.028

FC, Fold Change
FDR, False discovery ratio

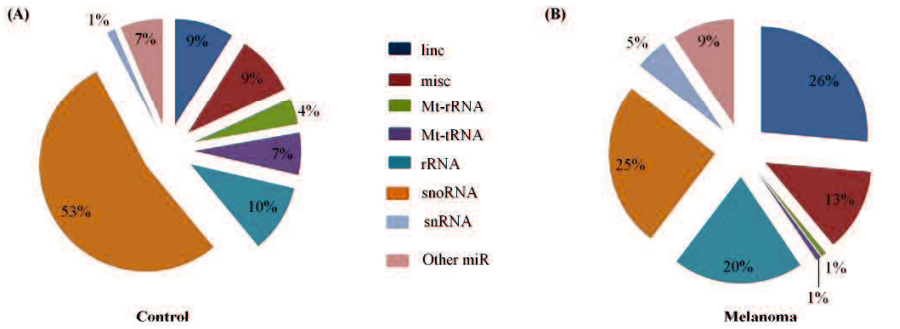

Figure 2-9. Eight RNA species were identified by small RNA sequencing in control and melanoma samples. (A, B) Reads percentage of each small RNA species in the control and melanoma samples are shown by pie plots.

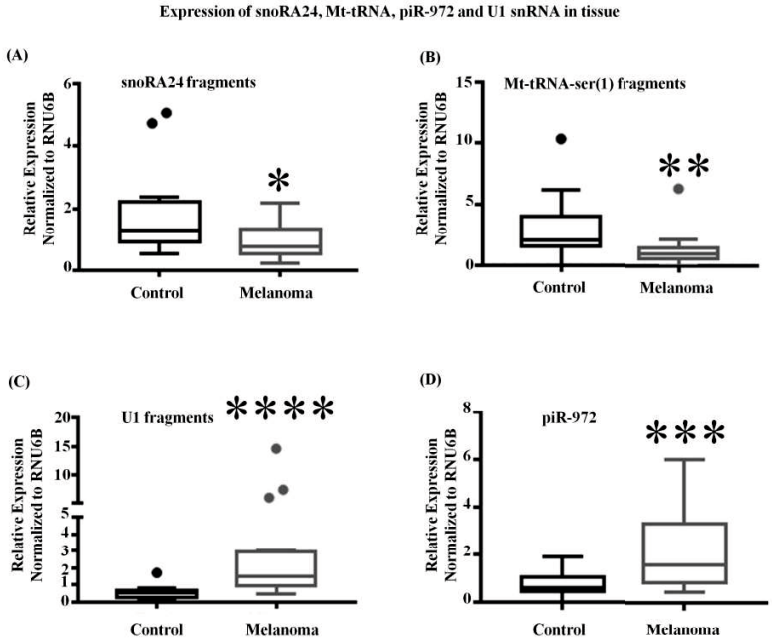

Figure 2-10. Relative expression of snoRA24, mt-tRNA, piR-972 and U1 snRNA in control (n = 12) and canine oral melanoma (n = 17). (A, B) snoRA24 and mt-tRNA were downregulated, and (C, D) U1 snRNA and piR-972 were upregulated. Y-axis represents relative miRNA expression levels in arbitrary units (Mann–Whitney test, *$P < 0.05$, **$P < 0.01$, ***$P < 0.001$, ****$P < 0.0001$)

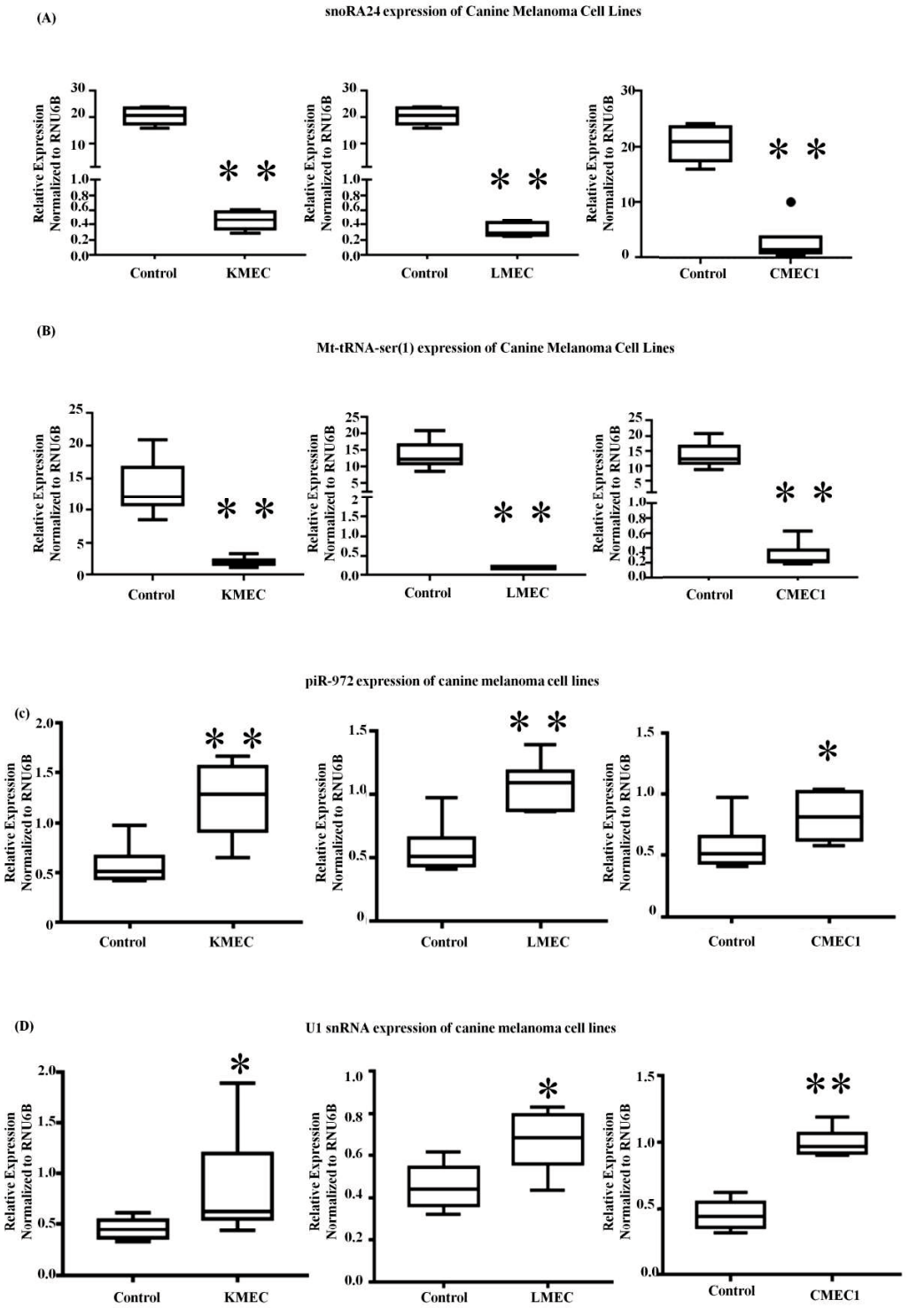
(A)
snoRA24 expression of Canine Melanoma Cell Lines
Relative Expression Normalized to RNU6B
Control
KMEC
LMEC
CMEC1
(B)
Mt-tRNA-ser(1) expression of Canine Melanoma Cell Lines
(c)
piR-972 expression of canine melanoma cell lines
(D)
U1 snRNA expression of canine melanoma cell lines

Figure 2-11. Relative expression of snoRA24, mt-tRNA, piR-972 and U1 snRNA in canine melanoma cell lines. (A, B) snoRA24 and mt-tRNA-*ser*(1) were downregulated, and (C, D) piR-972 and U1 snRNA were upregulated in KMEC, LMEC and CMEC1 cell lines. Y-axis represents relative miRNA expression levels in arbitrary units (Mann–Whitney test, $*P < 0.05$, $**P < 0.01$).

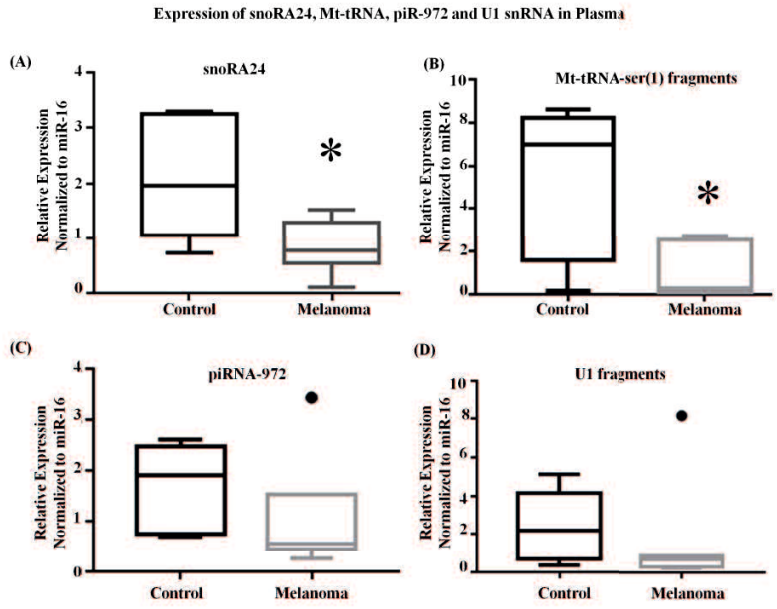

Figure 2-12. Relative expression of snoRA24, mt-tRNA, piR-972 and U1 snRNA in the plasma of canine oral melanoma patients. (A, B) snoRA24 and mt-tRNA were downregulated, however (C, D) piR-972 and U1 snRNA were not significantly changed in the plasma of canine oral melanoma patients. Y-axis represents relative miRNA expression levels in arbitrary units (Mann–Whitney test, $*P < 0.05$).

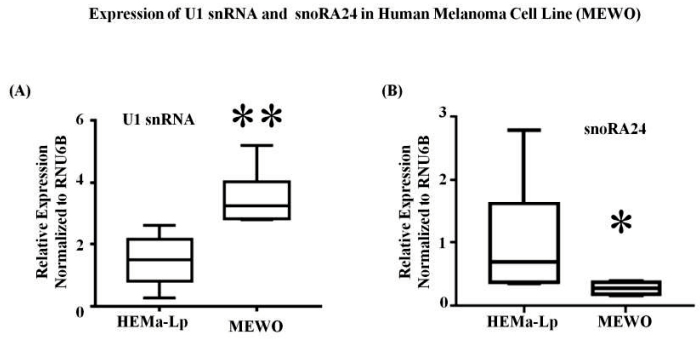

Figure 2-13. U1 snRNA and snoRA24 expression in human melanoma cell lines. (A, B) U1 snRNA was upregulated and snoRA24 was downregulated in a human melanoma cell line (MEWO) compared with an epidermal melanocytes culture (HEMa-Lp). Y-axis represents relative miRNA expression levels in arbitrary units (Mann–Whitney test, $*P < 0.05$, $**P < 0.01$).

Chapter 3

Transcriptome analysis of dog oral melanoma and its oncogenic analogy with human melanoma.

(Rahman, M *et al.*, 2019 *Oncol Rep*. Oct 25)

3.1 Abstract

Dogs have been considered as an excellent immunocompetent model for human melanoma due to the same tumor location and the common clinical and pathological features with human melanoma. However, the differences in the melanoma transcriptome between the two species have not been yet fully determined. Considering the role of oncogenes in melanoma development, in this study, I first characterized the transcriptome in canine oral melanoma and then compared the transcriptome with that of human melanoma. The global transcriptome from 8 canine oral melanoma samples and 3 healthy oral tissues were compared by RNA-Seq followed by RT-qPCR validation. The results revealed 2,555 annotated differentially expressed genes, as well as 364 novel differentially expressed genes. Dog chromosomes 1 and 9 were enriched with downregulated and upregulated genes, respectively. Along with 10 significant transcription site binding motifs; the NF-κB and ATF1 binding motifs were the most significant and 4 significant unknown motifs were identified among the upregulated differentially expressed genes. Moreover, it was found that canine oral melanoma shared >80% significant oncogenes (upregulated genes) with human melanoma, and JAK-STAT was the most common significant pathway between the species. The results identified a 429 gene signature in melanoma, which was up-regulated in both species; these genes may be good candidates for therapeutic

development. Furthermore, this study demonstrates that as regards oncogene expression, human melanoma contains an oncogene group that bears similarities with dog oral melanoma, which supports the use of dogs as a model for the development of novel therapeutics and experimental trials before human application.

3.2 Introduction

"Man's best friend" a phrase always referring to the domestic dog. However, in recent years, their friendship extends to diseases. Important insights in cancer have been obtained by investigating the dog's cancer. Dogs have been suggested as a model for several types of human cancer, including melanoma as a part of a growing field of research known as canine comparative oncology (47,124). Researchers studying human or canine cancers combine their scientific findings to more quickly understand what causes cancer and to develop new and less toxic therapies for people and our beloved pets. Melanoma is the most lethal cancer affecting humans and dogs. According to 'Cancer statistics, 2018' from the American Cancer Society, a total of 9,320 deaths were estimated in 2018, only in the US (113). However, the global incidence of melanoma is more of a concern (214). Cutaneous melanoma is the most common form of melanoma among individuals with fair skin, whereas non-cutaneous melanoma occurs in a greater proportion in populations of other ethnic groups (214,215). Oral melanoma is the most common melanoma type among dogs and accounts for 7% of all malignant tumors in dogs (216). The median progression-free survival of dogs with oral melanoma is <200 days even following excision and DNA vaccination (216,217).

It has recently been reported that human mucosal and canine oral melanoma bear more similar genetic alterations, such as copy number variations (CNVs), single nucleotide variations (SNVs), and mutations or deletions than human cutaneous melanoma (218). More similarities have also been observed in tumor location and histology with the mucosal than the cutaneous type (124,218). Moreover, the genomic classification of cutaneous melanoma has revealed a subtype without mutation that exhibits increased aggressiveness, such as mucosal melanoma (114,119). Due to these similarities between both species, dog oral melanoma has been suggested as a suitable model for both mucosal and triple wild-type human melanoma (119,123,124). Several genetic mutations or loss of function events observed in human melanoma have also been identified in dog oral melanoma, such as $BRAF^{V600E}$ (125), NRAS (Q61) mutation (123), loss function of phosphatase and tensin homolog (PTEN) (123) and c-KIT mutation and/or overexpression (126).

Genomic instability is a hallmark of cancer. Some aberrant genes promote cancer progression, while simultaneously inhibiting normal cellular process, whereas other deregulated genes occur as passenger alterations. The identification of specific cancer-causative genes may be effective for the development of therapeutic strategies against cancer. In this study, I used a novel technique to identify genes that are involved in

melanoma development. I hypothesized that cancer-causing genes include orthologous genes that are altered within the same type of cancer among different species. My hypothesis is an extension of cancer research that has been used for a number of years: Recurrent abnormalities among multiple cases are more likely to be causative factors than non-recurrent events. My view was that recurrently aberrant orthologous genes in the same type of cancer between two related species are the main causative agents for disease progression. I extended my analysis between dogs and humans, which share ancestral DNA and have a similar incidence of melanoma (30,124). This approach can better distinguish melanoma-causing genes from passenger aberrations, which may appear as a miscue in a single species investigation.

Previous reports have suggested dogs as a model for human melanoma. However, the genes and pathways involved in melanoma susceptibility have not yet been studied between species, at least to the best of my knowledge. In this study, I systematically analyzed and compared the canine and human melanoma transcriptome to address two objectives: To identify gene expression similarities between dog and human melanoma, and to examine common functional aspects of genes regulated during melanoma development between the species. I identified common differentially expressed genes (DEGs) between

the two species and revealed causative or active genes involved in the pathogenesis of melanoma, which may further aid in the development of more effective therapeutic approaches for melanoma in both species.

3.3 Results

3.3.1 RNA-seq.

RNA-seq was performed successfully for 11 samples (healthy controls, 3; melanoma, 8). Sequences were submitted to SRA databases (PRJNA527141). All sequence data were 2x100 bp in length with high quality metrics (>36 Phred score). The total number of read pairs ranged from 44 million to 47 million. Approximately 83% (range: 81-84%) of the read pairs were mapped to gene track (Canfam3.1). The percentage of genomic mapping was similar between the control and melanoma samples (means ± SD: 83.743±0.357 and 83.023±0.645%, respectively) (Figure. 3-14A), suggesting that no significant biases were introduced during data generation between the groups (P=0.133). Mapping statistics indicated that the data were of high quality and uniform (no outliers regarding the genome). Principal component analysis of the expressed genes revealed a clear separation of the control group from the melanoma group (Figure. 3-14B). The status of the top 20 expressed genes in the healthy group was compared with the expression in the melanoma group. In total, 11 of the top 20 expressed genes in the healthy group were not observed in the melanoma group (Figure 3-14C). *KRT13* was the most highly expressed gene in the controls and *MT-ATP6* was the most highly expressed gene in the melanoma

group (Appendix 3-13). Known melanoma oncogenes, such as *COL1A1*, *Vimentin,* and *SPARC*, were among the top 10 expressed genes in the melanoma group, while these genes were absent in the healthy group. These results revealed that the data had sufficient sequencing depth and were suitable for further differential expression analysis.

3.3.2 Identification and characterization of DEGs.

To identify DEGs in the melanoma samples, I set up the following stringent criteria: FDR <0.05, FC >2, and maximum group mean >5 (RPKM). This criterion identified 2,555 DEGs (Figure.3-15A), including 1,421 upregulated and 1,134 downregulated genes . The magnitude of the FC was higher in the downregulated group. In addition, 364 DEGs annotated by Ensembl were defined as novel genes, as they did not match species-specific entries in the UniProtKB/Swiss-Prot or RefSeq databases; these genes included 219 upregulated and 145 downregulated genes (Table 3-5 and Appendix 3-14).

I then classified the DEGs based on expression according to a previous study, with slight modifications (219). Genes were defined as very rare (5-15 RPKM), rare (16-99 RPKM), moderately abundant (100-499 RPKM), and abundant (>500 RPKM). The majority of genes were categorized as very rare (44.8%) and rare (45.5%), followed by moderately abundant (7.7%) and abundant (2.0%) (Figure. 3-15B). Similarly, the novel

genes were mostly categorized as very rare (45.32%) and rare (39.56%), followed by moderately abundant (12.91%) and abundant (2.2%) (Figure. 3-15C).

I then examined the 'on-off' genes in melanoma. Genes that were highly expressed (>5 RPKM maximum group mean) in one group with no expression in the other group (<1 RPKM min group mean) and FDR as '0' were defined as 'on-off' genes. I identified 321 'on-off' genes, including 80 'on' (upregulated) genes and 241 'off' (downregulated) genes (Appendix 3-15 and 16). Among the 'on' genes, *BGN*, *CXCL8*, and *PI3* were abundant genes (>500 RPKM), whereas 14 'off' genes, including 3 keratin genes (*KRT13*, *KRT71* and *KRT78*), were abundant. In the novel gene group, I identified 48 'on-off' genes (13 'on' and 35 'off' genes). Two genes were abundant (>500 RPKM) in each group (Appendix 3-17 and 18). The abundant 'on-off' genes are presented in Table 3-6.

To identify which chromosome harbored the majority of the DEGs, I analyzed the chromosomal location of all DEGs. I found that the highest number of upregulated genes (n=104) were on CFA_9 (dog chromosome 9) and the highest number of downregulated genes (n=96) were on CFA_1 (dog chromosome 1) (Figure. 3-15D and E). I also observed that 12 upregulated and 13 downregulated novel genes were located on CFA_9 and CFA_1, respectively (Appendix 3-14). Of note, the highest numbers of 'on' genes (n=8) and 'off' genes (n=26) were on CFA_9 and CFA_1, respectively (Appendix 3-15 and 16). When

sequence reads were mapped against these 2 chromosomes, there were missing peaks or new peaks (peaks were made by the mapped sequence in the region) in each group (Figure. 3-15F and G).

I then performed a functional analysis of the DEGs. Using the PANTHER classification system (220) DEGs produced 1,701 protein hits with 24 protein classes (Appendix 3-19A-B). The most abundant group of genes was in hydrolase (8.70%). Relatively higher percentages of upregulated genes were in the signaling molecule, enzyme modulator, receptor, extracellular matrix protein, defense/immunity protein, and cell adhesion molecule. Immuno-related genes are also investigated by comparing the immune-genes from ImmPort resources (221). I found 174 and 75 immunogenes in the up- and downregulated group, respectively. In both groups, antimicrobial-related immunogens were abundant (Appendix 3-19C). Subsequently, I performed overrepresentation enrichment analysis (ORA) and found chemokines and antimicrobials were 2 significant ($P<0.05$) terms in the upregulated group with the highest enrichment ratio (chemokines, 1.6; antimicrobials, 1.3), respectively. The term chemokines were most enriched in the downregulated group but did not bear statistical significance (data not shown).

3.3.3 GO, pathway and transcription factor analysis

GO analysis. I then analyzed the DEGs by WebGestalt using the GSEA method. GO analysis categorizes DEGs into 3 categories: i) Biological process (BP); ii) cellular component (CC); and iii) molecular function (MF). In total, 18 GO terms were significantly enriched (Figure. 3-16A). Defense response (GO: 0006952), cell-cell signaling (GO: 0007267), extracellular matrix (GO: 0031012), collagen trimer (GO: 0005581), cytokine receptor binding (GO: 0005126) and cytokine activity (GO: 0005125) were the top enriched terms in each category. Other significant GO terms (gliogenesis, taxis, immune response, growth factor activity, glycosaminoglycan binding, G-protein coupled receptor binding) related to the altered physiology during melanoma progression. Among the 18 significant GO terms, 9 were directly related to cytokines. Taken together, the GO results indicate that most DEGs are involved in cytokine-oriented functions.

Pathway analysis. I performed pathway analysis by 2 methods: GAGE and GSEA. In total, 9 common pathways were significantly enriched in both methods (Figure. 3-16B). To rank the pathways, the position of each analysis was taken and the average was examined. Cytokine-cytokine receptor interaction (CFA04060), focal adhesion (CFA04510) and ECM-receptor interaction (CFA04512) were the top 3 pathways. PI3K-

AKT (CFA04151) and TNF (CFA04668) signaling pathways were also present in my analysis.

Enriched transcription factor motif. To examine motifs up to 4 kb around the transcription start sites of the DEGs, I used GSEA within WebGestalt. In total, 10 transcription site binding motifs were significantly enriched in the upregulated DEGs (Figure. 3-16C). Among these 10, 6 were known and 4 were unknown motifs that do not match any known transcription factor binding site from the database (v7.4 TRANSFAC). The binding motifs for ATF1 and NF-κB were observed in the highest number of upregulated DEGs.

3.3.4 Cross species analysis of human and dog melanoma.

I analyzed 2 human melanoma RNA-seq from GEO datasets (please see Materials and methods). To evaluate the pattern of FC of the dog DEGs in human melanoma, I converted the genes to the human orthologues and compared the FC with the human melanoma study without considering statistical significance. The analysis of the human melanoma tissue results revealed that 63% of the upregulated genes and 40% of the downregulated genes had the same direction of FC between the species (Figure. 3-17A). In the case of human melanoma cell lines, I observed 58 and 47% similarities in FC, respectively (Appendix 3-20A). Of note, when I compared the statistically significant genes

between the species (FDR <0.05, FC ≥2; common DEGs), the percentage of shared upregulated genes increased (tissue, 88%; cell line, 62%) in both experiments (Figure. 3-17B and Appendix 3-20B, and Appendix 3-21-22). These findings indicate a marked overlap in upregulated genes or oncogenes between human and dog melanoma.

To further understand the association between human and dog tissue melanoma, I performed hierarchical clustering analysis. Common DEGs between the 2 melanoma (human and dog) tissue experiments were selected and expression values were considered from all other experiments for clustering. Clustering analysis of dog and human melanoma tissues, cell line and prostate cancer revealed that dog melanoma clustered together with a subset of human tissue melanoma samples (Figure. 3-17C). These results indicate the closer transcriptomic similarities between dog and human melanoma compared with other types of cancer. Prostate cancer data were included to indicate the dissimilarities in different types of cancer between the species.

I found that 429 upregulated melanoma signature genes, including 105 genes commonly upregulated in all 3 melanoma sets, 284 genes upregulated in human and dogs tissue melanoma, and 40 genes upregulated in cell line and dog melanoma, were the main causative driver genes for melanoma development (Appendix 3-23). Approximately half (41, 51%) of the on genes identified in dog melanoma samples were present in this group.

To examine the processes of melanoma development in the 2 species, I performed GSEA of common DEGs from 3 experiments. In total 10 pathways had an FDR <0.06 and 3 had a normalized enrichment score >2 (Figure. 3-17D). The top 3 pathways were immune and signaling related pathways. The leading edge genes of these pathways were also deregulated in a similar pattern in both species (Figure. 3-17D, lower panel).

I established a network from common DEGs by STRING and performed analysis by MCODE in Cytoscape. Twelve cluster networks were obtained (Figure. 3-17E). The majority of the genes of the first 3 networks encode signaling peptides. Genes in the first network are collagen and integrin genes (Figure. 3-17F; upper left panel). The second and third cluster genes are genes encoding cytokines-chemokines and growth factors (Figure. 3-17F; upper right and lower panels). As the FC of genes in the network was the same between the species, this indicated that these genes might exhibit similar melanoma promoting networking function between the species.

3.3.5 Validation of DEGs by RT-qPCR.

To confirm the result of RNA-seq I validated several genes by RT-qPCR. I confirmed that *COL7A1*, *AKT3*, *ERRFI1*, *IKBKB*, *NGF*, *IL6*, *MMP9*, and *EGFR* genes were

differentially expressed in dog melanoma (Figure. 3-17G). Similar fold changes of the genes were observed between RNA-seq and RT-qPCR.

3.4 Discussion

To the best of my knowledge, this is the first report of comprehensive RNA-seq in canine oral malignant melanoma. A previous study performed RNA-seq on canine cutaneous melanoma (155). Oral melanoma is the most frequent site for malignant melanoma compared with the cutaneous type (123,222). In addition, previous studies have demonstrated that oral melanoma in dogs can be used as a model for human melanoma (119,123,124).

The results of this study revealed that *COL1A1*, *SPARC*, and *VIM* were the top highly expressed DEGs in canine oral malignant melanoma. These genes have also been well studied in human melanoma or other types of cancer for their oncogenic behavior (223–226). In comparison, *KRT13*, *KRT71* and *S100A8* were not expressed in the melanoma group. In a study on human squamous cell carcinomas of the head and neck and esophagus, *KRT13* was found to be epigenetically silenced, while the chromosomal location of the *S100A8* gene was found to be frequently altered or deleted and downregulated (227,228). However, genes that are expressed in either of the group bear more significance than those with less magnitude of change. These genes bear more importance for biomarkers or therapeutic studies. I thus found the 80 genes that were expressed only in canine malignant melanoma (>5 RPKM maximum group mean)

compared with healthy tissue (<1 RPKM min group mean), with the aim of identifying genes that were turned on during melanoma progression. Using this criterion, *BGN*, *CXCL8*, and *PI3* were identified as 3 abundant genes in canine malignant melanoma. Only *CXCL8* was previously investigated in dogs to be increased in hemangiosarcoma (229). *BGN*, *CXCL8*, and *PI3* have previously been studied in human melanoma and other types of cancer (230–232). The abundant genes are only approximately 2% of the total DEGs. As highly expressed genes (abundant) are transcribed upon the essential demands of cells, their exact association with and involvement in melanoma progression warrants further investigation.

Cytogenic analysis of the DEGs revealed that CFA_1 harbored the majority of the 'off' genes or downregulated genes. Loss of alleles or abnormalities in HSA_1 (human chromosome 1) in human malignant melanoma was previously reported (233,234). This suggests that chromosome 1 is important in melanoma and the function in melanoma suppression is conserved in both species. I examined the distribution of DEGs in 24 protein classes and found the highest number of genes within the hydrolase category (220 genes). Most of the hydrolases were proteases (135 genes). Proteases are involved in regulatory signaling networks with kinases or other factors can function to transmit oncogenic signals in the tumor micro-environment. The Protein classification of these DEGs provides an

important foundation for further understanding of the pathogenesis of melanoma. Melanoma is one of the most immunogenic cancers. The immunogenic landscape of canine oral melanoma DEGs revealed the enrichment of chemokines and antimicrobials genes. Previous studies have proven that chemokines play specific roles in human melanoma tumor growth and metastasis (235,236). Chemokine-based therapy is also under continuous investigation (237). Moreover, antimicrobial immunogenes may enrich as a first line defense of the cancer cells, although many of them can regulate chemokines and other immunogenic signals.

GO analysis revealed that the majority of proteins encoded by DEGs were distributed in the extracellular domain or cytoplasm. I hypothesized that these proteins drive cells to undergo several physiological processes to generate the oncogenic microenvironment. In this study, different responses, cytokine and signaling process-related genes were enriched and were involved in G-protein, growth factor, glycosaminoglycan, and cytokine-related activity. G-protein-coupled receptors are key players in the regulation of various pathophysiological responses to initiate cancer development, including melanoma. GPCR-targeted drugs have exhibited excellent therapeutic benefits in human cancers (238). Another significant term, growth factor activity involved in cancer, was first discovered in the 1950s by Cohen *et al*. (239). Subsequent studies demonstrated various

roles of growth factors in the tumor microenvironment including in melanoma (240). Glycosaminoglycans and the conjugated proteins were reported to be involved in the tumor micro-environment and often perform crucial functions along with cytokine and growth factors (241).

In this study, I identified 9 pathways enriched in the DEGs using 2 methods to avoid possible bias. ECM receptor interaction, focal adhesion, protein digestion, and absorption, and cytokine receptor interaction were the most enriched pathways and along with 3 PI3K-AKT signaling pathways were previously reported to be involved in canine cutaneous melanoma (155). Pathway analysis has been useful for the analysis of experimental high-throughput biological data to facilitate data interpretation. For example, *IKKβ*, one of the major positive regulators of the NF-κB transcription factor, was found to be downregulated in canine oral melanoma (Appendix 3-24). However, several target genes of NF-κB were upregulated, indicating that NF-κB was activated. I also examined the transcription factors binding motifs that may represent the transcription factors of upregulated genes and found that the NF-κB binding motif was the most enriched. This suggests that NF-κB genes are activated through NF-κB-independent mechanisms or that NF-κB is activated through IKK*β*-independent mechanisms. However, when I analyzed the pathways for the commonly deregulated genes between humans and dogs, I found that

JAK-STAT was the most enriched pathway. Among the target genes of NF-κB, *STAT3*, *NF-κB1* and *RELA* share the highest number of genes (http://www.grnpedia.org/trrust/result.php?gene=STAT3&species=human&confirm=). This indicates that these target genes can be transactivated by either NF-κB or STAT3, or both factors. In this study, I found that 39 targets were upregulated in the dog melanoma data and 21 were significant. In the human data, among the 21 orthologues, 17 were upregulated (Appendix 3-25). These data again suggested that one or both of the transcription factors may be activated. As *IKKβ* was downregulated, I hypothesized that the canonical pathway was not activated in dogs. The target genes can be transcribed by either non-canonical or atypical pathways of NF-κB or by STAT3. A previous study also demonstrated that feedback loops exist between both signaling pathways. IL6, as one of the targets of NF-κB, can be regulated by STAT3 activation (242). IL6 was expressed in both human and dog melanoma. One study demonstrated that the pro-survival function of NF-κB was related to its functional interaction with the PI3K/AKT/mTOR signaling pathway. AKT engages mainly with IKKα instead of IKKβ in promoting NF-κB activation (243). NGF can activate NF-κB by the atypical pathway (244). Phosphorylation mediates the activation of STAT3 through TrkA by NGF (245). Therefore, IL6 may be a crucial regulator in melanoma initiation by regulating the STAT3/NF-κB loop, while the atypical NF-kB pathway is

maintained in dogs by NGF. Further studies are required to examine the potential for IL6 and NGF as novel therapeutic targets in melanoma for both species. RT-qPCR analysis confirmed the upregulation of *NGF*, *AKT*, and *IL6* and *IKKβ* downregulation in canine melanoma tissue samples.

Several studies have demonstrated clinicopathological and molecular similarities in melanoma between dogs and humans (119,123,246). However, to the best of my knowledge, no study to date has revealed the oncogenic transcriptomic similarities of melanoma between these species. In this study, I evaluated the common DEGs between the species. Among the upregulated genes in dog melanoma, 88 and 62% orthologous genes were also upregulated in human melanoma tissue and cell lines, respectively. In addition, among the 429 upregulated melanoma signature genes, 48 were previously reported in melanoma according to the Melanoma Gene Database (MGDB) (247) (Appendix 3-23). This result indicates that oncogenic functions of these genes for melanoma progression are conserved between the two species. Previous studies have also demonstrated that higher homology of known cancer genes, as well as mutation or inactivation events in cancer or other diseases are shared between these 2 species (123,248,249). The findings of this study further support the similarities in melanoma progression between dogs and humans. Several subtypes of melanoma have been identified in humans (114). Canine oral melanoma has

been suggested as a model for human mucosal and the triple wild-type subtype (119,123). The cluster analysis of this study with melanoma and prostate cancer revealed that dog melanoma clustered with a group of human tissue melanoma. These results again affirm previous studies that a human melanoma subtype is similar to dog melanoma. This study also demonstrates that the dog model will be more efficient to investigate or develop novel therapeutics compared with cell lines.

I also created a protein network using a human database. I speculated that deregulated proteins/genes in melanoma interact to drive disease progression. Functional association in melanoma has been found from the protein interaction network (250). In this study, each network cluster contained genes that perform similar functions, such as the first cluster that mostly contained collagen and integrins mainly involved with extracellular matrix-related functions. My results suggest that the same network exists in both species, as the genes show the same trend of expression in melanoma. The roles of collagen and integrins in cancer have been well studied (251,252). Potential therapeutic targets can be attained from this type of interaction network strategy, which is also reported by a previous study (250).

In conclusion, this study successfully identified the transcriptomic aberrations in canine oral melanoma. My evidence demonstrating the similarity of melanoma between the

2 species further emphasizes dogs as a suitable pre-clinical model for human melanoma. By comparing the melanoma transcriptome between the 2 species, I identified the key genes and molecular pathways for further study to develop more effective therapeutic approaches to melanoma.

3.5 Materials and methods

3.5.1 Tissue samples.

Canine oral melanoma tissue samples (n=17) were obtained following surgical resection (as a primary treatment for the melanoma patient) at the Kagoshima University veterinary teaching hospital. The patient's owners were informed prior to sample collection. The confirmed diagnosis was affirmed by the hospital. Tissue samples were maintained immediately in RNA*later*™ (Invitrogen; Thermo Fisher Scientific) following isolation and incubated overnight at 4ºC and then stored at -80ºC until further RNA extraction. Detailed information of the 17 samples is listed in Appendix 1-1A. Control oral tissues were obtained following surgical resection from healthy dogs (n=12) during routine anatomical practical training classes from the Kagoshima University shed. The site (oral melanoma or healthy oral tissue) and general surgical procedure for sample collection were the same between the healthy dogs and those with melanoma. Anesthesia was performed and maintained accordingly during the surgical procedure [pre-administration: Atropine sulfate 20 µg/kg (i.v.), Robenacoxib 2 mg/kg (i.v.); induction: Propofol ~5 mg/kg (i.v.); Maintenance: Sevoflurane 0.5-5% (inhalation)]. The anesthesia regimen was according to the American Animal Hospital Association (AAHA) guidelines (253). Palpebral and jaw

reflexes were used to confirm that the animals were fully anesthetized. Other monitoring parameters, such as temperature, heart and respiratory rate, blood pressure, oxygen saturation, end-tidal CO_2, etc. were continuously checked during this period. Animals were not euthanized as part of the current study. The study design and experimental protocols were approved by the university and the Kagoshima University veterinary teaching hospital ethics committee (KV0004).

3.5.2 RNA extraction and sequencing.

The *mir*Vana™ miRNA isolation kit (Thermo Fisher Scientific lnc.) was used to isolate total RNA from the tissues according to the manufacturer's protocol. RNA concentration was measured using a NanoDrop 2000c Spectrophotometer (Thermo Fisher Scientific lnc.). RNA quality and integrity was assessed using the Agilent 2100 Bioanalyzer (Agilent Technologies). The RNA integrity number (RIN) mean value for the tissue was 8.8 (range 7-10).

Following RNA isolation and quality assurance, small RNA libraries were prepared and sequenced by Hokkaido System Science Co., Ltd. The TruSeq RNA Sample Prep kit version 2 (Illumina) was used for library preparation. The low sample protocol was followed and input total RNA was 0.5 µg. Briefly, PolyA-containing mRNA was purified

using oligo-dT-attached magnetic beads. mRNA was fragmented into small sections following purification under an elevated temperature (94°C) using divalent cations. Fragmented mRNAs were copied into first-strand cDNA using reverse transcriptase with random primers. Second-strand cDNA synthesis was followed by DNA polymerase I and RNase H treatment. cDNA fragments underwent end repair process, a single addition of 'A' base and then ligation of adapters. The final cDNA library was created through purification and enrichment with PCR process.

3.5.3 Bioinformatics analysis.

For bioinformatics analysis, the below procedures and analyses were performed.

Reads processing and differential expression analysis. I received high quality reads from the sequencing facilities average Phred score >36. Sequencing data were imported into the CLC Bio Genomics Workbench (CLC Bio; Qiagen) as recommended by the manufacturer's manual (http://resources.qiagenbioinformatics.com). The normalization of reads, quality, ambiguity and adapter trimming or quality control was performed with the CLC Bio Genomics Workbench (versions 9 and 10). Paired end reads (100 bp) were further analyzed according to the RNA-seq analysis guide of the CLC Genomics Workbench. Default parameters were used during mapping and all other subsequent analyses. Briefly, during reads mapping to a genome, genome annotated with genes and transcripts were

selected and a mRNA track, gene track and a genome track Canis familiris.canfam3.1 were used (254). Reference sequences were downloaded using the workbench downloading option. During counting, the reads for expression values and the intact pairs were counted, while the broken pairs were ignored. The expression value was calculated in total counts, unique counts, transcripts per million, and reads per kilobase of exon model per million mapped reads (RPKM) (94). Differential Expression for the RNA-Seq tool was used to perform the statistical differential expression test. This tool followed a multi-factorial statistics based on a negative binomial Generalized Linear Model. The Wald test was used for comparison between the groups. I set the criteria for differential expression genes as false discovery rate (FDR) <0.05, fold change (FC) >2 (both upregulated and downregulated), and maximum group mean >5 (RPKM).

Cross species analysis of DEGs. I downloaded 3 RNA-seq datasets from the GEO database: GSE71747 for the human melanoma tissue, GSE88741 for the human melanoma cell line and GSE29155 for human prostate cancer. The datasets included for the cross-species analysis are illustrated in Appendix 3-26. Data were downloaded directly to the genomic workbench and the above-mentioned procedures and criteria were followed to analyze the reads. Human ortholog genes were collected by the BioMart tool within

Ensembl (255). Comparisons were drawn regarding the FC and with or without statistical significance of the ortholog genes between the species.

Gene ontology (GO), pathways and transcription factor analysis. GO and transcription factor analysis was performed by the WebGestalt (WEB-based GEne SeT AnaLysis Toolkit) (256) following the gene set enrichment analysis (GSEA) method. For pathway analysis, I blended 2 methods from WebGestalt and Pathview (257). I performed GSEA using the WebGestalt and Generally Applicable Gene-Set Enrichment (GAGE) by Pathview according to their default settings. Finally significant (q value or FDR <0.05) pathways from the two methods were selected.

Network analysis. Common DEGs were uploaded to STRING (https://string-db.org/) to obtain the protein interaction network (169). The parameter for the confidence score was set to 7. Cytoscape 3.5.1 (https://cytoscape.org/) was used to analyze the network (168). Closed networks were considered during network construction both in STRING and Cytoscape. MCODE algorithm was used within the Cytoscape application for cluster network analysis.

3.5.4 RT-qPCR.

Total RNA (250 ng) was reverse transcribed into cDNA using the ReverTra Ace® qPCR RT Master Mix with gDNA Remover (Toyobo). RT-qPCR was performed using a

TaqMan® Fast Advanced Master Mix kit (Thermo Fisher Scientific Inc.) and a StepOne Plus™ Real Time PCR system (Applied Biosystems; Thermo Fisher Scientific Inc.). Optimal reagent concentration and reaction condition described in the manufacturer's instructions were followed. The thermocycling conditions used for qPCR were as follows: 50°C for 2 min, 95°C for 20 sec; followed by 40 cycles of denaturation at 95°C for 1 sec and annealing/extension at 60°C for 20 sec. The $2^{-\Delta\Delta Cq}$ method was used to determine gene expression levels (258). RT-qPCR reactions of undetermined Cq were assigned Cq=36 cycle. GAPDH was used as a quantitative normalization reference. Primer sequences of the TaqMan Gene Expression assays are available in the following IDs: Glyceraldehyde 3-phosphate dehydrogenase (GAPDH; Cf04419463), collagen type VII alpha 1 chain (COL7A1; Cf02690281), AKT serine/threonine kinase 3 (AKT3; Cf02704523), ERBB receptor feedback inhibitor 1 (ERRFI1; Cf02653684), inhibitor of nuclear factor kappa B kinase subunit beta (IKBKB; Cf02695869), nerve growth factor (NGF; Cf02697134), epidermal growth factor receptor (EGFR; CF02626541), matrix metalloproteinase 9 (MMP9; CF02621845) and interleukin (IL)6 (Cf02624282).

3.5.5 *Statistical analysis*.

GraphPad Prism 7 (www.graphpad.com) was used for statistical analysis. Hierarchical clustering analysis was performed on $\log_{10}$ ratio with every gene expression

from each sample. Hierarchical clustering was done with Euclidean distance metrics and complete linkage algorithm. Comparisons between the group (healthy, n=12; melanoma, n=17) of the RT-qPCR data were performed using the Mann-Whitney U-test. A P-value <0.05 was considered to indicate a statistically significant difference.

Table 3-5. Top 20 novel differentially expressed genes in canine oral melanoma.

Ensembl ID	Chromosome	Region	Max group mean	Log_2 fold change	FDR P-value
ENSCAFG00000023728	17	61715810..61716667	6965.176802	-13.0728668	0
ENSCAFG00000029470	7	Complement (43565980..43569673)	4441.530653	-6.317147271	8.66135E-15
ENSCAFG00000018586	4	67701614..67703002	1576.83413	-1.476555989	0.044341327
ENSCAFG00000032057	26	27624214..27624534	1030.146501	6.625580707	3.22992E-14
ENSCAFG00000031806	26	27626671..27632004	645.9357198	7.033040174	0
ENSCAFG00000030258	8	Complement (72906321..73387840)	585.378127	7.09342349	0
ENSCAFG00000017655	30	Complement (35713470..35737559)	554.1272685	1.5182161	0.02925338
ENSCAFG00000000471	12	742518..744376	502.6434471	-14.74161241	0
ENSCAFG00000031786	26	27605067..27616302	497.5464419	7.498002132	0
ENSCAFG00000015206	21	40680858..40685074	476.1739252	7.802839134	0

ENSCAFG00000030164	X	Complement (82986436..82986741)	473.8678307	-1.319491428	0.025365105
ENSCAFG00000019812	6	Complement (42202578..42207944)	360.4657394	-2.977400921	4.13027E-06
ENSCAFG00000023111	17	Complement (60984425..60987378)	354.3255735	-1.423676	0.00159774
ENSCAFG00000016966	30	27636259..27664073	309.6540468	2.174448832	0.018722413
ENSCAFG00000032259	9	Complement (37617977..37622560)	298.0600534	-8.627843471	0
ENSCAFG00000019141	X	Complement (119204969..119205259)	277.0573496	-1.266862717	0.016078337
ENSCAFG00000032358	8	Complement (72847361..72852219)	268.1075815	5.707864264	5.27351E-11
ENSCAFG00000029493	26	27620223..27620543	264.9025566	6.875187743	1.58428E-08
ENSCAFG00000014627	3	60899870..60901258	261.1790712	8.044118048	1.11703E-08
ENSCAFG00000012022	17	59698670..59701290	254.5146118	-4.447052200	8.66135E-15

FDR, false discovery rate.

Table 3-6. Abundant 'on-off' genes in canine oral melanoma.

Name	Chromosome	Max group mean	Log_2 fold change	FDR P-value
BGN	X	750.6354384	5.44424503	0
CXCL8	13	718.7157383	8.318634019	0
PI3	24	625.5995841	8.475895656	0
KRT13	9	19890.23609	-11.27810332	0
KRT71	27	7541.688327	-15.13319019	0
S100A8	7	5616.157022	-6.39785469	0
ARSF	X	1426.603766	-12.19831506	0
TGM3	24	1376.03872	-15.43829609	0
AQP3	11	1324.472821	-11.7832697	0
S100A14	7	1165.913739	-9.555767692	0
SPRR3	17	1090.426813	-13.23899417	0
S100A2	7	1023.838115	-8.469980831	0
SFN	2	769.2134926	-8.549424168	0
RHCG	3	723.8378326	-12.84073049	0
SPINK5	2	646.388121	-11.37480897	0
S100A16	7	549.0286762	-6.490015324	0
KRT78	27	508.5240706	-11.77812871	0
ENSCAFG00000031806	26	645.936	7.03304	0
ENSCAFG00000030258	8	585.378	7.09342	0
ENSCAFG00000023728	17	6965.18	-13.073	0
ENSCAFG00000000471	12	502.643	-14.742	0

FDR, false discovery rate.

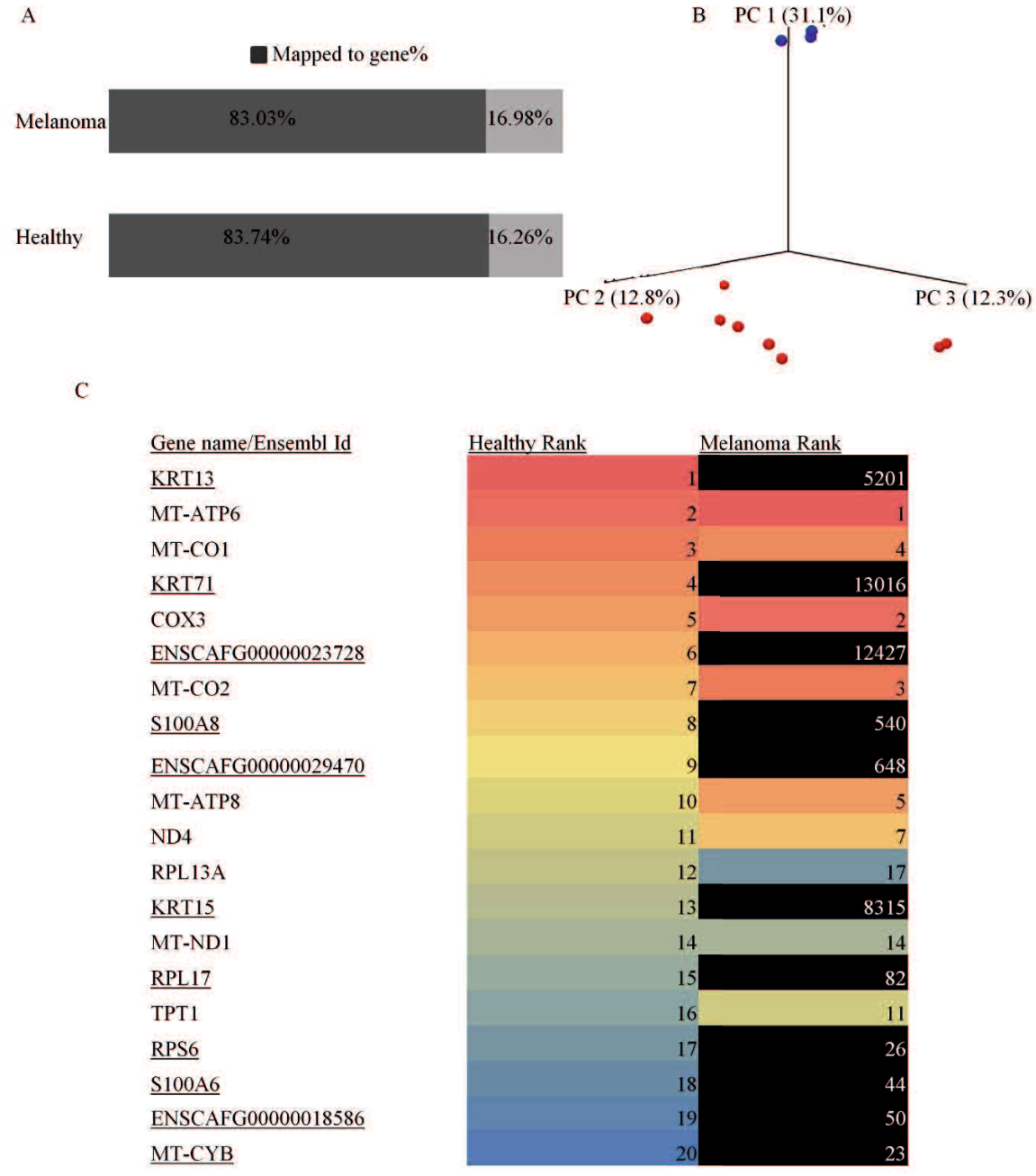

Figure 3-14. Reads characterization of RNA-seq from canine oral melanoma. (A) Mapped percentage of the reads against the reference genome. Percentages of the mapped reads were estimated with the average percentage of mapped reads from each group. Healthy,

n=3; melanoma; n=8. (B) Principal component analysis of variance from transformed RNA seq reads counts for whole transcriptome by CLC Workbench. Axis indicates the variance contribution. Blue is for healthy and red is for melanoma samples. (C) Comparison of top twenty expressed genes in healthy (n=3) and melanoma (n=8) group. Number and color gradient (red to blue) were used to indicate highest to lowest ranking. Uncommon genes between the groups are underlined and positions are marked black color in melanoma. PC, principal component.

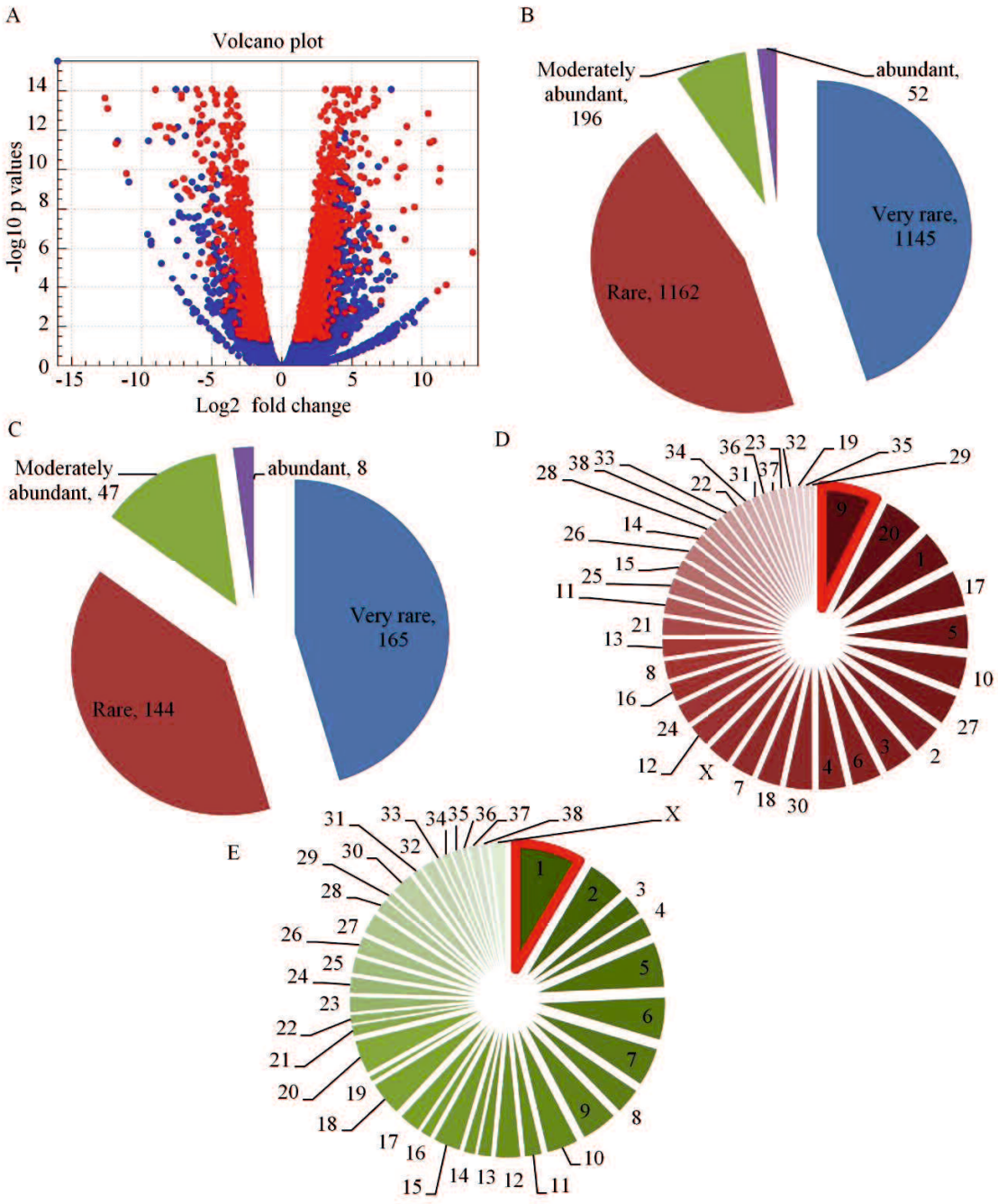
A
Volcano plot
-log10 p values
Log2 fold change
B
Moderately abundant, 196
abundant, 52
Very rare, 1145
Rare, 1162
C
Moderately abundant, 47
abundant, 8
Very rare, 165
Rare, 144
D
E

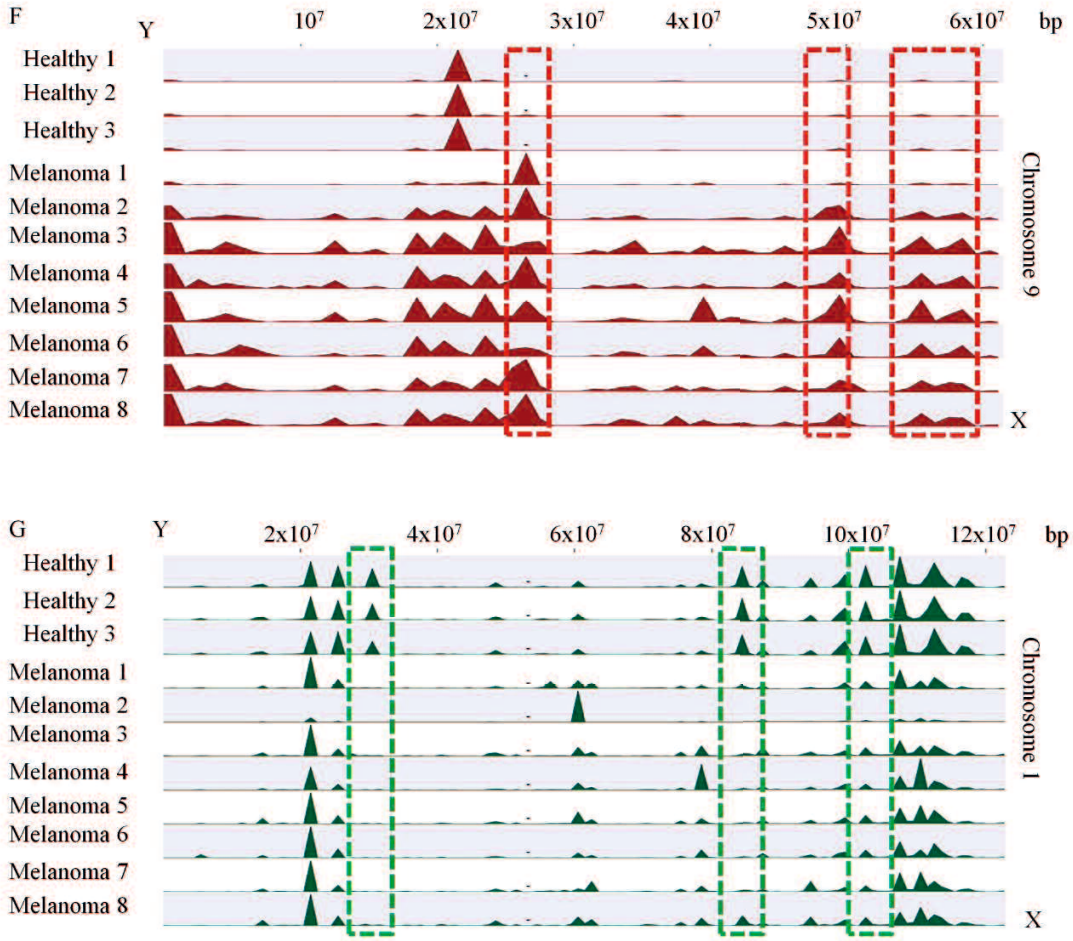

Figure 3-15. Differentially expressed genes from RNA-seq and their chromosomal location. (A) Volcano plot representing the differential expression of genes from RNA-seq. Each dot indicates one gene. A red dot indicates significant genes according to my stringent criterion, (FC) >2 and maximum group mean >5 (RPKM). The x-axis indicates the Log2 fold change of the genes comparing healthy and melanoma group; the y-axis indicates the -Log_{10} false discovery rate (FDR). (B and C) Overall expression abundance of known and novel differentially expressed genes respectively. Numbers indicate the number of genes in each category: Very rare (5-15 RPKM), rare (16-99 RPKM), moderately abundant (100-499 RPKM) and abundant (>500 RPKM). (D and E) Chromosomal locations of differentially expressed genes. Numbers indicate the corresponding chromosome identity.

The chromosome with the highest number of differentially expressed genes is indicated by the red border; (D) upregulated and (E) downregulated genes in the chromosomal locations. (F and G) Reads mapped from each individual sample to the CFA_1 and CFA_9 regions from RNA-seq. Dotted lines indicated the mapped sequence variation of every sample between the groups. The X is the length of the chromosome and Y is the mapped sequences of each sample.

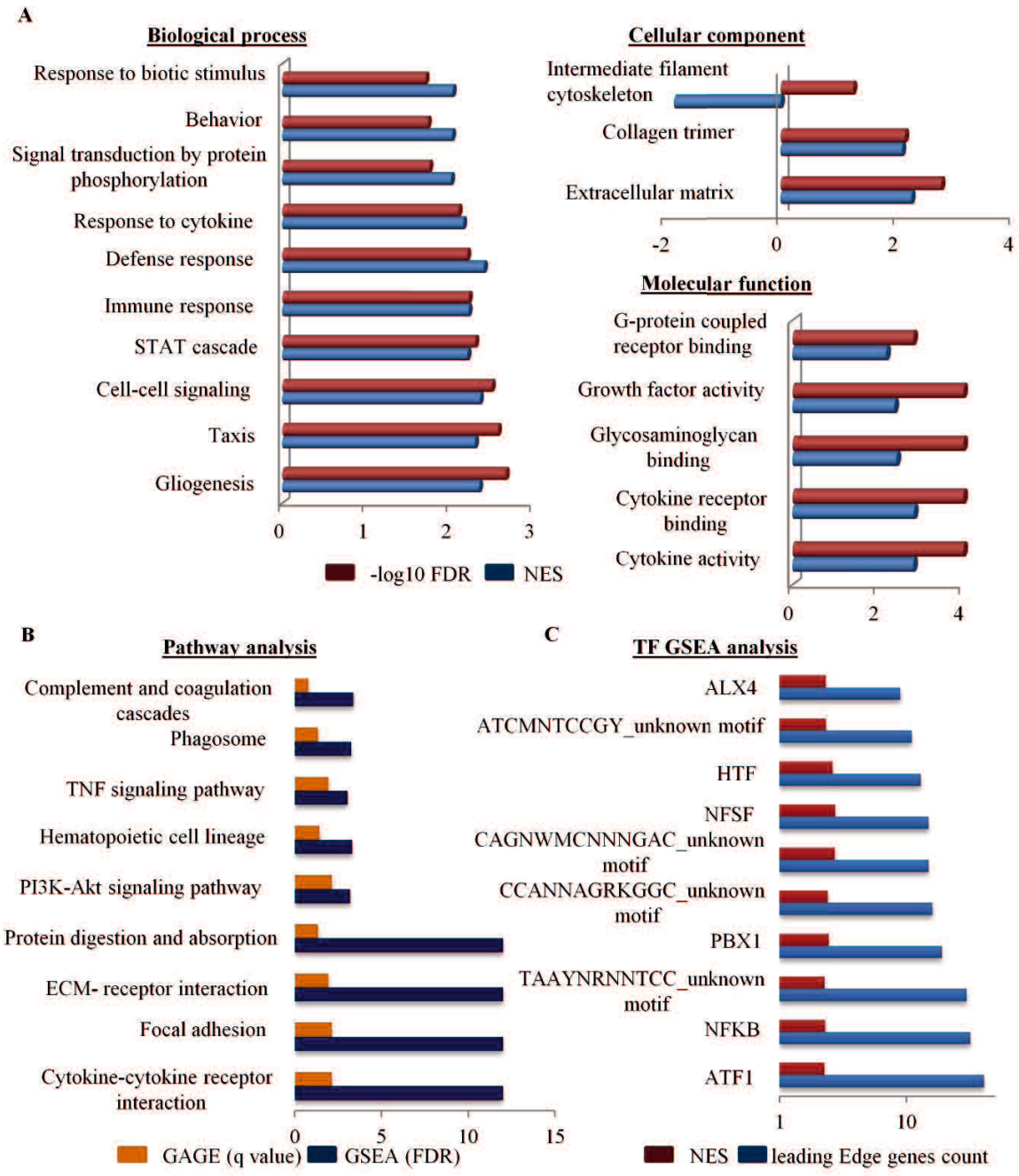
A
Biological process
Response to biotic stimulus
Behavior
Signal transduction by protein phosphorylation
Response to cytokine
Defense response
Immune response
STAT cascade
Cell-cell signaling
Taxis
Gliogenesis
0
1
2
3
-log10 FDR
NES
Cellular component
Intermediate filament cytoskeleton
Collagen trimer
Extracellular matrix
-2
0
2
4
Molecular function
G-protein coupled receptor binding
Growth factor activity
Glycosaminoglycan binding
Cytokine receptor binding
Cytokine activity
0
2
4
B
Pathway analysis
Complement and coagulation cascades
Phagosome
TNF signaling pathway
Hematopoietic cell lineage
PI3K-Akt signaling pathway
Protein digestion and absorption
ECM- receptor interaction
Focal adhesion
Cytokine-cytokine receptor interaction
0
5
10
15
GAGE (q value)
GSEA (FDR)
C
TF GSEA analysis
ALX4
ATCMNTCCGY_unknown motif
HTF
NFSF
CAGNWMCNNNGAC_unknown motif
CCANNAGRKGGC_unknown motif
PBX1
TAAYNRNNTCC_unknown motif
NFKB
ATF1
1
10
NES
leading Edge genes count

Figure 3-16. Gene Ontology, pathway and transcription factor (TF) analysis of the differentially expressed genes. (A) Gene Ontology analysis of significant terms in biological process (BP), cellular component (CC) and molecular function (MF). Blue bars indicate the normalized enrichment score (NES); red bars indicate the -log false discovery rate (FDR). (B) Pathways that were significant between two methods are shown. The x-axes represent the -log value of generally applicable gene set enrichment (GAGE) q value and gene set enrichment analysis (GSEA) FDR. (C) Enriched TFs are shown with NES and number of leading edge genes in log scale at the x-axis.

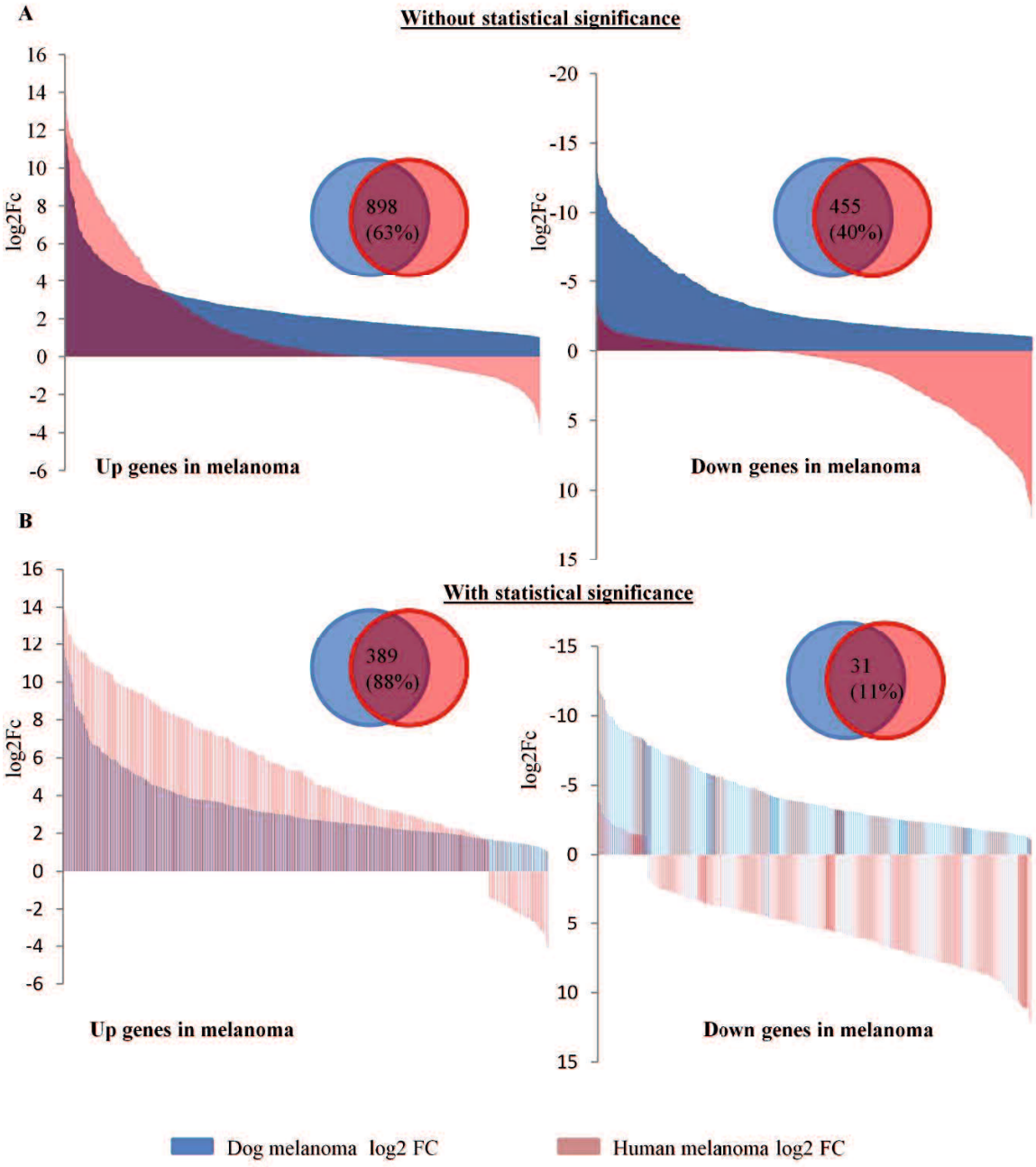
A
Without statistical significance
log2Fc
898
(63%)
Up genes in melanoma
455
(40%)
Down genes in melanoma
B
With statistical significance
389
(88%)
Up genes in melanoma
31
(11%)
Down genes in melanoma
Dog melanoma log2 FC
Human melanoma log2 FC

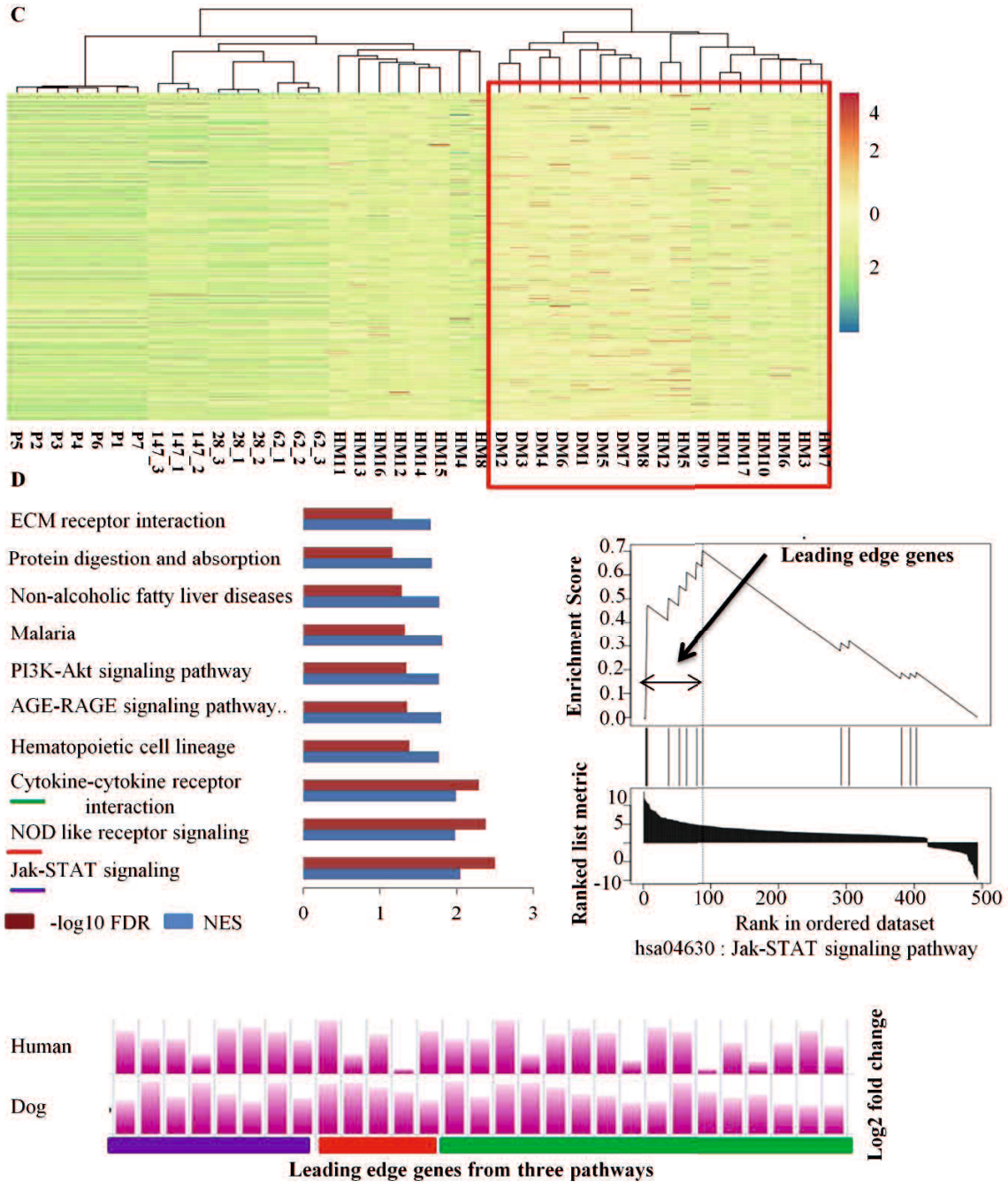
C
4
2
0
2
P5 P2 P3 P4 P6 P1 P7 147_3 147_1 147_2 28_3 28_1 28_2 62_1 62_2 62_3 HM11 HM13 HM16 HM12 HM14 HM15 HM4 HM8
DM2 DM3 DM4 DM6 DM1 DM5 DM7 DM8 HM2 HM5 HM9 HM1 HM17 HM10 HM6 HM3 HM7
D
ECM receptor interaction
Protein digestion and absorption
Non-alcoholic fatty liver diseases
Malaria
PI3K-Akt signaling pathway
AGE-RAGE signaling pathway..
Hematopoietic cell lineage
Cytokine-cytokine receptor interaction
NOD like receptor signaling
Jak-STAT signaling
-log10 FDR
NES
0 1 2 3
Enrichment Score
Leading edge genes
Ranked list metric
Rank in ordered dataset
hsa04630 : Jak-STAT signaling pathway
Human
Dog
Log2 fold change
Leading edge genes from three pathways

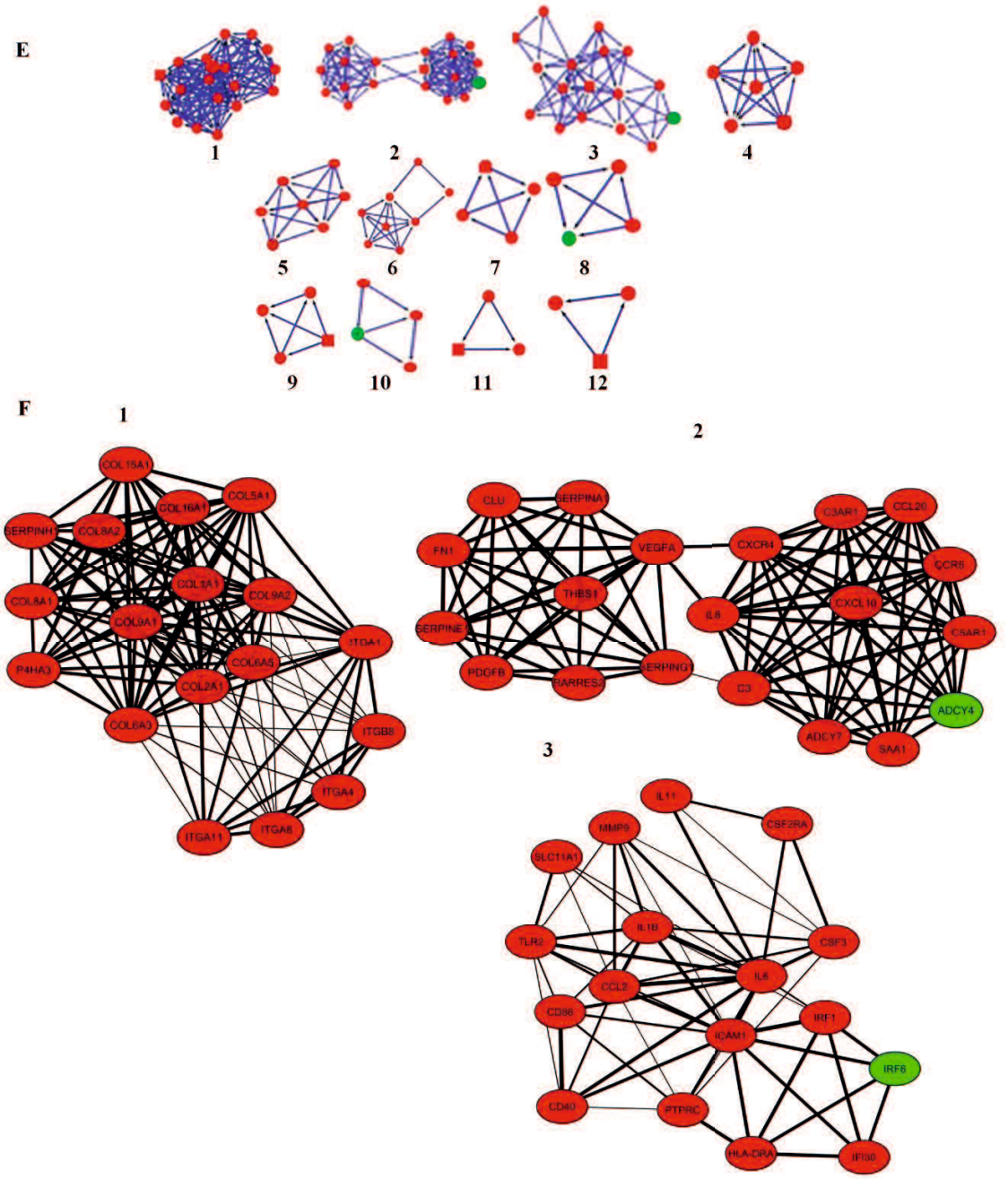
E
1
2
3
4
5
6
7
8
9
10
11
12
F
1
COL15A1
COL5A1
COL16A1
SERPINH1
COL8A2
COL1A1
COL8A1
COL9A2
COL9A1
ITGA1
P4HA3
COL6A5
COL2A1
COL6A3
ITGB8
ITGA4
ITGA11
ITGA8
2
CLU
SERPINA1
FN1
VEGFA
THBS1
SERPINE1
PDGFB
SERPING1
BARRES2
CXCR4
C3AR1
CCL20
CCR5
IL8
CXCL10
C5AR1
C3
ADCY4
ADCY7
SAA1
3
IL11
MMP9
CSF2RA
SLC11A1
IL1B
TLR2
CSF3
IL6
CCL2
CD86
IRF1
ICAM1
IRF8
CD40
PTPRC
HLA-DRA
IFI30

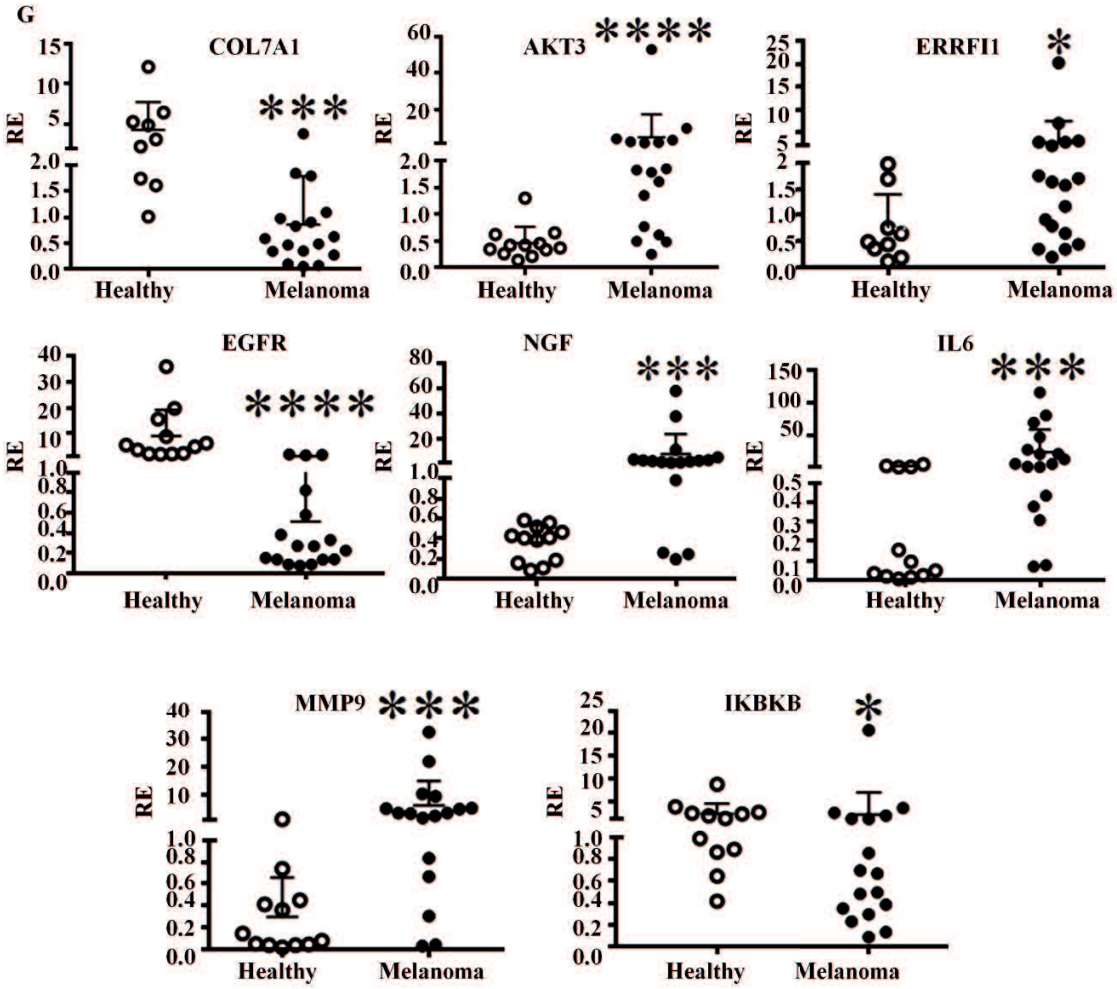

Figure 3-17. Differentially expressed genes between human and dog melanoma. (A and B) Gene fold change (FC) between the species with or without considering statistical significance in dog melanoma. Numbers and percentages of common up- and downregulated genes are shown in the overlapping region. The x-axis is the number of genes and the y-axis indicates the FC. (C) Heatmap with cluster analysis showing the expression of common oncogenes between prostate cancer cell lines (LNCaP-P1-P7), human melanoma cell lines [SK_MEL_28 (28_1-3), SK_MEL_147 (147_1-3), UACC_62 (62_1-3)], canine oral melanoma (DM_1-8) and human tissue melanoma (HM_1-17). The color gradient on the right indicates the expression values. Euclidean hierarchical clustering with complete linkage was used. Dog and human clustered together is indicated within the

red line. (D) Common enriched pathways between humans and dogs. Schematic on top right panel indicates how leading edge genes were defined. Fold changes of the leading edge genes from the top 3 pathways in both species are shown on the bottom panel. FDR, false discovery rate; NES, normalized enrichment score (E) Schematic presentation of 12 network clusters established by the common differentially expressed genes. (F) The first three clusters are shown in which a node indicates a gene and the lines between them indicate the edge. Red color indicates upregulated genes and green represents downregulated genes. (G) Relative expression of COL7A1 (healthy control, n=9), AKT3, ERRFI1, EGFR, NGF, IL6, MMP9 and IKBKB genes examined by RT-qPCR in healthy oral tissue (n=12) and oral melanoma (n=17). $^{*}P<0.05$, $^{***}P<0.01$, $^{****}P<0.0001$. The bars indicate standard deviation (SD). RE, relative expression; COL7A1, collagen type VII alpha 1 chain; AKT3, AKT serine/threonine kinase 3; ERRFI1, ERBB receptor feedback inhibitor 1; EGFR, epidermal growth factor receptor; NGF, nerve growth factor; IL6, interleukin 6; MMP9, matrix metallopeptidase 9; IKBKB, inhibitor of nuclear factor kappa B kinase subunit beta.

Conclusion

To the best of my knowledge, this study is the first portrait of comprehensively studied COM transcriptome by next generation sequencing. I successfully reveal the transcriptomic aberration of COM and find its analogy with the human melanoma. Among the non-coding RNA transcriptome, I first reveal the altered expression of miRNAs and confirm their expression by qPCR. Studied miRNA's targets have significant correlation as like their human study. Important miRNAs with respect to human and dog melanoma is explored. These findings facilitate to know the role of miRNA in melanoma and contribute in further miRNA based therapeutic development. Additionally, indicates the suitability of dog for miRNA based therapeutic development for both species. During my small non-coding RNAs analysis, I find not only miRNA but also some new type of small RNAs like snRNA, snoRNAs, tRNA fragments and piRNAs are differentially expressed. The expression pattern of these small RNAs are same between tissue and cell line but different in plasma. Also the expression pattern of the snRNA and snoRNA are conserved in human melanoma. So, not only miRNA but also other types of non-coding RNAs are aberrantly expressed in melanoma. Most importantly conserved expression pattern in human melanoma emphasize their involvement in melanoma pathogenesis. During the analysis of coding part of the transcriptome, I observe the annotated and novel differentially expressed

genes. Cross species analysis of the mRNA transcriptome reveals the similarities between the 2 species. Moreover, key/driver genes and molecular pathways are listed by comparing the melanoma transcriptome. This study successfully identified the coding transcriptome aberrations in canine oral melanoma. By comparing the melanoma transcriptome between the 2 species, I identified the key genes and molecular pathways for further study to develop more effective therapeutic approaches to melanoma.

The evidence from my whole transcriptome analysis demonstrates the similarity of melanoma between the 2 species. I show that similarities exist in the both non-coding and coding part of the transcriptome. Moreover, the interaction between non-coding and coding part are also conserved between the 2 species. These emphasize dogs as a suitable pre-clinical model for human melanoma. My study may significantly contribute in future to develop more effective therapeutic approaches in the field of comparative oncology.

Acknowledgments

Glory is to Allah and all praises to him who gives the opportunity and makes successful accomplishment of this doctorate program. I would like to give my first, sincere, thankful and deepest sense of gratitude to my respected Ph.D supervisor Professor Dr. Naoki Miura who selected me as a student under his supervision. I am also very grateful to him for his precious help, guidance, support and continuous encouragement during the study period.

I would like to express my sincere gratitude to my co-supervisors for their helpful suggestion and constructive comments during the study period. Special thanks to Professor Dr. Fujiki Makoto, Dr Okamoto Yoshiharu, and Dr. Osamu Yamato for their technical support for my experiment. I am also very thankful to Professor Chikara Kubota and Associate Professor Takahashi Masashi for their helpful suggestion and enthusiastic words.

I also owe special thanks to Associate professor Yasuo Saitoh and Tomoko Iwanaga for their helpful technical suggestion during my research writing. I would like to thanks Associate Professor Dr.Tatsunori Masatani for his help and appreciation during my research presentation.

Acknowledgments

I am very grateful to my senior Dr. Yu Chang Lai for his countless help, appreciation and direction about the research project. I also indebted to Masuda Ayako who was always helped me including my academic and non-academic issues. I also thank to Jin, Kaho, Kasumi, Fumi, Baba, Habibi, Jump, Soma, Chise, and Chandana who often helped me in some way, during the course of the work. I am very thankful to Mizuki Ando who was always very kind and helpful to my family which helped me to keep forward my research work.

I'm humbled and appreciative to the Kagoshima City Hall authority for their support during my study period.

I would like to express my deepest sense of gratitude to the Ministry of Education, Culture, Sports, Science and Technology (MEXT) to support financially during my study period in Japan.

I am also very indebted to my respected teacher Professor Dr. Mahbub Alam from the department of medicine, Faculty of Veterinary Science, Bangladesh Agricultural University, Mymensingh Bangladesh who implanted the dream of Ph.D and helped me to ride on the track.

Finally, the best gratitude and love is for my father and mother who gave me the foundation of education. I also thankful to my daughter and my wife for sacrificing their time and allow me to keep up the research work.

Appendix

Appendix 1-1A. Signalment characteristics and WHO clinical stage of the 17 canine oral malignant melanomas

COM tissue specimen for NGS and qPCR					
No	Age (Years)	Sex	Breed	WHO Stage	NGS(N) or qPCR (q)
T1	12.7	Male	Miniature	IV	N and q
T2	14.8	Male	Mongrel	IV	N and q
T3	10	Male	Golden Retriever	IV	N and q
T4	10.11	Male	Miniature	I	q
T5	7.11	Male	Miniature	I	q
T6	10.9	Male	Miniature	IV	q
T7	12	Male	Shiba	IV	q
T8	13	Male	Pomerania	I	q
T9	10.3	Male	Yorkshire	IV	q
T10	10.2	Male	Chiwawa	IV	N and q
T11	12.4	Female	Miniature	IV	q
T12	14.6	Female	Miniature	II	q
T13	15.2	Female	Mongrel	IV	N and q
T14	12.11	Male	Miniature	IV	N and q
T15	12.4	Male	Shiba and Miniature cross	IV	N and q
T16	15.2	Female	Mongrel	IV	N and q
T17	10.8	Male	Miniature	IV	q

Appendix 1-1B. Clean sequencing reads from the normal and melanoma individual libraries.

Column ID	**Normal**	
Sample Name	Reads	Reads After adapter treaming
Nomal1	31719088	19015734
Nomal2	34437764	15742516
Nomal3	37308370	16280411
Total	103465222	51038661
	Melanoma	
Melanoma1	29554264	15993157
Melanoma2	28585813	13852584
Melanoma3	28264207	10101754
Melanoma4	27946191	11432175
Melanoma5	29796066	13157883
Melanoma6	36882368	22866409
Melanoma7	57273744	42202229
Melanoma8	27785482	12462538
Total reads	266088135	142068729

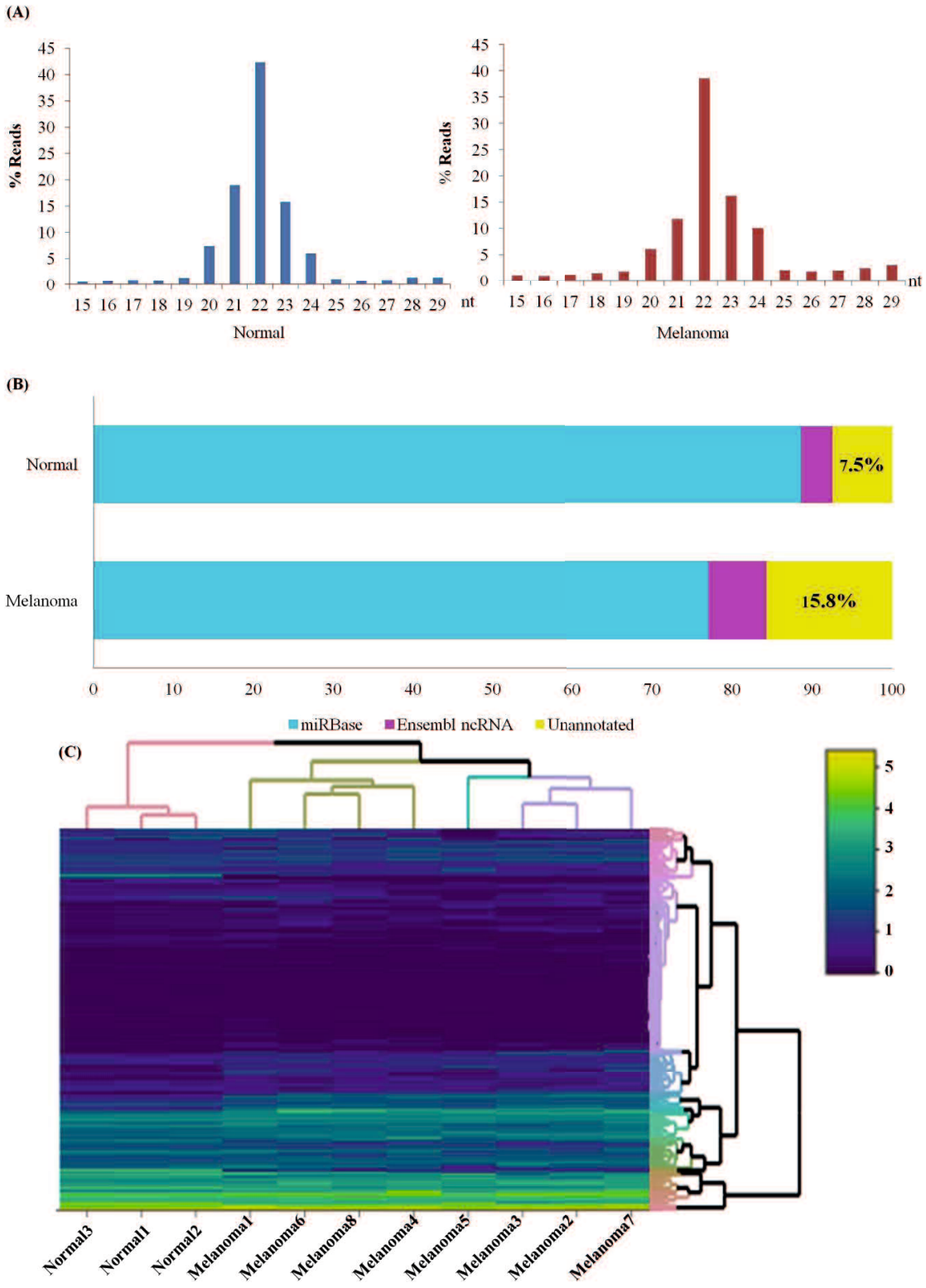
(A)
% Reads
45
40
35
30
25
20
15
10
5
0
15 16 17 18 19 20 21 22 23 24 25 26 27 28 29
nt
Normal
Melanoma
(B)
Normal
Melanoma
7.5%
15.8%
0 10 20 30 40 50 60 70 80 90 100
miRBase
Ensembl ncRNA
Unannotated
(C)
5
4
3
2
1
0
Normal3
Normal1
Normal2
Melanoma1
Melanoma6
Melanoma8
Melanoma4
Melanoma5
Melanoma3
Melanoma2
Melanoma7

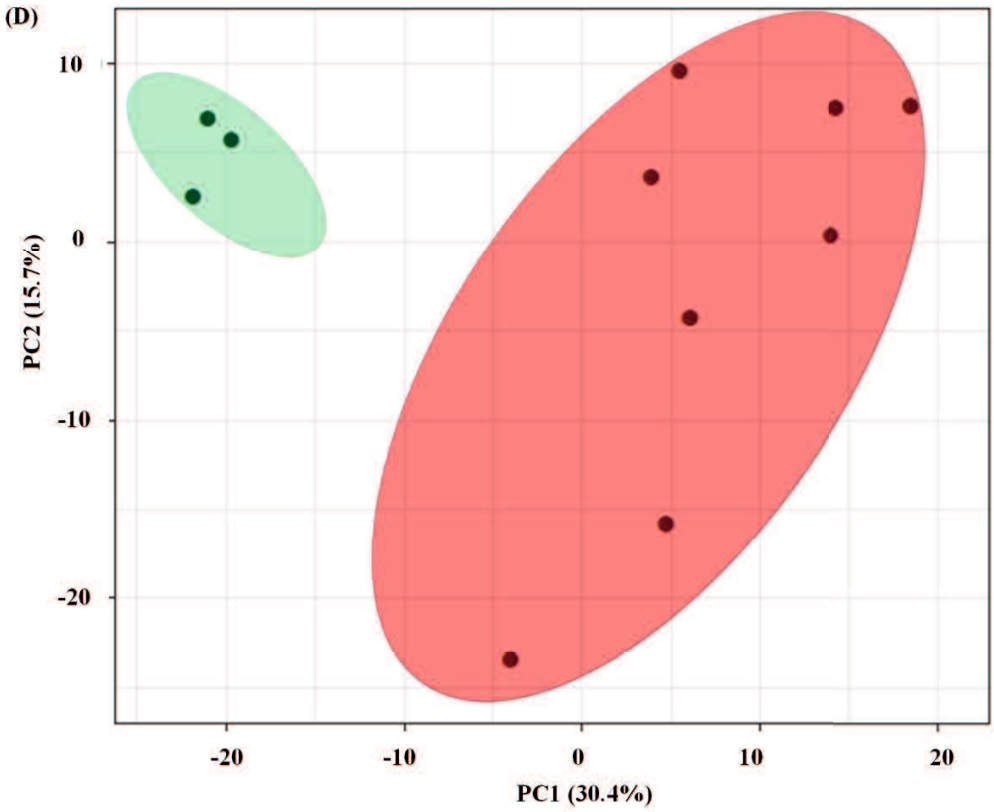

Appendix 1-2. Profile of small RNA reads in canine oral melanoma: (a) Length distribution of clean reads in the normal and melanoma libraries; (b) Percentages of the clean reads annotated by the miRBase and Ensembl non-coding RNA databases; c) Unsupervised Euclidean hierarchical clustering by the miRNA normalized expression values in the normal and melanoma libraries, The colour scale (upper right) indicates the expression values; (d) Principal component analysis (PCA) of normal (green) and melanoma (pink) samples. The miRNAs read counts were normalized and transformed before PCA.

Appendix 1-3. Differentially expressed microRNAs in canine oral melanoma

miR	Stand	Species	FC [1]	FDR [2]	Chr [3]
mir-8884	Mature 3'	Canis familiaris	4.03	3.46E-02	8
mir-107	Mature 3'	Canis familiaris	4.25	2.1E-02	28
mir-8859b	Mature 3'	Canis familiaris	4.28	2.79E-02	18
mir-421	Mature 3'	Canis familiaris	4.41	2.78E-02	X
mir-190a	Mature 5'	Canis familiaris	5.33	4.45E-02	30
mir-454	Mature 3'	Homo sapiens	5.69	1.27E-02	9
mir-335	Mature 5'	Canis familiaris	5.77	1.77E-02	14
mir-132	Mature 3'	Homo sapiens	5.97	5.93E-03	9
mir-301a	Mature 3'	Canis familiaris	6.88	2.5E-03	9
mir-330	Mature 5'	Canis familiaris	7.19	2.06E-03	1
mir-21	Mature 5'	Homosapiens//Canis familiaris	7.60	4.2E-04	9
mir-423//mir-423a	Mature 5'	Homosapiens//Canis familiaris	8.69	5.81E-03	9
mir-363	Mature 3'	Canis familiaris	9.62	3.00E-04	X
mir-146b	Mature 5'	Homosapiens//Canis familiaris	15.32	1.62E-03	28
mir-140	Mature 3'	Homo sapiens	23.03	6.27E-03	5
mir-9-2//mir-9-3//mir-9-1	Mature 5'	Canis familiaris	62.71	3.36E-07	3,7
mir-223	Mature 3'	Canis familiaris	37.49	8.16E-04	X

mir-383	Mature 5'	Homosapiens//Canis familiaris	207.48	2.43E-04	16
mir-450b	Mature 5'	Canis familiaris	60.14	3.09E-08	X
mir-196a-2	Mature 5'	Canis familiaris	990.94	2.54E-08	27
mir-371	Mature 5'	Canis familiaris	22.75	5.67E-05	1
mir-542	Mature 3'	Canis familiaris	131.06	1.80E-09	X
mir-130b	Mature 3'	Canis familiaris	14.17	9.51E-05	26
mir-424	Mature 5'	Homo sapiens	57.02	4.06E-09	X
mir-450a	Mature 5'	Canis familiaris	24.21	4.06E-05	X
mir-106a	Mature 5'	Homo sapiens	17.84	1.27E-05	X
mir-301b	Mature 3'	Canis familiaris	13.51	7.86E-05	26
mir-20b	Mature 5'	Canis familiaris	38.45	3.51E-07	X
mir-18b	Mature 5'	Canis familiaris	27.73	7.00E-06	X
mir-424	Mature 3'	Homosapiens//Canis familiaris	71.56	8.27E-07	X
let-7a-1//let-7a-3//let-7a-2	Mature 5'	Homosapiens//Canis familiaris	-3.27	1.58E-02	10,5
mir-126	Mature 5'	Homosapiens//Canis familiaris	-3.56	1.75E-02	9
mir-125a	Mature 5'	Canis familiaris	-4.56	6.52E-03	1
let-7b	Mature 5'	Canis familiaris	-3.40	1.66E-02	10
mir-101-2//mir-101-1	Mature 3'	Canis familiaris	-3.19	1.71E-02	1,5
mir-1271	Mature 5'	Canis familiaris	-4.32	1.72E-02	4
mir-183	Mature 5'	Homosapiens//Canis	-3.55	2.25E-02	14

		familiaris			
mir-26b	Mature 5'	Homo sapiens	-2.76	4.42E-02	37
mir-29c//mir-29c-1//mir-29c-2	Mature 3'	Homosapiens//Canis familiaris	-4.20	3.68E-03	7
mir-152	Mature 3'	Homosapiens//Canis familiaris	-3.24	3.16E-02	9
mir-1260a	Mature 5'	Homo sapiens	-3.43	2.72E-02	4
mir-378i	Mature 5'	Homo sapiens	-3.11	3.27E-02	3
mir-708	Mature 5'	Homosapiens//Canis familiaris	-3.87	3.22E-02	21
mir-31	Mature 5'	Canis familiaris	-3.55	4.32E-02	11
mir-143	Mature 5'	Homo sapiens	-3.79	3.46E-02	4
mir-1468	Mature 5'	Canis familiaris	-5.32	2.69E-03	X
mir-145	Mature 3'	Homo sapiens	-5.54	6.97E-04	4
let-7c	Mature 5'	Homosapiens//Canis familiaris	-5.91	2.88E-04	31
mir-379	Mature 5'	Homosapiens//Canis familiaris	-5.97	1.89E-02	8
mir-147	Mature 3'	Canis familiaris	-7.034	1.62E-03	30
mir-96	Mature 5'	Canis familiaris	-9.00	7.86E-05	14
mir-99a-1//mir-99a-2	Mature 5'	Canis familiaris	-12.07	4.9E-04	31,5
mir-452	Mature 5'	Canis familiaris	-16.75	9.86E-05	X
mir-409	Mature 5'	Homo sapiens	-16.85	2.12E-07	8
mir-95	Mature 3'	Canis familiaris	-17.61	1.12E-04	3

mir-224	Mature 5'	Canis familiaris	-28.17	1.14E-07	X
mir-375	Mature 3'	Canis familiaris	-38.64	6.83E-14	37
mir-141	Mature 3'	Homo sapiens	-153.25	0	27
mir-429	Mature 3'	Canis familiaris	-314.72	2.88E-22	5
mir-205	Mature 5'	Canis familiaris	-320.15	0	7
mir-200c	Mature 3'	Homosapiens//Canis familiaris	-376.31	2.93E-22	27
mir-200a	Mature 3'	Homo sapiens	-520.66	1.41E-27	5
mir-200b	Mature 3'	Homo sapiens	-663.46	0	5
mir-203a//mir-203	Mature 3'	Homosapiens//Canis familiaris	-854.25	0	8

[1] Fold change. [2] False discovery rate. [3] Chromosome

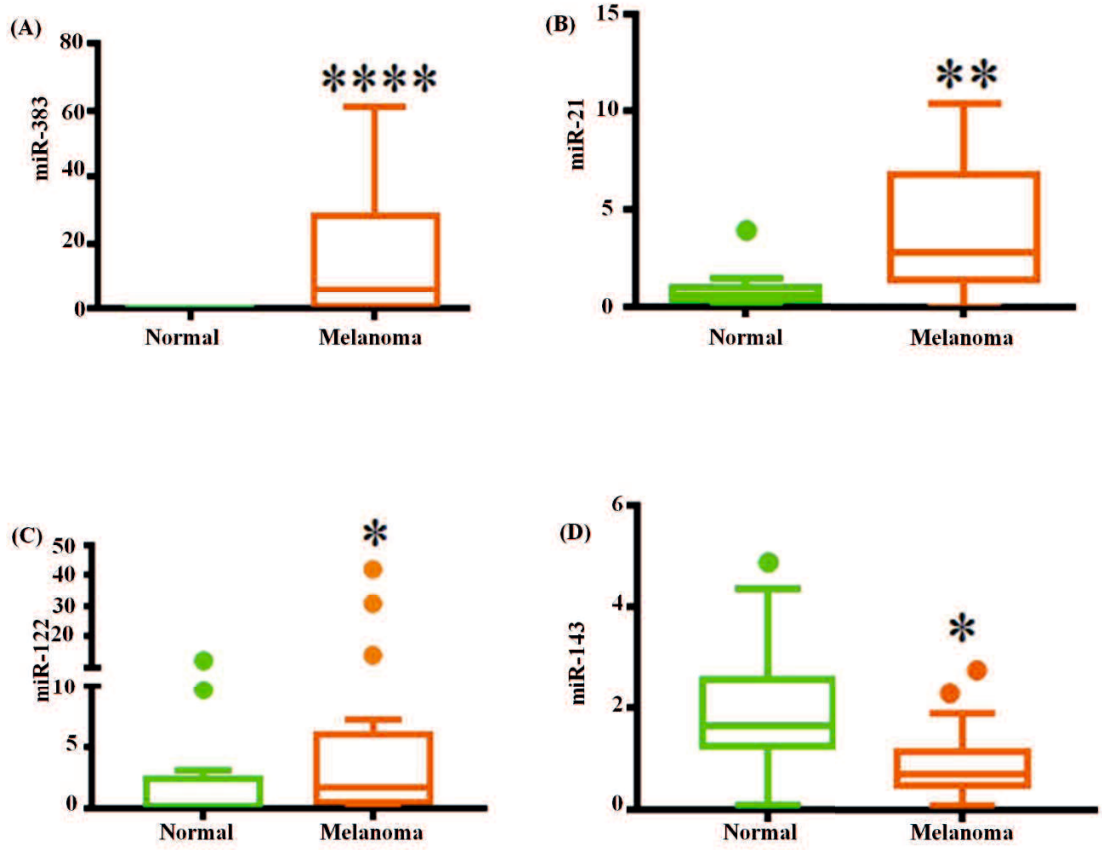

Appendix 1-4. Differential miRNA expression in COM. (a-c) Relative expression of up-regulated miR-383, 21 and 122; (d) Relative expression of down-regulated miR-143. The Y-axes indicates the relative miRNA expression levels normalized against RNU6B (normal n=12, melanoma n=17; Mann-Whitney test followed by Tukey's test; *P <0.05, **P <0.01, ****P <0.0001)

(A)

Dog PAX9 ENST00000361487.6 3' UTR length: 4013

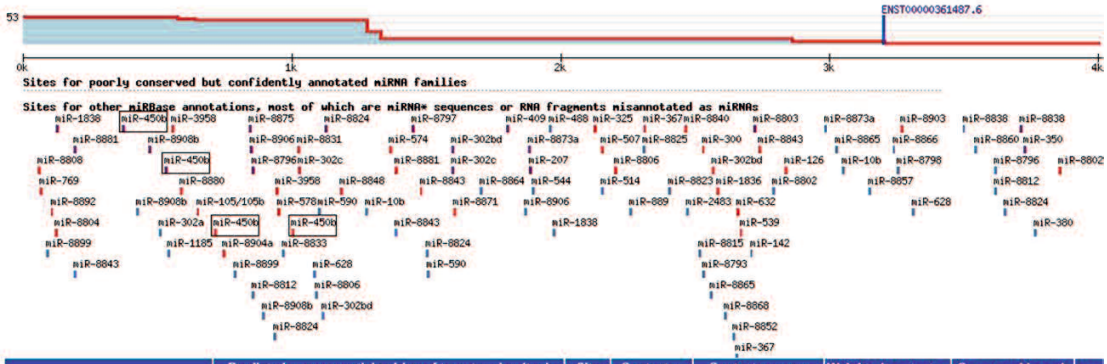

	Predicted consequential pairing of target region (top) and miRNA (bottom)	Site type	Context++ score	Context++ score percentile	Weighted context++ score	Conserved branch length	P_{CT}
Position 380-387 of PAX9 3' UTR cfa-miR-450b	5' ...GCAAUUGUUGAGAUUUUGCAAAA... 3' UAAGUCCUUGUAUAACGUUUU	8mer	-0.22	96	-0.22	0.153	N/A
Position 544-551 of PAX9 3' UTR cfa-miR-450b	5' ...AGAUGACCUAUUUUGUUGCAAAA... 3' UAAGUCCUUGUAUAACGUUUU	8mer	-0.19	94	-0.19	0	N/A
Position 735-741 of PAX9 3' UTR cfa-miR-450b	5' ...UUUUUUUCUUUCUUUUUGCAAAG... 3' UAAGUCCUUGUAUAACGUUUU	7mer-m8	-0.03	50	-0.03	0.233	N/A
Position 1033-1039 of PAX9 3' UTR cfa-miR-450b	5' ...UUAAUGUGAAACGCUUUGCAAAG... 3' UAAGUCCUUGUAU AACGUUUU	7mer-m8	-0.08	78	-0.07	0.153	N/A

```
      .....350.....360.....370.....380.....390.....400.....410.....420.....430.....440.....
Dog   JCAACCUGAACUUUUGAAACGUGCAA----UUGUU---GAGA-UUUUGC-AAAAUC----AAUAAAGGAAACUACAU-------AUAGAAAA------AAAA----AGUUAUGCUAUACCCUCUAAUCAAAUAA-
Human JCAACCUGAACUUUUGAAAUGUGCAA----UUGUU---GAGA-UUUUGC-AAAAUC----AAUAAAGGAAAAUACUU-------AUAG---------AAAA----AAUUAUGCUACACCCUCUAAUCAAAUAU-
```

(B)

Dog ACVR2A ENST00000241416.7 3' UTR length: 3560

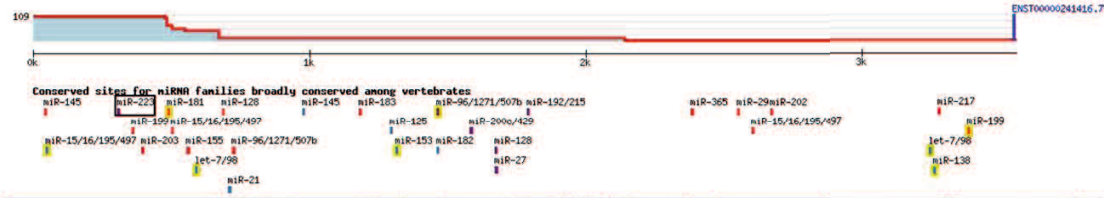

	Predicted consequential pairing of target region (top) and miRNA (bottom)	Site type	Context++ score	Context++ score percentile	Weighted context++ score	Conserved branch length	P_{CT}
Position 305-312 of ACVR2A 3' UTR cfa-miR-223	5' ...AAUCAAGUGUUUGAA-AACUGACA... 3' CCCCAUAAACUGUUUGACUGU	8mer	-0.46	98	-0.46	3.283	0.29

```
      260.....270.....280.....290.....300.....310.....320.....330.....340.....350.....360.....
Dog   ICUCCAAAU--C---AAGGAUC-UUUUGGACCU--GGCU-AAUCAAGUGU-UUG--AAAACUGACAUCAGAUUUC-----UAAAUGUCUGUCGG---AA---GACACUAAUUCC-UUAAAUGAACUACUGCUA---
Human ICUCCAAAU--C---AAGGAUC-UUUUGGACCU--GGCU-AAUGGAGUGU-UUG--AAAACUGACAUCAGAUUUC-----UUAAUGUCUGUCAG---AA---GACACUAAUUCC-UUAAAUGAACUACUGCU----
```

(C)

Dog NDRG2 ENST00000298687.5 3' UTR length: 852

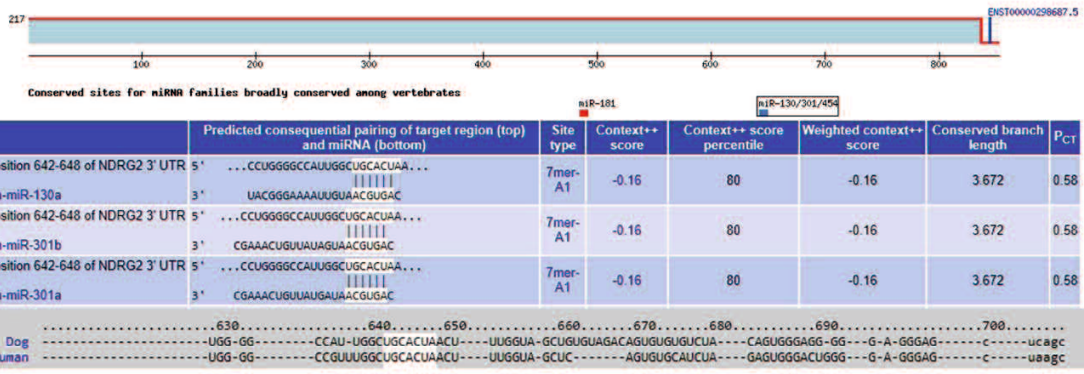

	Predicted consequential pairing of target region (top) and miRNA (bottom)	Site type	Context++ score	Context++ score percentile	Weighted context++ score	Conserved branch length	P_{CT}
Position 642-648 of NDRG2 3' UTR cfa-miR-130a	5' ...CCUGGGGCCAUUGGCUGCACUAA... 3' UACGGGAAAAUUGUAACGUGAC	7mer-A1	-0.16	80	-0.16	3.672	0.58
Position 642-648 of NDRG2 3' UTR cfa-miR-301b	5' ...CCUGGGGCCAUUGGCUGCACUAA... 3' CGAAACUGUUAUAGUAACGUGAC	7mer-A1	-0.16	80	-0.16	3.672	0.58
Position 642-648 of NDRG2 3' UTR cfa-miR-301a	5' ...CCUGGGGCCAUUGGCUGCACUAA... 3' CGAAACUGUUAUGAUAACGUGAC	7mer-A1	-0.16	80	-0.16	3.672	0.58

```
                    .....630.............640.....650.....660.....670.....680.....690.....700.....
Dog   --------------------UGG-GG--------CCAU-UGGCUGCACUAACU----UUGGUA-GCUGUGUAGACAGUGUGUGUCUA----CAGUGGGAGG-GG---G-A-GGGAG------c-----ucagc
Human --------------------UGG-GG--------CCGUUUGGCUGCACUAACU----UUGGUA-GCUC-------AGUGUGCAUCUA----GAGUGGGACUGGG---G-A-GGGAG------c-----uaagc
```

Appendix 1-5. Predicted conserved target binding site of miR-450b-PAX9, miR-223-ACVR2A and miR-301a-NDRG2 from TargetScan: (a-c). Predicted binding sites of respective miRNA-mRNA are conserved between human and dog.

Appendix 1-6. Over representation analysis of the down-regulated miRNAs target genes against cancer and other databases

Cancer Gene Census		
Gene Set	Enrichments	P-Value
oncogene	1.11	8.80E-2
fusion	1.04	4.42E-01
others	1.01	5.77E-01
tumor suppresor genes	0.84	9.66E-01
GLAD4U databases		
Cell Transformation, Neoplastic	2.13	5.48E-12
Neoplastic Processes	1.73	5.64E-10
Neoplasm Invasiveness	1.81	5.95E-09
Chromosome Aberrations	1.66	3.59E-06
Neoplasms, Squamous Cell	1.53	7.39E-06
Neoplasms	1.40	8.42E-06
Leukemia, Myeloid, Acute	1.80	9.46E-06
Neoplasm Metastasis	1.55	1.12E-05
Translocation, Genetic	1.51	1.34E-05
Leukemia	1.52	1.58E-05
OMIM databases		
Colorectal cancer	22.23	1.64E-06
Diabetes mellitus, noninsulin-dependent	12.88	4.82E-06
Lung canceralveolar cell carcinoma, included	18.31	4.87E-06
Leukemia, acute myeloid	14.82	1.52E-05
Juvenile myelomonocytic leukemia	37.35	3.87E-05
Intervertebral disc disease	31.12	7.64E-05
Osteoporosis	31.12	7.64E-05
Tetralogy of fallot	23.34	2.09E-04
Breast cancer	10.38	5.06E-04
Myocardial infarction, susceptibility tomyocardial infarction	15.56	7.85E-04

Appendix 1-7A. Down-regulated miRNAs target transcription factor (34)

Gene symbol	Gene name
ATF2	activating transcription factor 2(ATF2)
BMI1	BMI1 proto-oncogene, polycomb ring finger(BMI1)
CITED2	Cbp/p300 interacting transactivator with Glu/Asp rich carboxy-terminal domain 2(CITED2)
E2F6	E2F transcription factor 6(E2F6)
ETV4	ETS variant 4(ETV4)
EYA1	EYA transcriptional coactivator and phosphatase 1(EYA1)
EYA3	EYA transcriptional coactivator and phosphatase 3(EYA3)
EYA4	EYA transcriptional coactivator and phosphatase 4(EYA4)
FOXJ3	forkhead box J3(FOXJ3)
FOXN2	forkhead box N2(FOXN2)
FOXP1	forkhead box P1(FOXP1)
HOXA5	homeobox A5(HOXA5)
HOXB2	homeobox B2(HOXB2)
HOXB6	homeobox B6(HOXB6)
ID1	inhibitor of DNA binding 1, HLH protein(ID1)
MTF2	metal response element binding transcription factor 2(MTF2)
NAB1	NGFI-A binding protein 1(NAB1)
NKRF	NFKB repressing factor(NKRF)
NR2C2	nuclear receptor subfamily 2 group C member 2(NR2C2)
PITX2	paired like homeodomain 2(PITX2)
PLAGL2	PLAG1 like zinc finger 2(PLAGL2)
POU2F1	POU class 2 homeobox 1(POU2F1)
RFXANK	regulatory factor X associated ankyrin containing protein(RFXANK)
RNF144A	ring finger protein 144A(RNF144A)
SP4	Sp4 transcription factor(SP4)
TBX18	T-box 18(TBX18)
TEAD1	TEA domain transcription factor 1(TEAD1)
TSC22D1	TSC22 domain family member 1(TSC22D1)
TTLL4	tubulin tyrosine ligase like 4(TTLL4)
VDR	vitamin D (1,25- dihydroxyvitamin D3) receptor(VDR)
ZFAND6	zinc finger AN1-type containing 6(ZFAND6)
ZFR	zinc finger RNA binding protein(ZFR)
ZNF174	zinc finger protein 174(ZNF174)
ZNF275	zinc finger protein 275(ZNF275)

Appendix 1-7B. Up-regulated miRNAs target transcription factor (33)

Gene symbol	Gene name
ALX1	ALX homeobox 1(ALX1)
BNC2	basonuclin 2(BNC2)
CLOCK	clock circadian regulator(CLOCK)
CREB1	cAMP responsive element binding protein 1(CREB1)
DMTF1	cyclin D binding myb like transcription factor 1(DMTF1)
E2F1	E2F transcription factor 1(E2F1)
FAM20C	FAM20C, golgi associated secretory pathway kinase(FAM20C)
FOXF2	forkhead box F2(FOXF2)
IRF4	interferon regulatory factor 4(IRF4)
IRF9	interferon regulatory factor 9(IRF9)
KCNIP3	potassium voltage-gated channel interacting protein 3(KCNIP3)
KLF5	Kruppel like factor 5(KLF5)
MBNL2	muscleblind like splicing regulator 2(MBNL2)
MECP2	methyl-CpG binding protein 2(MECP2)
MEF2C	myocyte enhancer factor 2C(MEF2C)
MLLT10	myeloid/lymphoid or mixed-lineage leukemia; translocated to, 10(MLLT10)
MXI1	MAX interactor 1, dimerization protein(MXI1)
NR4A2	nuclear receptor subfamily 4 group A member 2(NR4A2)
OPTN	optineurin(OPTN)
PPARG	peroxisome proliferator activated receptor gamma(PPARG)
RB1	RB transcriptional corepressor 1(RB1)
SMARCE1	SWI/SNF related, matrix associated, actin dependent regulator of chromatin, subfamily e, member 1(SMARCE1)
TCF7L1	transcription factor 7 like 1(TCF7L1)
TGFB1I1	transforming growth factor beta 1 induced transcript 1(TGFB1I1)
TULP4	tubby like protein 4(TULP4)
VEZF1	vascular endothelial zinc finger 1(VEZF1)
ZNF106	zinc finger protein 106(ZNF106)
ZFP91	ZFP91 zinc finger protein(ZFP91)
ZKSCAN1	zinc finger with KRAB and SCAN domains 1(ZKSCAN1)
ZMYND11	zinc finger MYND-type containing 11(ZMYND11)
ZNF25	zinc finger protein 25(ZNF25)
ZNF362	zinc finger protein 362(ZNF362)
ZNF706	zinc finger protein 706(ZNF706)

Appendix 1-8A. Centrality measures of the down-miR-TFs network

Name	Degree unDir	Betweenness unDir
miR-126	8	624.1707
FOXN2	7	468.996
BMI1	5	513.5405
MTF2	7	328.1401
miR-183	4	493.2195
E2F6	5	371.776
ATF2	4	462.0376
PLAGL2	5	346.5784
NR2C2	5	314.7015
miR-141	7	184.9902
miR-200a	7	184.9902
HOXA5	4	288.2461
EYA4	4	287.1757
EYA3	4	240.7778
miR-26b	3	305.2306
miR-429	5	162.008
miR-200C	5	162.008
miR-224	3	217.9321
miR-708	3	215.3048
miR-203	3	202.4925
NAB1	4	141.5243
POU2F1	3	183.4897
miR-31	3	181.3361
TSC22D1	4	135.0135
EYA1	4	127.1013
miR-29c	3	155.9466
CITED2	3	128.5187
ID1	2	178.7648
let-7a	4	88.01872
let-7b	4	88.01872
let-7c	4	88.01872
miR-452	3	106.9105
miR-200b	4	77.83935
miR-205	3	98.6442

FOXJ3	3	62.76508
PITX2	3	55.94286
NKRF	2	81.71066
TBX18	2	71.12229
FOXP1	3	45.44023
SP4	2	58.20149
ZFR	3	38.42038
TEAD1	2	42.46944
miR-143	2	41.72976
miR-101	2	32.58413
ZFAND6	3	3.152525
TTLL4	3	1.5
ZNF275	3	1.5
miR-125a	2	2
HOXB2	1	0
HOXB6	1	0
RFXANK	1	0
VDR	1	0
miR-1271	1	0
ETV4	1	0
miR-152	1	0
miR-378i	1	0
RNF144A	1	0
miR-96	1	0
ZNF174	1	0

Appendix 1-8B. Centrality measures of the Up-miR-TFs network

Name	Degree unDir	Betweenness unDir
CREB1	12	375.086
CLOCK	11	632.3675
miR-20b	11	389.3206
miR-106a	10	252.2331
PPARG	10	171.4987
MECP2	8	139.5748
miR-9	7	533.7517
RB1	7	213.1603
miR-454	6	71.72027
miR-301a	6	60.50574
miR-371	6	153.1827
miR-130b	6	60.50574
miR-301b	6	60.50574
MEF2C	6	374.621
BNC2	5	215.9453
miR-450b	5	134.3094
SMARCE1	5	188.1774
MLLT10	4	2.95
FOXF2	4	2.95
miR-21	4	146.3551
miR-424	4	72.14337
E2F1	4	35.43737
KLF5	4	135.0854
IRF9	4	31.6513
ZFP91	3	15.99994
miR-196a	3	102.6522
MBNL2	3	41.64914
ZNF362	3	13.10051
IRF4	3	22.85
NR4A2	3	1.833333
ZNF706	2	96
miR-132	2	4.590909
miR-423	2	2
miR-363	2	96
TULP4	2	188

miR-223	2	188
DMTF1	2	4.457326
MXI1	2	0.770707
ZNF25	2	0.770707
KCNIP3	2	0
TGFB1I1	2	4.12479
TCF7L1	2	16.16178
miR-107	1	0
miR-421	1	0
miR-190a	1	0
ALX1	1	0
VEZF1	1	0
ZNF106	1	0
FAM20C	1	0
ZKSCAN1	1	0
OPTN	1	0
ZMYND11	1	0
miR-450a	1	0

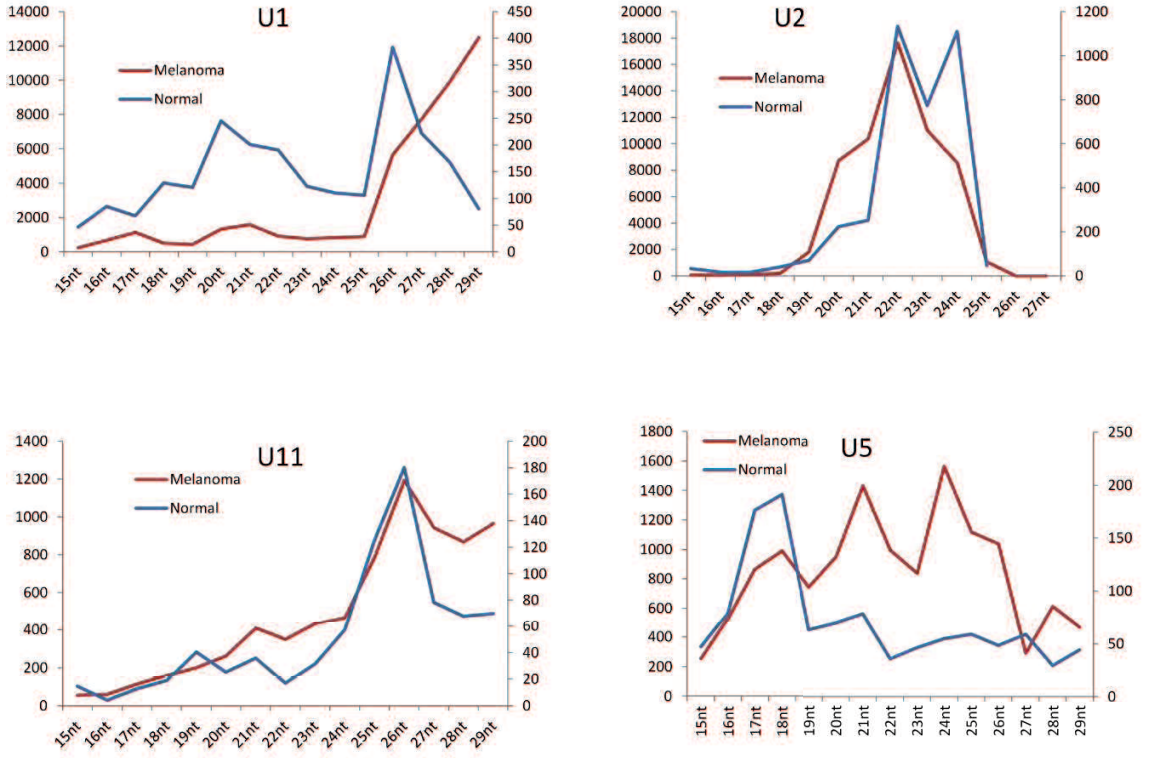

Appendix 2-9. Fragment length distribution of U1, U2, U11 and U5. Y-axis represent the percent RPM on the and X-axis is the length of the fragments.

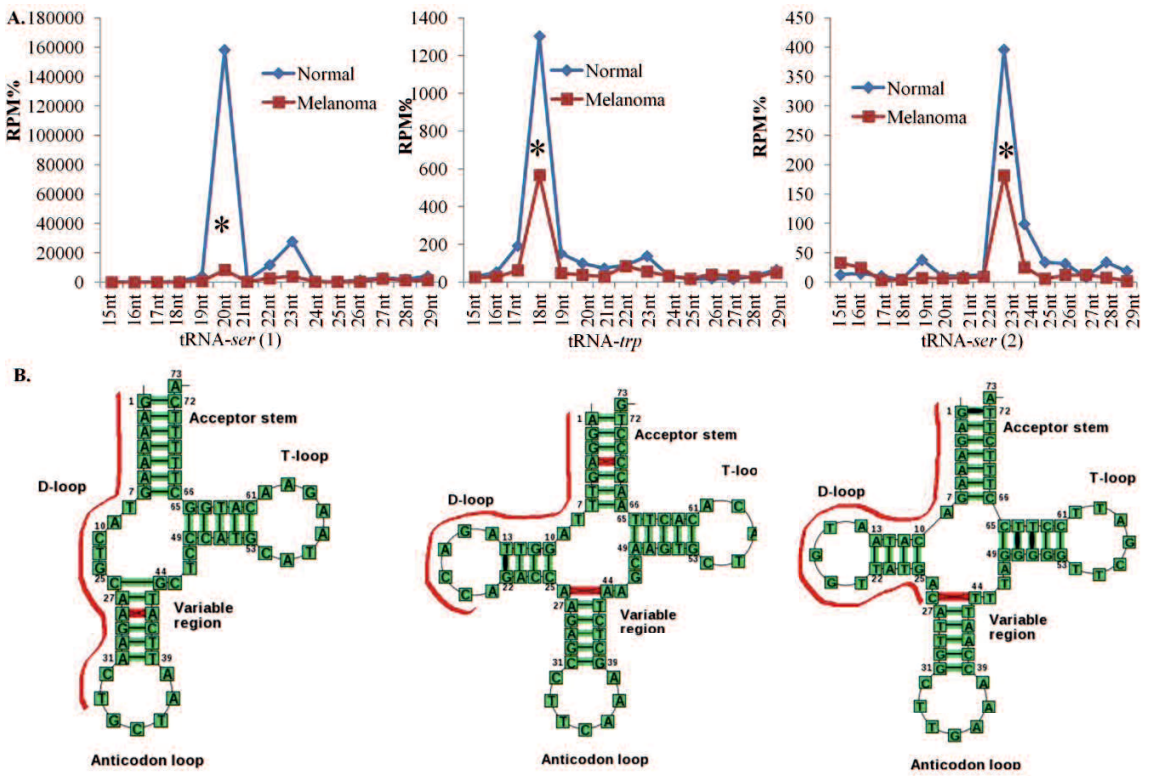

Appendix 2-10. Read length distribution of tRNA fragments from sequencing data count. (A) All three cases specific length of t-RNA fragment is significantly less in melanoma. (B) Site of the tRNA fragments in the clover leafed structure of tRNA. All three originated from the 5´tRH/5´tRF. Student t-test was performed, *P < 0.05.

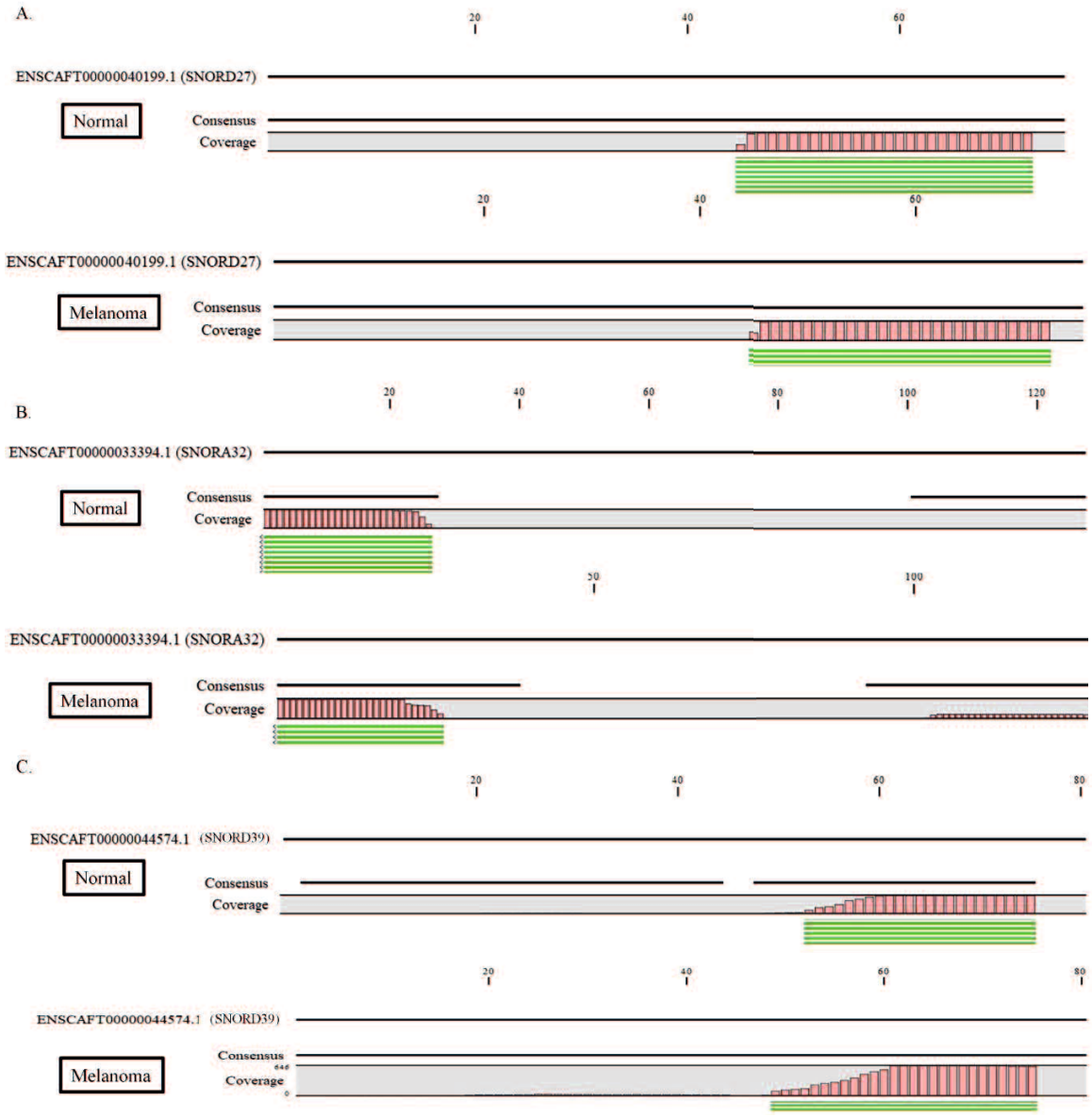
A.
ENSCAFT00000040199.1 (SNORD27)
Normal
Consensus
Coverage
ENSCAFT00000040199.1 (SNORD27)
Melanoma
Consensus
Coverage
B.
ENSCAFT00000033394.1 (SNORA32)
Normal
Consensus
Coverage
ENSCAFT00000033394.1 (SNORA32)
Melanoma
Consensus
Coverage
C.
ENSCAFT00000044574.1 (SNORD39)
Normal
Consensus
Coverage
ENSCAFT00000044574.1 (SNORD39)
Melanoma
Consensus
Coverage

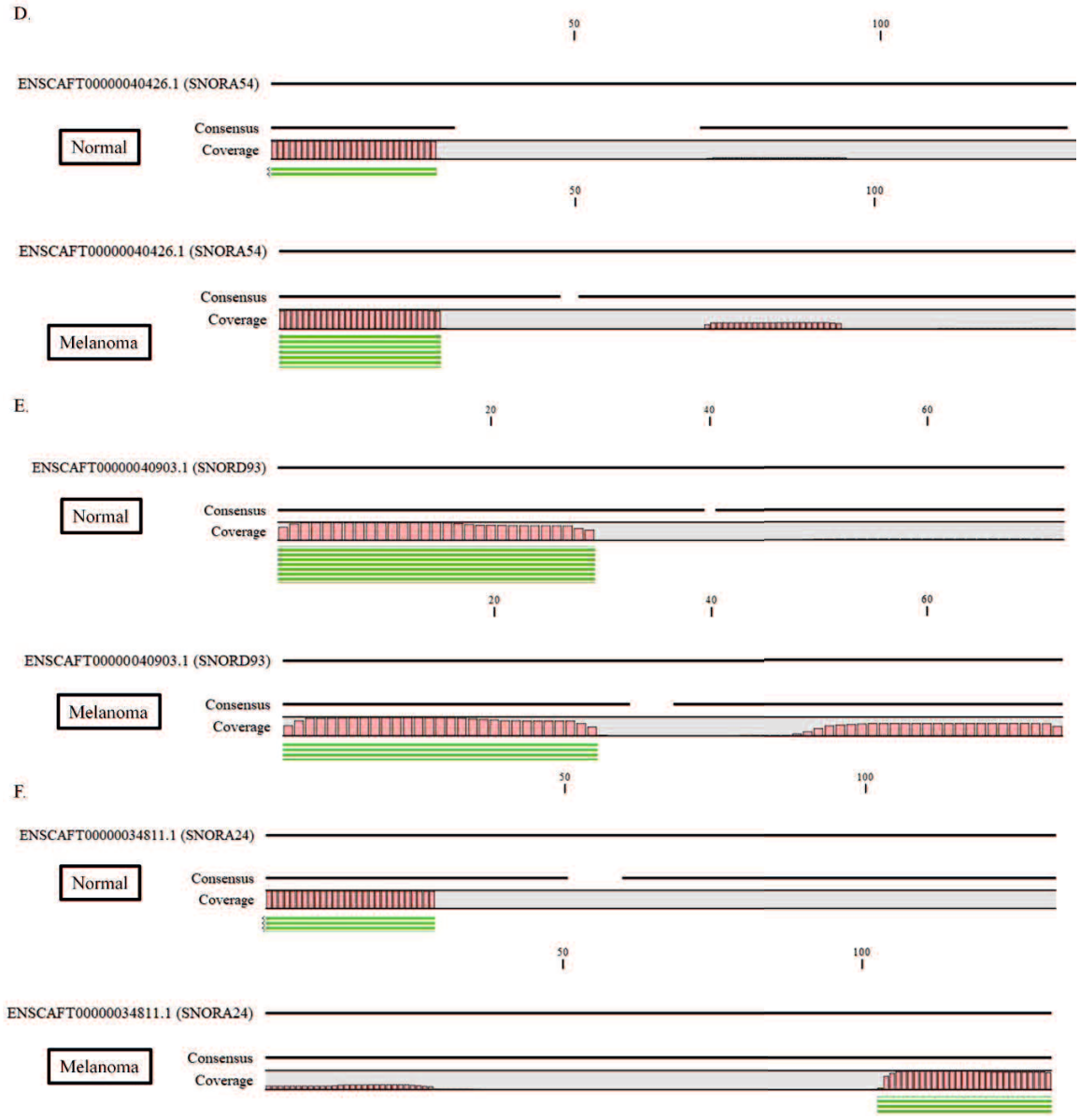
D.
50
100
ENSCAFT00000040426.1 (SNORA54)
Normal
Consensus
Coverage
50
100
ENSCAFT00000040426.1 (SNORA54)
Consensus
Coverage
Melanoma
E.
20
40
60
ENSCAFT00000040903.1 (SNORD93)
Normal
Consensus
Coverage
20
40
60
ENSCAFT00000040903.1 (SNORD93)
Melanoma
Consensus
Coverage
50
100
F.
ENSCAFT00000034811.1 (SNORA24)
Normal
Consensus
Coverage
50
100
ENSCAFT00000034811.1 (SNORA24)
Melanoma
Consensus
Coverage

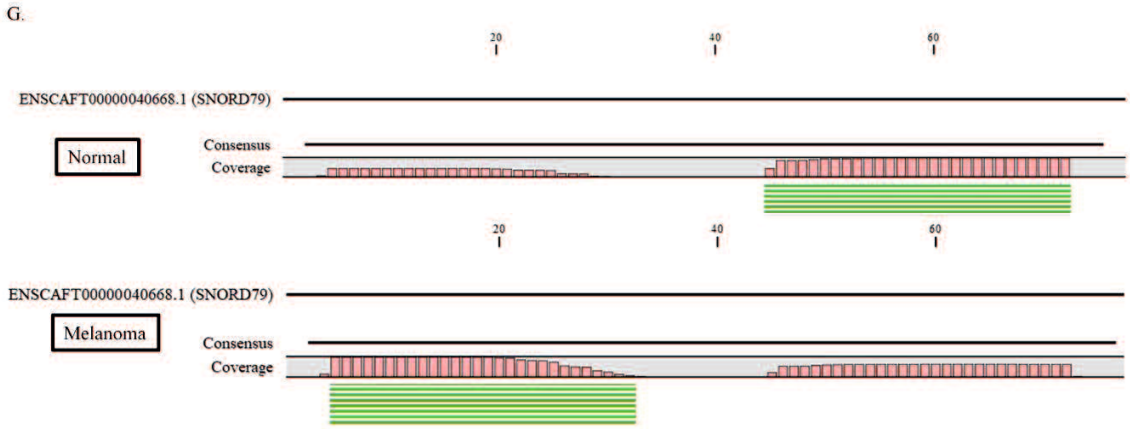

Appendix 2-11. Read mapping of the snoRNA fragments. (A-E) snoRD27, snoRA32, snoRA39, snoRA54, snoRA93 fragments mapping against to the reference. Fragments in normal and melanoma mapped in the same site (3′ or 5′) (F) snoRA24 fragments mapped in the 3′ site in normal and 5′ site in melanoma. (G) snoRD79 fragments mapped in the 5′ site in normal and 3′ site in melanoma.

A. U1 in human genome blastn

Results for BLASTN against Human GRCh38 (Genomic sequence)

Job details

Job name	BLASTN against Human GRCh38 (Genomic sequence)
Species	Human (Homo sapiens)
Assembly	GRCh38
Search type	BLASTN (NCBI Blast)

Download results file

Perfect match with human RNAU1

Results table

Show All entries — Show/hide columns (2 hidden) — Filter

Genomic Location	Overlapping Gene(s)	Orientation	Query start	Query end	Length	Score	E-val	%ID
KI270713:21884-21912 [Sequence]	RF00003	Reverse	1	29	29 [Sequence]	58.0	2e-06	100.00 [Alignment]
CHR_HSCHR1_4_CTG31:144551802-144551830 [Sequence]	RF00003	Reverse	1	29	29 [Sequence]	58.0	2e-06	100.00 [Alignment]
CHR_HSCHR1_4_CTG31:144560691-144560719 [Sequence]	RF00003	Reverse	1	29	29 [Sequence]	58.0	2e-06	100.00 [Alignment]
14:34546826-34546854 [Sequence]	RNU1-27P	Forward	1	29	29 [Sequence]	58.0	2e-06	100.00 [Alignment]
14:34556249-34556277 [Sequence]	RNU1-28P	Reverse	1	29	29 [Sequence]	58.0	2e-06	100.00 [Alignment]
6:13214168-13214196 [Sequence]	PHACTR1, RNU1-11P	Forward	1	29	29 [Sequence]	58.0	2e-06	100.00 [Alignment]
1:16514145-16514173 [Sequence]	RNU1-1	Reverse	1	29	29 [Sequence]	58.0	2e-06	100.00 [Alignment]
1:16666808-16666836 [Sequence]	AL137796.2, RNU1-3	Reverse	1	29	29 [Sequence]	58.0	2e-06	100.00 [Alignment]
1:16740628-16740656 [Sequence]	AL021920.3, CROCC, CROCCP4, RNU1-4	Forward	1	29	29 [Sequence]	58.0	2e-06	100.00 [Alignment]
1:16896092-16896120 [Sequence]	CROCC, RNU1-2	Forward	1	29	29 [Sequence]	58.0	2e-06	100.00 [Alignment]

B. snoRA24 in human genome blastn

Results for BLASTN against Human GRCh38 (Genomic sequence)

Job details

Job name	BLASTN against Human GRCh38 (Genomic sequence)
Species	Human (Homo sapiens)
Assembly	GRCh38
Search type	BLASTN (NCBI Blast)

Download results file

Perfect match with human snoRA24

Results table

Show/hide columns (2 hidden) — Filter

Genomic Location	Overlapping Gene(s)	Orientation	Query start	Query end	Length	Score	E-val	%ID
3:128714678-128714705 [Sequence]	RF00399	Reverse	1	28	28 [Sequence]	48.1	0.002	96.43 [Alignment]
4:118279190-118279216 [Sequence]	SNHG8, SNORA24	Forward	1	27	27 [Sequence]	46.1	0.006	96.30 [Alignment]
12:66681559-66681580 [Sequence]	GRIP1	Forward	4	25	22 [Sequence]	44.1	0.024	100.00 [Alignment]
15:65285567-65285591 [Sequence]	PARP16, SNORA24B	Reverse	1	25	25 [Sequence]	42.1	0.095	96.00 [Alignment]

Appendix 2-12. BLASTN result of U1 snRNA and snoRA24 primer sequences against human GRCh38. (A-B) U1 snRNA and snoRA24a canine primer's were perfectly match with the human U1 snRNA and snoRA24a sequence.

Appendix 3-13. Top 20 expressed genes in the control and melanoma.

Name	Chr. No	Identifier	RPKM	RE%	Rank
KRT13	9	ENSCAFG00000023449	19890.2361	5.43095	1
MT-ATP6	MT	ENSCAFG00000022729	8786.4994	2.39912	2
MT-CO1	MT	ENSCAFG00000022723	7944.76051	2.16928	3
KRT71	27	ENSCAFG00000007233	7541.68833	2.05923	4
COX3	MT	ENSCAFG00000022730	7229.27704	1.97392	5
ENSCAFG00000023728	17	ENSCAFG00000023728	6965.1768	1.90181	6
MT-CO2	MT	ENSCAFG00000022726	6290.5654	1.71761	7
S100A8	7	ENSCAFG00000017557	5616.15702	1.53347	8
ENSCAFG00000029470	7	ENSCAFG00000029470	4441.53065	1.21274	9
MT-ATP8	MT	ENSCAFG00000022728	3456.0191	0.94365	10
ND4	MT	ENSCAFG00000022735	2864.80131	0.78222	11
RPL13A	1	ENSCAFG00000029892	2271.34387	0.62018	12
KRT15	9	ENSCAFG00000023529	1949.26113	0.53224	13
MT-ND1	MT	ENSCAFG00000022713	1874.1061	0.51172	14
RPL17	7	ENSCAFG00000019044	1831.89455	0.50019	15
TPT1	22	ENSCAFG00000004533	1780.72188	0.48622	16
RPS6	11	ENSCAFG00000001615	1763.05161	0.48139	17
S100A6	7	ENSCAFG00000017553	1728.78217	0.47204	18
ENSCAFG00000018586	4	ENSCAFG00000018586	1576.83413	0.43055	19
MT-CYB	MT	ENSCAFG00000022742	1563.5178	0.42691	20

Melanoma-Top 20 expressed genes

Name	**Chr. No**	**Identifier**	**RPKM**	**RE%**	**Rank**
MT-ATP6	MT	ENSCAFG00000022729	6066.67774	1.76435	1
COX3	MT	ENSCAFG00000022730	5040.20294	1.46582	2
MT-CO2	MT	ENSCAFG00000022726	4804.66925	1.39733	3
MT-CO1	MT	ENSCAFG00000022723	4564.04515	1.32735	4
MT-ATP8	MT	ENSCAFG00000022728	2274.78453	0.66157	5
COL1A1	9	ENSCAFG00000017018	1955.6742	0.56876	6
ND4	MT	ENSCAFG00000022735	1932.22042	0.56194	7
GAPDH	27	ENSCAFG00000015077	1760.063	0.51187	8
SPARC	4	ENSCAFG00000017855	1592.01338	0.463	9
VIM	2	ENSCAFG00000004529	1540.70219	0.44808	10
TPT1	22	ENSCAFG00000004533	1448.55914	0.42128	11

ACTG1	9	ENSCAFG00000005734	1374.25346	0.39967	12
FTH1_1	11	ENSCAFG00000030465	1298.52499	0.37765	13
MT-ND1	MT	ENSCAFG00000022713	1280.29762	0.37234	14
APOE	1	ENSCAFG00000004617	1241.31668	0.36101	15
B2M	30	ENSCAFG00000013633	1095.02626	0.31846	16
RPL13A	1	ENSCAFG00000029892	1074.56403	0.31251	17
RPL8	13	ENSCAFG00000001677	1072.15928	0.31181	18
COL1A2	14	ENSCAFG00000002069	1065.72002	0.30994	19
DCT	22	ENSCAFG00000005323	1058.98851	0.30798	20

Chr, chromosome

RPKM, reads per kilobase of exon model per million mapped reads

RE, relative expression

Common genes between the group were marked by color

Appendix 3-14. Novel differentially expressed genes in canine oral melanoma

ENSEMBL ID	Chromosome	Max group mean	Log_2 fold change	FDR p-value
ENSCAFG00000035504	1	11.84891334	7.990528544	1.31565E-06
ENSCAFG00000035871	1	5.375183724	7.858276269	0.01533349
ENSCAFG00000023074	1	9.83181066	6.418872648	5.7903E-06
ENSCAFG00000028453	1	7.091847892	5.113753787	0
ENSCAFG00000030509	1	5.393395026	4.896990937	3.22992E-14
ENSCAFG00000004730	1	111.3153548	4.789783319	7.84708E-13
ENSCAFG00000030746	1	36.46314253	4.549518428	1.35577E-10
ENSCAFG00000024425	1	6.161866656	3.389076645	2.94408E-05
ENSCAFG00000002660	1	7.11058835	3.113049903	2.8645E-05
ENSCAFG00000034249	1	41.54709691	2.691535635	2.44909E-09
ENSCAFG00000030943	1	52.56424385	2.386679663	1.76591E-08
ENSCAFG00000030942	1	52.34896342	2.36467677	1.76278E-08
ENSCAFG00000000399	1	11.97511614	2.316532168	0.005801799
ENSCAFG00000002392	1	11.44992494	1.415091641	0.005701833
ENSCAFG00000002916	1	26.62715237	1.252462889	0.01181013
ENSCAFG00000029151	1	60.47632563	1.218044508	0.034309245
ENSCAFG00000032711	1	16.53203716	-1.045037185	0.047474182
ENSCAFG00000003594	1	43.24507089	-1.1589629	0.019255889
ENSCAFG00000005006	1	11.39903325	-1.4548379	0.000762331
ENSCAFG00000002083	1	45.65808914	-1.926537472	0.000134483
ENSCAFG00000024085	1	5.312288797	-2.038063452	0.017015946
ENSCAFG00000000026	1	52.16175897	-2.152982301	4.44868E-06
ENSCAFG00000024191	1	9.8497097	-3.439525742	1.70002E-05
ENSCAFG00000002237	1	38.26297143	-3.651258288	0.022543198
ENSCAFG00000024559	1	9.089560057	-4.332120047	1.01157E-07
ENSCAFG00000035737	1	5.477306783	-4.584600635	8.63545E-09
ENSCAFG00000028993	1	93.05584988	-6.8596193	0
ENSCAFG00000031912	1	58.0192795	-7.403607581	0
ENSCAFG00000031824	1	10.21649406	-8.437873099	0
ENSCAFG00000033364	2	9.855645082	4.17238559	7.67944E-06
ENSCAFG00000005852	2	47.36075855	2.787247621	1.10304E-07
ENSCAFG00000007705	2	31.23562827	2.030196141	0.000294183
ENSCAFG00000012763	2	32.73403954	1.971982951	4.26304E-05
ENSCAFG00000003894	2	24.03981851	-5.165133229	0
ENSCAFG00000024733	2	25.4897546	-6.636421529	0

ENSCAFG00000014627	3	261.1790712	8.044118048	1.11703E-08
ENSCAFG00000010220	3	5.213834539	3.403507705	0.000210201
ENSCAFG00000016695	3	21.17512727	2.204762499	0.020735339
ENSCAFG00000013979	3	36.23293284	1.454838813	0.022144068
ENSCAFG00000015372	3	13.40211576	-1.528951959	0.003999528
ENSCAFG00000029013	3	41.20800914	-2.588867658	8.75518E-08
ENSCAFG00000036387	4	5.085521306	3.208929883	0.00579167
ENSCAFG00000028981	4	7.574157432	2.270852079	0.003657978
ENSCAFG00000011612	4	45.74082332	-1.052773667	0.038699369
ENSCAFG00000018586	4	1576.83413	-1.476555989	0.044341327
ENSCAFG00000040164	4	19.53998725	-2.447553939	2.27964E-06
ENSCAFG00000023144	4	5.896396964	-6.703027754	2.46133E-14
ENSCAFG00000016093	4	209.8511735	-7.279550499	8.66135E-15
ENSCAFG00000019807	5	13.27244991	6.05652362	5.81285E-12
ENSCAFG00000020220	5	19.75182685	4.987324055	1.28365E-06
ENSCAFG00000036707	5	11.42749399	4.069413256	9.99231E-09
ENSCAFG00000030394	5	9.203802558	3.908964196	0.031418318
ENSCAFG00000023925	5	12.6187247	3.203036116	1.03401E-05
ENSCAFG00000023902	5	6.580662588	2.890178889	0.003875369
ENSCAFG00000032273	5	83.67336552	2.007087472	0.004897718
ENSCAFG00000020333	5	18.2536878	1.48077867	0.04592475
ENSCAFG00000018611	5	8.108729222	-1.280853437	0.024794219
ENSCAFG00000020027	5	24.99885637	-1.654232768	0.001019657
ENSCAFG00000017001	5	5.032567544	-1.706048205	0.017349885
ENSCAFG00000031282	5	6.241250231	-2.300600643	0.001457624
ENSCAFG00000017933	5	8.222279668	-3.117410396	1.3081E-09
ENSCAFG00000016475	6	6.207350609	5.555615085	9.46773E-09
ENSCAFG00000014493	6	9.411892563	5.450061274	1.28977E-10
ENSCAFG00000019365	6	5.720406352	2.007330901	0.000161649
ENSCAFG00000018181	6	81.18196135	1.743825912	0.002028509
ENSCAFG00000019210	6	36.15229119	1.717054924	0.001184475
ENSCAFG00000030466	6	60.39843434	1.593961838	0.015172906
ENSCAFG00000011354	6	13.31082009	1.371791741	0.02691254
ENSCAFG00000032470	6	9.667412844	1.352943984	0.022931305
ENSCAFG00000020150	6	179.6286941	-1.452402091	0.02867968
ENSCAFG00000019812	6	360.4657394	-2.977400921	4.13027E-06
ENSCAFG00000019353	6	17.82418593	-8.62334277	0
ENSCAFG00000013653	6	60.03999718	-9.608857975	0

ENSCAFG00000023230	6	110.0280698	-9.755172915	0
ENSCAFG00000020241	6	183.9605566	-9.904211295	0
ENSCAFG00000030657	7	6.094502238	6.126157191	5.0791E-13
ENSCAFG00000030095	7	31.17087967	5.292306471	1.15748E-10
ENSCAFG00000030495	7	6.406529733	4.38151355	7.06626E-10
ENSCAFG00000011151	7	5.696123664	2.282051734	9.1904E-06
ENSCAFG00000031490	7	71.5800605	2.167537672	0.049096317
ENSCAFG00000030770	7	18.3538727	2.101136582	1.93306E-05
ENSCAFG00000031543	7	5.121222149	1.477593476	0.016524158
ENSCAFG00000028771	7	9.071423725	1.418545759	0.008394907
ENSCAFG00000010830	7	9.944699234	1.288792253	0.030262585
ENSCAFG00000024483	7	5.499134371	-1.469320418	0.026980851
ENSCAFG00000014066	7	5.351742552	-1.638390844	0.005260481
ENSCAFG00000031930	7	127.3999434	-1.731021626	0.000118146
ENSCAFG00000017072	7	11.00622815	-1.964315844	0.000573783
ENSCAFG00000016844	7	8.40582253	-2.29490768	0.001070859
ENSCAFG00000024748	7	12.05486525	-2.34597306	0.000391652
ENSCAFG00000019080	7	11.71493088	-4.997440461	0
ENSCAFG00000011523	7	21.3442383	-6.257916114	0
ENSCAFG00000029470	7	4441.530653	-6.317147271	8.66135E-15
ENSCAFG00000031147	7	132.7355295	-9.052401579	0
ENSCAFG00000031078	8	22.29379605	9.615694414	0.002058616
ENSCAFG00000029996	8	184.8595736	7.343536104	0
ENSCAFG00000030993	8	26.2898926	7.146712593	1.64319E-08
ENSCAFG00000030258	8	585.378127	7.09342349	0
ENSCAFG00000030900	8	60.2735056	7.063696675	9.06275E-09
ENSCAFG00000023944	8	8.551984464	6.691074533	0.000477606
ENSCAFG00000028509	8	195.5497797	6.6020349	8.66135E-15
ENSCAFG00000030001	8	5.544994499	6.499263655	0.000605242
ENSCAFG00000024111	8	36.42339286	6.496687056	1.49372E-10
ENSCAFG00000030894	8	7.883838361	6.234718094	9.40513E-06
ENSCAFG00000030284	8	6.602370696	6.215628147	5.08115E-05
ENSCAFG00000035669	8	9.852235555	6.048882373	2.52329E-13
ENSCAFG00000032358	8	268.1075815	5.707864264	5.27351E-11
ENSCAFG00000014670	8	54.39790355	4.177243121	4.76952E-14
ENSCAFG00000024864	8	29.84926746	4.001831338	5.84382E-11
ENSCAFG00000013905	8	33.00828872	-1.587328465	0.002468675
ENSCAFG00000013883	8	10.89481935	-1.70571124	3.69751E-05

ENSCAFG00000030662	8	56.02102778	-2.881399708	1.53398E-07
ENSCAFG00000030682	8	44.28513998	-3.493394761	2.31026E-11
ENSCAFG00000030632	8	69.62308674	-5.57089491	0
ENSCAFG00000004595	9	5.316570014	9.669021308	0.000930388
ENSCAFG00000031869	9	95.18178455	6.076742279	0
ENSCAFG00000024792	9	11.45011491	4.492638067	1.52219E-13
ENSCAFG00000024944	9	13.08670208	3.884699418	2.08442E-12
ENSCAFG00000029405	9	18.14755016	3.641717992	5.57726E-12
ENSCAFG00000020060	9	14.74740628	3.366275782	7.16723E-06
ENSCAFG00000005705	9	8.84341831	2.993692916	7.379E-05
ENSCAFG00000035696	9	13.56535106	2.432402494	7.52262E-06
ENSCAFG00000031537	9	18.53592654	2.005974341	0.001801798
ENSCAFG00000017532	9	13.5607973	1.730496006	0.001705415
ENSCAFG00000019510	9	31.15019746	1.689203167	0.005314997
ENSCAFG00000011598	9	76.3149409	1.314715694	0.039670467
ENSCAFG00000004905	9	51.40954779	-1.736000438	0.012913181
ENSCAFG00000014799	9	40.18589901	-1.831410924	0.008093531
ENSCAFG00000015156	9	14.58251434	-1.925719996	0.006109203
ENSCAFG00000029346	9	68.10763129	-2.067691372	0.001392657
ENSCAFG00000032099	9	26.07743078	-2.284337191	1.33048E-06
ENSCAFG00000012998	9	12.65787595	-2.328934235	0.001104143
ENSCAFG00000013770	9	21.07570069	-2.737397316	4.45846E-12
ENSCAFG00000029478	9	28.43608154	-3.755747176	4.57446E-09
ENSCAFG00000028642	9	10.93521375	-4.307119162	3.35055E-07
ENSCAFG00000032290	9	29.05642424	-6.60423219	0
ENSCAFG00000032259	9	298.0600534	-8.627843471	0
ENSCAFG00000030805	9	226.851523	-13.83146445	0
ENSCAFG00000030326	10	10.51433181	6.950486503	6.28947E-14
ENSCAFG00000000072	10	22.4997321	2.875203787	6.27621E-09
ENSCAFG00000001689	10	6.405037111	2.697530043	0.000203552
ENSCAFG00000000415	10	117.5359313	2.572415781	0.002637691
ENSCAFG00000030366	10	11.36498223	-1.407651586	0.000961291
ENSCAFG00000023004	10	8.312458864	-1.917253801	0.003657978
ENSCAFG00000030654	11	9.454107243	5.012443858	6.3712E-09
ENSCAFG00000001675	11	26.12739629	3.19227453	0.017608957
ENSCAFG00000000497	11	6.090285607	2.71770156	0.007294829
ENSCAFG00000030323	11	5.490964011	-1.776399549	0.001371287
ENSCAFG00000030529	11	33.47633953	-2.783080879	3.52938E-07

ENSCAFG00000025172	11	13.7708214	-2.976886011	0.049304964
ENSCAFG00000003564	12	28.32039123	7.018257499	8.97162E-07
ENSCAFG00000000686	12	32.97688229	3.377376433	1.64505E-08
ENSCAFG00000023691	12	9.531165787	3.165363812	0.003127103
ENSCAFG00000000492	12	70.16028245	2.851333741	6.56334E-07
ENSCAFG00000002008	12	10.77399764	2.171941847	4.63379E-06
ENSCAFG00000030835	12	7.263951396	2.063464127	0.01402659
ENSCAFG00000000447	12	55.03136949	1.961293592	0.00279692
ENSCAFG00000023724	12	77.94689605	1.278705939	0.011633011
ENSCAFG00000002230	12	10.35125429	-4.282669952	2.1475E-08
ENSCAFG00000024271	12	100.093464	-5.169063803	0
ENSCAFG00000033670	12	5.114319465	-8.57494298	0
ENSCAFG00000000613	12	5.405141424	-8.885612115	2.06869E-06
ENSCAFG00000040421	12	20.76619667	-9.340422965	0
ENSCAFG00000031682	12	12.54351205	-9.53393842	1.67156E-14
ENSCAFG00000000471	12	502.6434471	-14.74161241	0
ENSCAFG00000028960	13	86.42977166	10.6431215	1.13093E-08
ENSCAFG00000025016	13	85.47879686	9.152385829	8.84452E-11
ENSCAFG00000036767	13	9.800816163	6.400432043	2.82928E-05
ENSCAFG00000000798	13	5.037333716	5.469184203	0.024137533
ENSCAFG00000037056	13	5.668552626	3.34473999	0.00572879
ENSCAFG00000030437	13	9.257080107	2.481089364	0.029366224
ENSCAFG00000035602	13	13.93981873	1.87956864	0.00017421
ENSCAFG00000032430	13	121.6158135	-9.458522801	0
ENSCAFG00000030958	14	237.833792	9.555686481	1.52219E-13
ENSCAFG00000002440	14	23.26639053	2.407251465	9.21693E-07
ENSCAFG00000002448	14	31.40147285	1.631262334	0.018899332
ENSCAFG00000033183	14	5.367650894	-2.002234974	0.001280894
ENSCAFG00000036275	14	7.722634884	-2.031970763	0.001984224
ENSCAFG00000008273	15	59.21192407	7.311770646	1.59123E-08
ENSCAFG00000003087	15	8.033511329	2.1511169	0.008591691
ENSCAFG00000004887	15	6.911189519	1.964593226	0.003811336
ENSCAFG00000035346	15	31.53484296	1.876929663	0.009888794
ENSCAFG00000028627	15	5.552740778	1.772338319	0.009847107
ENSCAFG00000005575	16	57.64510766	3.647908552	1.00655E-13
ENSCAFG00000037515	16	107.6213567	3.125051818	6.6514E-07
ENSCAFG00000004543	16	6.816617907	2.642941407	0.00192538
ENSCAFG00000006478	16	32.35042328	-1.893927576	4.70684E-05

ENSCAFG00000003530	16	6.866790759	-2.841989642	6.36442E-09
ENSCAFG00000003221	16	17.00845423	-8.852779959	0
ENSCAFG00000023369	17	12.43810628	9.025580649	0.004531852
ENSCAFG00000015584	17	25.34159938	7.620806798	7.28711E-08
ENSCAFG00000031753	17	111.6859735	6.812037186	0
ENSCAFG00000029676	17	29.49818068	6.608920443	7.56579E-08
ENSCAFG00000011504	17	21.58928444	6.435067104	0
ENSCAFG00000032691	17	27.74508545	5.464913358	4.41417E-07
ENSCAFG00000013697	17	5.681752854	5.172695622	1.78488E-09
ENSCAFG00000008716	17	22.37250093	3.67559889	8.66135E-15
ENSCAFG00000004676	17	7.881443769	2.992185762	2.60136E-05
ENSCAFG00000032813	17	64.87938002	2.510340205	3.77766E-05
ENSCAFG00000033956	17	26.30909345	2.123570876	4.29007E-05
ENSCAFG00000028873	17	8.120066373	2.041988643	0.014279887
ENSCAFG00000039320	17	22.53598103	2.011665176	0.000546326
ENSCAFG00000003477	17	93.43666748	1.841033118	0.002423496
ENSCAFG00000009798	17	15.86203471	1.390682937	0.007833443
ENSCAFG00000023111	17	354.3255735	-1.423676	0.00159774
ENSCAFG00000031309	17	5.674618292	-3.981567365	1.59672E-06
ENSCAFG00000007239	17	29.116383	-4.040764465	1.96716E-05
ENSCAFG00000012022	17	254.5146118	-4.4470522	8.66135E-15
ENSCAFG00000031502	17	16.70667691	-6.186774316	2.46133E-14
ENSCAFG00000033334	17	9.289585898	-10.98779122	1.67709E-09
ENSCAFG00000029234	17	13.6321999	-11.39229998	0
ENSCAFG00000023728	17	6965.176802	-13.0728668	0
ENSCAFG00000030793	18	6.906168635	6.89767843	1.47317E-07
ENSCAFG00000010913	18	21.30361322	2.195604751	3.61531E-06
ENSCAFG00000015053	18	7.572474683	1.810140892	0.004391949
ENSCAFG00000016171	18	6.733095434	1.501024767	0.030352477
ENSCAFG00000015082	18	8.752443586	1.490000824	0.045476794
ENSCAFG00000040425	18	7.649864509	-1.325652033	0.01134781
ENSCAFG00000010698	18	6.782613348	-1.421643737	0.031085516
ENSCAFG00000032173	18	161.6327199	-1.635174338	0.012537178
ENSCAFG00000038408	18	25.56853282	-1.839577047	0.006360489
ENSCAFG00000029403	18	71.23147697	-1.857241406	0.001143626
ENSCAFG00000037290	19	6.609443672	4.039669048	0.002519664
ENSCAFG00000005717	19	8.98263234	1.829891314	0.02855777
ENSCAFG00000037999	19	6.75690743	-8.773042538	0

ENSCAFG00000023396	20	9.624830908	7.377000459	2.54697E-11
ENSCAFG00000013645	20	14.58263198	5.116795935	4.22058E-06
ENSCAFG00000012879	20	31.50231251	4.689566062	0.000262534
ENSCAFG00000013805	20	18.11678566	4.241772322	1.46624E-10
ENSCAFG00000016245	20	13.5365478	3.895977936	1.80398E-10
ENSCAFG00000029989	20	62.67518044	1.592139584	0.002547595
ENSCAFG00000006577	20	40.15492665	1.28581714	0.02463222
ENSCAFG00000017892	20	23.26026818	1.216476764	0.034039575
ENSCAFG00000014978	20	44.7787123	-1.867886567	0.000179305
ENSCAFG00000031302	20	38.82323666	-3.440591213	2.29073E-08
ENSCAFG00000031469	20	6.183341835	-3.554588434	1.04883E-12
ENSCAFG00000015206	21	476.1739252	7.802839134	0
ENSCAFG00000029553	21	235.7557557	7.375427473	0
ENSCAFG00000040603	21	5.899703212	2.139710831	0.031223123
ENSCAFG00000004384	21	137.7959713	2.085913471	0.000124446
ENSCAFG00000029218	21	8.301400317	1.154016603	0.029484632
ENSCAFG00000008336	21	42.02752093	-1.492066625	0.016314754
ENSCAFG00000004857	21	193.3028437	-3.431779804	0.032584178
ENSCAFG00000040404	21	7.232160967	-7.903831499	4.07182E-08
ENSCAFG00000030587	22	33.93408748	3.311947415	3.03031E-05
ENSCAFG00000023746	22	6.424778002	-1.202632832	0.037449692
ENSCAFG00000004602	22	16.16257142	-1.468739242	0.005107483
ENSCAFG00000006540	23	43.98782211	2.815493009	1.50359E-05
ENSCAFG00000031320	23	13.37876644	-1.207485628	0.023938064
ENSCAFG00000031852	23	33.98901851	-1.648026364	0.001182034
ENSCAFG00000008181	23	10.37684255	-3.032187454	3.82046E-07
ENSCAFG00000040319	23	6.340588935	-3.213854659	7.35688E-12
ENSCAFG00000039338	23	14.47409395	-3.231006457	8.89525E-10
ENSCAFG00000028903	23	5.042668697	-4.802915121	1.26197E-05
ENSCAFG00000036793	23	22.84208458	-5.348127779	9.46275E-08
ENSCAFG00000012157	24	27.75430569	6.023733686	0.001071397
ENSCAFG00000007435	24	11.52251298	2.198838745	0.00188214
ENSCAFG00000025524	24	61.67024069	2.065881024	2.0265E-05
ENSCAFG00000009480	24	7.485922906	1.987419966	0.039159775
ENSCAFG00000012643	24	23.97548078	-1.428645618	0.004722781
ENSCAFG00000008000	24	217.8956333	-2.140894775	1.36735E-06
ENSCAFG00000007115	25	6.367529963	1.887623723	0.003275596
ENSCAFG00000008369	25	6.6227376	1.573426641	0.019255889

ENSCAFG00000008104	25	13.03920661	-3.687323509	1.25089E-07
ENSCAFG00000010555	25	11.53777457	-3.939533063	0.000211828
ENSCAFG00000012788	25	5.111924429	-9.542291866	4.13199E-12
ENSCAFG00000031160	25	6.145862568	-10.29637654	0
ENSCAFG00000030158	25	21.35338743	-11.67289691	0
ENSCAFG00000023843	26	32.84709867	10.89789493	0.00034417
ENSCAFG00000031637	26	160.0894375	10.16536199	2.46133E-14
ENSCAFG00000032706	26	46.76126804	10.09829385	2.20328E-09
ENSCAFG00000015176	26	15.83001965	9.31746543	0.00226455
ENSCAFG00000031196	26	117.3001854	9.280131794	7.81035E-14
ENSCAFG00000032328	26	34.33406501	9.151918636	8.40715E-08
ENSCAFG00000029323	26	60.91962248	8.5101226	6.83077E-11
ENSCAFG00000030555	26	70.23522946	8.373409718	2.46133E-14
ENSCAFG00000032325	26	166.3718066	8.158170961	2.63822E-12
ENSCAFG00000024720	26	165.9629161	7.838425146	0
ENSCAFG00000031733	26	15.87122419	7.759508157	9.13843E-08
ENSCAFG00000029236	26	45.97768312	7.625813359	7.06014E-14
ENSCAFG00000032078	26	87.1774074	7.621481734	0
ENSCAFG00000013622	26	32.90772055	7.517514898	7.24938E-07
ENSCAFG00000031786	26	497.5464419	7.498002132	0
ENSCAFG00000031273	26	40.32579269	7.398822446	6.86836E-12
ENSCAFG00000031403	26	76.27499128	7.25233011	9.19387E-12
ENSCAFG00000031806	26	645.9357198	7.033040174	0
ENSCAFG00000030935	26	21.92585697	7.031104073	4.09152E-10
ENSCAFG00000031653	26	50.61092742	6.987647103	0
ENSCAFG00000029493	26	264.9025566	6.875187743	1.58428E-08
ENSCAFG00000028850	26	20.40777678	6.801055021	4.00728E-09
ENSCAFG00000032057	26	1030.146501	6.625580707	3.22992E-14
ENSCAFG00000032249	26	14.74547498	6.507410735	1.41156E-07
ENSCAFG00000014432	26	37.83913442	6.172905188	3.00835E-09
ENSCAFG00000023160	26	9.705257788	5.54375583	0.000141606
ENSCAFG00000030602	26	6.156205964	5.524318344	0.000112626
ENSCAFG00000032195	26	66.24015321	5.370346958	1.23187E-08
ENSCAFG00000029467	26	6.275652456	5.285486988	4.81461E-05
ENSCAFG00000028847	26	7.350395084	5.15195901	9.28871E-05
ENSCAFG00000031415	26	151.0779026	5.126069552	5.94329E-07
ENSCAFG00000028814	26	5.475298382	3.744628212	5.5012E-10
ENSCAFG00000014043	26	9.315090207	3.520563144	9.23561E-07

ENSCAFG00000006533	26	9.378420819	3.287958478	2.28852E-07
ENSCAFG00000015433	26	55.64363616	-1.606026549	0.001567768
ENSCAFG00000014154	26	11.23365129	-3.678529071	0
ENSCAFG00000034742	27	6.366787228	7.737310383	0.000480128
ENSCAFG00000036159	27	59.58527103	5.961706723	4.8607E-05
ENSCAFG00000031299	27	133.7284285	3.70632318	4.76952E-14
ENSCAFG00000016263	27	229.9063389	2.632377517	9.01311E-08
ENSCAFG00000016252	27	7.216717465	2.43881255	0.004374991
ENSCAFG00000031081	27	12.15543778	1.452481677	0.023456803
ENSCAFG00000014684	27	216.6154061	1.196683782	0.027762038
ENSCAFG00000008380	27	18.09306778	-1.708711291	0.002133287
ENSCAFG00000011417	27	108.3009024	-3.178978325	0.002201465
ENSCAFG00000007209	27	143.4421203	-6.043971873	4.26733E-07
ENSCAFG00000008119	29	9.083695237	1.445388418	0.047246834
ENSCAFG00000030471	30	29.01707307	4.061389152	7.2252E-06
ENSCAFG00000017107	30	43.70962071	2.731781862	4.3467E-08
ENSCAFG00000016966	30	309.6540468	2.174448832	0.018722413
ENSCAFG00000017708	30	65.81016401	1.822977056	0.00139088
ENSCAFG00000030087	30	19.27988597	1.677261956	0.003829301
ENSCAFG00000017655	30	554.1272685	1.5182161	0.02925338
ENSCAFG00000017975	30	7.228569269	-1.477224269	0.047283246
ENSCAFG00000013769	30	65.48987731	-3.102552092	8.98877E-09
ENSCAFG00000013154	30	82.1977666	-3.453941172	0
ENSCAFG00000008972	30	18.17520593	-4.959292407	0
ENSCAFG00000009568	31	5.362325892	6.348564651	8.64095E-09
ENSCAFG00000037434	31	37.49518033	2.832063332	2.06068E-06
ENSCAFG00000029022	31	204.9706601	2.554388904	0.000397991
ENSCAFG00000009086	31	25.30822967	2.05434979	9.84932E-05
ENSCAFG00000009065	31	6.434569406	1.536579467	0.006931285
ENSCAFG00000031278	31	10.60218043	-1.157224371	0.032407784
ENSCAFG00000009129	31	13.70062538	-1.507501325	0.00196152
ENSCAFG00000008291	31	14.77854181	-2.25846266	0.006010454
ENSCAFG00000038174	31	14.95569581	-9.290770871	0
ENSCAFG00000024769	32	64.71316476	-6.263568502	0
ENSCAFG00000010410	32	14.27186699	-8.615062238	0
ENSCAFG00000009117	33	11.04003445	-1.464479006	0.0049994
ENSCAFG00000012865	33	37.63126618	-6.290328255	0
ENSCAFG00000008984	34	19.14360198	1.794916741	0.000773881

ENSCAFG00000014222	34	5.180445543	1.303804658	0.013960161
ENSCAFG00000011068	34	6.140061191	-1.513028369	0.037963785
ENSCAFG00000029800	35	37.09904872	1.515849715	0.008714697
ENSCAFG00000009857	35	46.49861294	-1.292701179	0.01823561
ENSCAFG00000033502	35	5.620149551	-1.668664762	0.023291739
ENSCAFG00000030080	36	17.93809951	1.63806603	0.001442281
ENSCAFG00000013060	36	22.21006783	-1.261552467	0.018093887
ENSCAFG00000039936	37	5.27704554	3.076432914	0.000718333
ENSCAFG00000029635	37	193.3391254	-1.571657714	0.00778852
ENSCAFG00000014615	37	15.62828231	-2.177023096	0.022497851
ENSCAFG00000032355	37	13.74313386	-2.694748773	7.18752E-05
ENSCAFG00000036759	38	6.651710318	8.358300704	0.0183053
ENSCAFG00000013015	38	63.84569112	4.162792086	1.67156E-14
ENSCAFG00000013035	38	14.89495302	2.600307096	4.91593E-05
ENSCAFG00000031225	38	5.538333357	1.791742128	0.00343815
ENSCAFG00000035312	38	8.672052101	-6.442356139	0
ENSCAFG00000031355	X	12.57006146	7.220553637	7.72752E-08
ENSCAFG00000017231	X	30.62323839	3.888384804	0.000130448
ENSCAFG00000016072	X	13.9090449	2.666327857	0.000273256
ENSCAFG00000019141	X	277.0573496	-1.266862717	0.016078337
ENSCAFG00000030164	X	473.8678307	-1.319491428	0.025365105
ENSCAFG00000012234	X	123.0443004	-1.520430058	0.003480336
ENSCAFG00000013713	X	17.44095908	-1.833305593	0.000542333
ENSCAFG00000015485	X	128.9887531	-2.337384697	2.48492E-05
ENSCAFG00000019159	X	15.09504116	-3.174399164	0.004468031

genes in CFA1
genes in CFA9

FDR, false discovery rate

CFA, canis familiaris

Appendix 3-15. On genes among the DEGs in canine oral melanoma

Name	Chromosome	Max group mean	Log_2 fold change	FDR p-value
BGN	X	750.6354384	5.44424503	0
CXCL8	13	718.7157383	8.318634019	0
PI3	24	625.5995841	8.475895656	0
SMPDL3A	1	335.9104413	6.23191243	0
CCL2	9	302.6210063	6.954792344	0
SLC2A3	27	199.6855496	5.598058625	0
COL9A2	15	176.5921335	5.412189889	0
SAA1_2	21	174.8578142	9.213325616	0
SERPINE1	6	150.3106455	6.521012952	0
SOX10	10	145.4978994	4.888647866	0
SPP1	32	135.5664837	8.621911023	0
SEMA7A	30	122.2285749	6.330537393	0
EDIL3	3	111.0295024	5.883237274	0
L1CAM	X	108.0680806	5.476332277	0
MATN4	24	98.99814302	7.759292564	0
COL11A1	6	83.54422941	11.55017046	0
SOCS3	9	67.11431284	5.265940518	0
SERPINA1	8	66.87881825	6.24878167	0
TNC	11	66.02479843	6.664087639	0
PLP1	X	64.1002786	4.445243008	0
NES	7	57.12356477	4.821129461	0
PYCR1	9	56.5875883	4.351680632	0
MARCKSL1	2	55.4823409	4.294400236	0
CHI3L1	7	54.53271717	7.868381299	0
COL2A1	27	54.10774133	10.36199764	0
ACAN	3	50.1107608	10.46073103	0
PLEK	10	46.67881402	5.51083778	0
COL9A1	12	41.98627672	9.375337519	0
COL9A3	24	41.57551242	8.411393341	0
IL1B	17	40.81758304	9.979670367	0
ADAMTS4	38	36.64656404	7.530108375	0
IGSF11	33	36.5180056	4.688153859	0
ESM1	4	33.64843512	6.654032082	0
RGS2	38	33.45685671	4.969950737	0

TUBB4A	20	32.984893	5.423221335	0
TMEM176B	16	31.74275472	4.3080645	0
UCHL1	3	31.70497382	6.080937609	0
SLC35F1	1	31.27766386	5.816710967	0
ART3	32	30.49449802	4.143724776	0
GEM	29	29.98151751	4.530547767	0
ST6GALNAC3	6	29.23087882	8.243724801	0
RLBP1	3	28.98452562	8.71996617	0
FADS1	18	28.41153634	4.564978271	0
INSC	21	28.18181586	5.310384396	0
SORCS1	28	26.80615162	4.813094558	0
CHSY1	3	26.00790821	3.498935818	0
DUSP4	16	25.45685187	5.007013785	0
CCL8	9	24.72356943	6.236176168	0
INHBA	18	24.61957437	5.735849396	0
ADAM12	28	24.35623078	7.876380279	0
FFAR2	1	24.35586759	7.672564831	0
SLC11A1	37	24.05122675	4.53015279	0
CXCR4	19	22.27558403	3.793069705	0
SLC16A3	9	21.76429775	4.161894929	0
TNIK	34	19.51839693	4.792793663	0
MBOAT2	17	18.23938883	5.249162506	0
GJC1	9	17.11586399	4.385813844	0
IGF2BP2	34	16.76377122	4.071408692	0
A2M	27	16.57721136	4.338114778	0
SLC37A2	5	16.44347492	4.403598924	0
SCARF2	26	15.87954748	4.477028826	0
CSF3R	15	15.83849636	5.612821052	0
MMP9	24	15.19461628	6.728881362	0
C5AR1	1	14.65109832	4.973092761	0
FOXD3	5	14.25774904	5.80396222	0
TREM2	12	13.96815761	6.088030738	0
ADAMTS7	3	13.81198604	4.777863618	0
VASH2	7	13.58460851	5.048378371	0
RUNX3	2	13.24629468	3.730023224	0
FAM178B	10	13.20160425	6.023586124	0
GDF11	10	12.30694328	4.337278568	0
FZD2	9	12.24540935	5.15308087	0

MS4A7	21	11.32327689	4.467772962	0
DOK5	24	9.644779425	5.120629828	0
COL8A2	15	8.940308919	6.70697219	0
PDZRN3	20	8.346289524	4.293455462	0
SLC2A6	9	7.656551098	4.848285143	0
TNFSF9	20	7.610733382	5.475211044	0
HCK	24	6.575744695	4.471370016	0
ADGRE1	20	5.89952385	6.303668571	0

Genes in chromosome 9 colored red

FDR, false discovery rate

Appendix 3-16. Off genes in DEGs in canine oral melanoma

Name	Chromosome	Max group mean	Log_2 fold change	FDR p-value
KRT13	9	19890.23609	-11.27810332	0
KRT71	27	7541.688327	-15.13319019	0
S100A8	7	5616.157022	-6.39785469	0
ARSF	X	1426.603766	-12.19831506	0
TGM3	24	1376.03872	-15.43829609	0
AQP3	11	1324.472821	-11.7832697	0
S100A14	7	1165.913739	-9.555767692	0
SPRR3	17	1090.426813	-13.23899417	0
S100A2	7	1023.838115	-8.469980831	0
SFN	2	769.2134926	-8.549424168	0
RHCG	3	723.8378326	-12.84073049	0
SPINK5	2	646.388121	-11.37480897	0
S100A16	7	549.0286762	-6.490015324	0
KRT78	27	508.5240706	-11.77812871	0
PERP	1	425.0318481	-8.339934272	0
GPX2	8	421.0816574	-8.94888878	0
TRIM29	5	399.6917575	-9.963230323	0
JUP	9	392.6518664	-4.917058359	0
MALL	17	368.7054814	-6.942210838	0
HSPA2	8	359.5941666	-5.719842035	0
HOPX	13	348.4567723	-8.446232254	0
CRNN	17	329.4546465	-13.23498636	0
PPL	6	316.8138888	-5.925841609	0
KRT3	27	284.9690046	-11.5287632	0
PKP1	7	264.2402015	-9.97491112	0
LYPD3	1	253.4635322	-11.98501	0
CESdD1	2	242.3369351	-9.074733907	0
TGM1	8	198.4040362	-8.598541013	0
A2ML1	27	192.0014741	-11.68778195	0
PDZK1IP1	15	188.871261	-8.449622852	0
EPS8L1	1	188.6684038	-9.850882677	0
DSG3	7	181.8460663	-9.188266586	0
CEACAM1	1	175.1950229	-5.598487054	0
EVPL	9	174.4026625	-7.83401447	0

TUBA4A	37	173.6161404	-3.660833864	0
MAL2	13	171.869597	-8.425049634	0
DSC2	7	167.1611035	-9.046837738	0
PDLIM2	25	163.3938192	-4.086152736	0
DSG1	7	157.6500116	-11.14337884	0
BARX2	5	153.2732291	-8.928156407	0
ENDOU	27	146.5467812	-10.28185326	0
KLF5	22	140.6824284	-5.235251895	0
XDH	17	136.0175304	-6.284603096	0
CST6	18	132.7387439	-7.931622359	0
NQO2	35	132.3729592	-4.249273859	0
SERPINB5	1	131.8707576	-8.009000575	0
PLA2G4E	30	131.7089616	-11.56597866	0
RAB25	7	119.8805087	-8.850339947	0
TMEM40	20	119.1956888	-6.613357439	0
C17orf64	9	118.7326899	-4.643270197	0
LYPD2	13	117.9723538	-11.90277481	0
TMPRSS11B	13	116.7217861	-10.92330889	0
FAR2	27	116.2202206	-4.331541322	0
GMDS	35	114.0219233	-3.408339763	0
MPZL2	5	112.2013084	-7.85328996	0
ZNF185	X	111.3300308	-8.382905376	0
CNFN	1	110.6681351	-11.95449818	0
SPINT2	1	108.9695695	-4.002896704	0
EPS8L2	18	108.9080551	-9.136373848	0
C6orf132	12	108.4889688	-9.944674018	0
PROM2	17	96.99216499	-9.166619181	0
FAM3B	31	88.80701186	-7.276605709	0
NCCRP1	1	82.22099537	-9.355733866	0
COL17A1	28	81.8956081	-6.941030185	0
GDPD2	X	77.85340637	-8.802339306	0
SDR16C5	29	76.90958799	-4.952598006	0
EHF	18	74.20591096	-8.795046291	0
FAM84A	17	71.77350126	-6.674520814	0
CLDN7	5	71.28433678	-8.835003177	0
GDA	1	70.50485567	-6.832127371	0
SCEL	22	69.64286873	-7.742400007	0
HEBP2	1	69.09456765	-3.759529488	0

PLEKHN1	5	66.84102914	-4.443524281	0
EPHA1	16	66.45172064	-7.946281305	0
KLK13	1	65.02592188	-10.13612317	0
ADH4	32	63.99430127	-4.158050237	0
ESRP1	29	63.92067475	-5.892612427	0
AOX4	37	60.56542979	-14.72852032	0
BNIPL	17	59.66141244	-7.187272907	0
LRAT	15	57.67829118	-5.723888362	0
TMPRSS11D	13	56.92664447	-9.634077799	0
CHST2	23	55.45352498	-4.181653073	0
CLCA2	6	54.48585804	-8.190137593	0
KRTDAP	1	54.33789416	-11.09403133	0
ALOX12	5	54.06128613	-9.164408556	0
CABP7	26	53.76159879	-9.567082013	0
LAD1	7	52.65142816	-6.891889737	0
C1orf56	17	52.63065403	-6.386077061	0
DSC3	7	51.40139622	-6.648335402	0
TTC22	5	50.29803546	-11.1495017	0
DUOXA1	30	50.21815698	-7.019517562	0
ARG1	12	49.60814265	-6.277971196	0
MBOAT1	35	49.52901996	-3.918167764	0
KRT23	9	49.09132421	-10.393661	0
SPTBN2	18	47.49138337	-7.366144613	0
SYTL1	2	47.40785241	-5.728325717	0
PLEKHG6	27	45.85035153	-6.179629637	0
IL20RB	23	45.78583859	-7.475325507	0
GRHL3	2	45.50188756	-6.302418543	0
RHOV	30	45.30762005	-7.537606319	0
MUC1	7	44.44088729	-8.588611826	0
CYP2S1	1	43.98564679	-6.256130234	0
NECTIN4	38	43.51791614	-8.500449702	0
TP63	34	42.46840701	-8.07667911	0
HS3ST1	3	42.33630969	-4.831068594	0
FAM3D	20	42.15501103	-8.803523301	0
CLIC3	9	42.02216527	-4.265788985	0
GALNT12	11	41.89259721	-3.826535249	0
SLC5A1	26	41.68426716	-8.934676382	0
CLIP4	17	41.60297447	-5.158483888	0

ANKRD35	17	40.40621862	-7.443869519	0
PKP3	18	40.07215199	-6.367002512	0
GRHL1	17	39.79987313	-4.780505725	0
CDSN	12	39.76682735	-11.85574382	0
ESRP2	5	39.50157807	-7.693655986	0
SOX15	5	39.47297421	-9.51471629	0
CGN	17	38.80144712	-7.775395193	0
SPINT1	30	38.580219	-3.827957932	0
IL20RA	1	38.49181689	-8.348959308	0
SMPDL3B	2	38.21618713	-9.918698068	0
SPINK7	4	38.03730634	-9.855097766	0
TMPRSS11E	13	36.42410118	-7.352274898	0
RIPK4	31	35.78680706	-7.856906774	0
TMEM54	2	35.63985487	-5.580536098	0
C6orf15	12	35.51311619	-10.76461291	0
STAP2	20	35.02659593	-6.243554927	0
IRF6	7	34.49076457	-7.991614378	0
HSD17B2	5	34.03444573	-9.10628083	0
POF1B	X	33.84606903	-12.73266555	0
CLDN4	6	33.50129554	-6.457999422	0
PPP1R13L	1	33.37160131	-4.085268758	0
ANKK1	5	33.27515374	-9.338431467	0
FAM83G	5	32.79341847	-5.365068721	0
ELF5	18	32.75766934	-9.374368486	0
TMPRSS4	5	31.46008299	-9.434065004	0
AANAT	9	30.89220658	-11.21422557	0
KYNU	19	30.07507193	-6.749045979	0
EPHX2	25	29.96399416	-4.034886823	0
TREH	5	29.56405015	-8.549458864	0
CSTA	33	29.54043546	-10.14908405	0
LRMP	27	29.04498102	-4.779188461	0
BICDL2	6	28.98819319	-7.82788282	0
GDPD3	6	28.94879417	-4.347563411	0
ATP12A	25	28.65361365	-11.94139841	0
RAB27B	1	28.61134622	-6.003524089	0
TMPRSS11A	13	28.35601638	-8.104809826	0
RDH12	8	28.3262372	-7.560892775	0
KRT80	27	27.62915494	-8.68144252	0

GGT6	5	27.38341327	-8.535082222	0
TMPRSS13	5	27.28094265	-9.770239081	0
CNKSR1	2	27.00110021	-4.281848536	0
AP1M2	20	26.91699275	-5.356706606	0
ALS2CL	20	26.21858236	-4.206422748	0
ZBED2	33	26.08682324	-6.297105636	0
SH3RF2	2	26.06971098	-7.179493255	0
IL36RN	17	26.01093733	-9.341129084	0
PDIA2	6	25.85662469	-7.110683038	0
RUFY4	37	25.82301633	-6.689425763	0
TMEM45B	5	25.7123222	-10.13047238	0
B3GNT5	34	25.71219665	-4.055454124	0
C1GALT1	14	25.55569358	-3.078975639	0
GPR87	23	25.11729782	-7.518683088	0
CYP2F1	1	24.91217599	-10.64725496	0
IL36B	17	24.29830764	-10.1884871	0
EXPH5	5	24.04954658	-7.422051039	0
ARHGEF37	4	23.90091682	-4.101988366	0
GRHL2	13	22.95302906	-7.090051723	0
NKPD1	1	22.63283821	-8.452922601	0
GSDMC	13	22.60636832	-9.603398397	0
DUOXA2	30	22.27003137	-7.920336383	0
SLC23A1	2	21.20754115	-8.789255736	0
NUAK2	38	20.87615921	-4.534815198	0
TMEM184A	6	20.28052305	-6.865285987	0
MUC13	33	19.58598328	-7.564317637	0
CDC42BPG	18	19.29081546	-4.858554731	0
ST14	5	18.81560139	-5.234973033	0
FAM83F	10	17.64987761	-8.156806194	0
TNK1	5	17.1922582	-6.714137634	0
GRTP1	22	17.16713588	-6.089605064	0
CHST4	5	16.38817655	-6.030041784	0
TPRG1	34	16.24330446	-9.144849835	0
CA13	29	16.06240131	-4.572811377	0
CYP4F22	20	16.00054878	-8.448566843	0
ENPP3	12	15.73591122	-6.955233073	0
VSIG8	38	15.4742638	-8.595329762	0
SULT2B1	1	15.38530237	-11.06719657	0

GRB7	9	14.78124309	-7.210497176	0
PERM1	5	14.56814103	-4.328570776	0
PINLYP	1	14.43747612	-8.900605552	0
UOX	6	14.12314725	-9.99558118	0
EPCAM	10	14.02221204	-5.9102022	0
SLC16A14	25	13.98914226	-5.833867393	0
CRYBG2	2	13.71330124	-9.316434578	0
RERG	27	13.46529789	-4.210980897	0
CERS3	3	13.37680942	-6.390784606	0
B3GNT3	20	13.06437493	-9.677046242	0
MAP3K9	8	12.9655026	-5.213603812	0
TFCP2L1	19	12.78063181	-6.855905113	0
SH3YL1	17	12.30152916	-8.164356369	0
CBD103	16	12.14940309	-6.623107681	0
KLK10	1	12.04110114	-11.29032103	0
VSIG10L	1	11.72203298	-4.021121331	0
NIPAL4	4	11.36823391	-5.636521888	0
FAM83B	12	11.35691949	-6.902951987	0
TSPAN1	15	11.23532252	-7.626618447	0
KRT24	9	10.9282437	-7.795783141	0
LAMB4	18	10.76789625	-7.738614171	0
KLC3	1	10.21558535	-4.983898262	0
FAT2	4	10.10026093	-7.059346028	0
PLB1	17	10.03151038	-6.820846713	0
KRT76	27	10.00303904	-7.781596414	0
RASAL1	26	9.914484962	-5.231825243	0
GCNT3	30	9.64100525	-8.821882395	0
OTX1	10	9.400832053	-7.139509013	0
EPN3	9	9.340281336	-6.719854591	0
PPFIA3	1	9.307617618	-4.786054379	0
HAL	15	9.052170666	-9.167994737	0
URAD	25	8.662519843	-9.477314423	0
PLCH2	5	8.556582898	-7.22832828	0
WNT7B	10	8.282207381	-6.459758306	0
RHBG	7	8.252745845	-4.975324328	0
TMEM229A	14	8.074741564	-6.99224761	0
PATJ	5	7.964707289	-5.054861007	0
ATP2C2	5	7.856871558	-5.28363047	0

TGM5	30	7.828857404	-8.385477976	0
DUOX2	30	7.47593459	-8.551717179	0
CASZ1	2	7.327772011	-4.909469545	0
SLC52A3	24	7.094603109	-6.983622534	0
SLC5A9	15	7.019467879	-10.90095694	0
OCLN	2	6.800594627	-5.707425329	0
FRRS1	6	6.47276621	-4.522727843	0
RASEF	1	6.345978805	-7.734390047	0
CARD14	9	6.160800999	-9.618344576	0
STRA8	16	5.998313291	-9.447989179	0
BAIAP3	6	5.615411704	-4.978535361	0
CNDP1	1	5.595804245	-7.640356862	0
ADGRF4	12	5.516455443	-7.474817855	0
SLC22A18	18	5.439037365	-6.232460287	0
PRSS8	6	5.383872336	-8.192263369	0
SLC19A3	25	5.214792847	-8.886948941	0
RNF39	35	5.14620547	-8.393614658	0

Genes in the chromosome 1 colored green

FDR, false discovery rate

Appendix 3-17. On genes among novel genes in canine oral melanoma

Name	Chromosome	Max group mean	Log_2 fold change	FDR p-value
ENSCAFG00000031806	26	645.936	7.03304	0
ENSCAFG00000030258	8	585.378	7.09342	0
ENSCAFG00000031786	26	497.546	7.498	0
ENSCAFG00000015206	21	476.174	7.80284	0
ENSCAFG00000029553	21	235.756	7.37543	0
ENSCAFG00000029996	8	184.86	7.34354	0
ENSCAFG00000024720	26	165.963	7.83843	0
ENSCAFG00000031753	17	111.686	6.81204	0
ENSCAFG00000031869	9	95.1818	6.07674	0
ENSCAFG00000032078	26	87.1774	7.62148	0
ENSCAFG00000031653	26	50.6109	6.98765	0
ENSCAFG00000011504	17	21.5893	6.43507	0
ENSCAFG00000028453	1	7.09185	5.11375	0

FDR, false discovery rate

Appendix 3-18. Off genes among novel genes in canine oral melanoma

Name	Chromosome	Max group mean	Log_2 fold change	FDR p-value
ENSCAFG00000023728	17	6965.18	-13.073	0
ENSCAFG00000000471	12	502.643	-14.742	0
ENSCAFG00000032259	9	298.06	-8.6278	0
ENSCAFG00000030805	9	226.852	-13.831	0
ENSCAFG00000020241	6	183.961	-9.9042	0
ENSCAFG00000031147	7	132.736	-9.0524	0
ENSCAFG00000032430	13	121.616	-9.4585	0
ENSCAFG00000023230	6	110.028	-9.7552	0
ENSCAFG00000024271	12	100.093	-5.1691	0
ENSCAFG00000028993	1	93.0558	-6.8596	0
ENSCAFG00000013154	30	82.1978	-3.4539	0
ENSCAFG00000030632	8	69.6231	-5.5709	0
ENSCAFG00000024769	32	64.7132	-6.2636	0
ENSCAFG00000013653	6	60.04	-9.6089	0
ENSCAFG00000031912	1	58.0193	-7.4036	0
ENSCAFG00000012865	33	37.6313	-6.2903	0
ENSCAFG00000032290	9	29.0564	-6.6042	0
ENSCAFG00000024733	2	25.4898	-6.6364	0
ENSCAFG00000003894	2	24.0398	-5.1651	0
ENSCAFG00000030158	25	21.3534	-11.673	0
ENSCAFG00000011523	7	21.3442	-6.2579	0
ENSCAFG00000040421	12	20.7662	-9.3404	0
ENSCAFG00000008972	30	18.1752	-4.9593	0
ENSCAFG00000019353	6	17.8242	-8.6233	0
ENSCAFG00000003221	16	17.0085	-8.8528	0
ENSCAFG00000038174	31	14.9557	-9.2908	0
ENSCAFG00000010410	32	14.2719	-8.6151	0
ENSCAFG00000029234	17	13.6322	-11.392	0
ENSCAFG00000019080	7	11.7149	-4.9974	0
ENSCAFG00000014154	26	11.2337	-3.6785	0
ENSCAFG00000031824	1	10.2165	-8.4379	0
ENSCAFG00000035312	38	8.67205	-6.4424	0
ENSCAFG00000037999	19	6.75691	-8.773	0

ENSCAFG00000031160	25	6.14586	-10.296	0
ENSCAFG00000033670	12	5.11432	-8.5749	0

FDR, false discovery rate

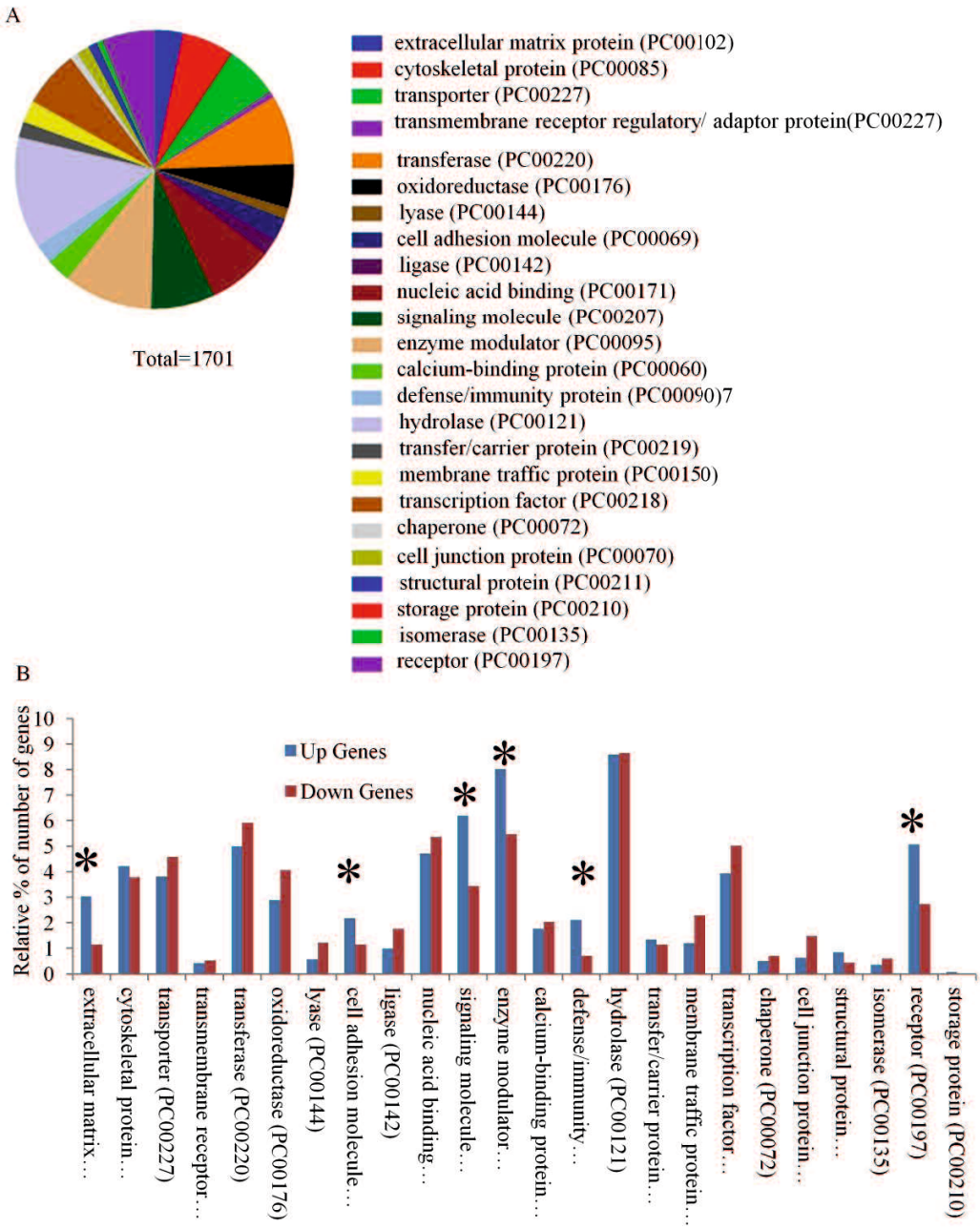
A
Total=1701
extracellular matrix protein (PC00102)
cytoskeletal protein (PC00085)
transporter (PC00227)
transmembrane receptor regulatory/ adaptor protein(PC00227)
transferase (PC00220)
oxidoreductase (PC00176)
lyase (PC00144)
cell adhesion molecule (PC00069)
ligase (PC00142)
nucleic acid binding (PC00171)
signaling molecule (PC00207)
enzyme modulator (PC00095)
calcium-binding protein (PC00060)
defense/immunity protein (PC00090)7
hydrolase (PC00121)
transfer/carrier protein (PC00219)
membrane traffic protein (PC00150)
transcription factor (PC00218)
chaperone (PC00072)
cell junction protein (PC00070)
structural protein (PC00211)
storage protein (PC00210)
isomerase (PC00135)
receptor (PC00197)
B
Relative % of number of genes
Up Genes
Down Genes
extracellular matrix…
cytoskeletal protein…
transporter (PC00227)
transmembrane receptor…
transferase (PC00220)
oxidoreductase (PC00176)
lyase (PC00144)
cell adhesion molecule…
ligase (PC00142)
nucleic acid binding…
signaling molecule…
enzyme modulator…
calcium-binding protein…
defense/immunity…
hydrolase (PC00121)
transfer/carrier protein…
membrane traffic protein…
transcription factor…
chaperone (PC00072)
cell junction protein…
structural protein…
isomerase (PC00135)
receptor (PC00197)
storage protein (PC00210)

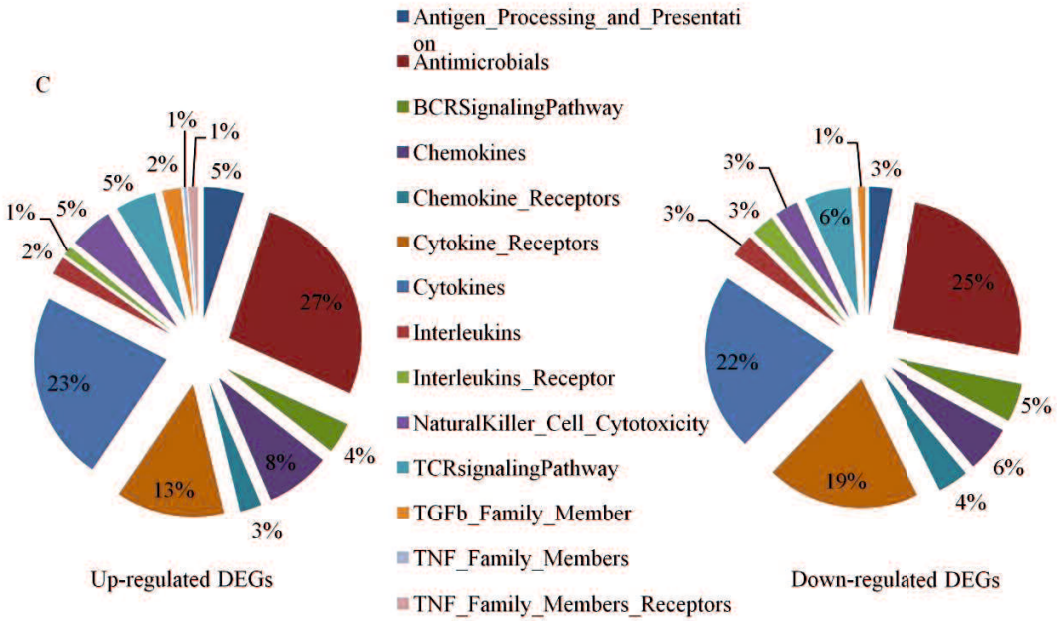

Appendix 3-19. Protein classification of differentially expressed genes using the PANTHER protein classification database. (A) Chart of the distribution of the genes in the 24 protein classes. (B) Bar graph of percentages of up- and downregulated genes in each class. Percent of relative differences between the up- and downregulated genes in each protein class 1< marked with *. (C) Landscape of immunogens in canine oral melanoma. Percentage of immunogens of each terms under the up and down-regulated DEGs groups.

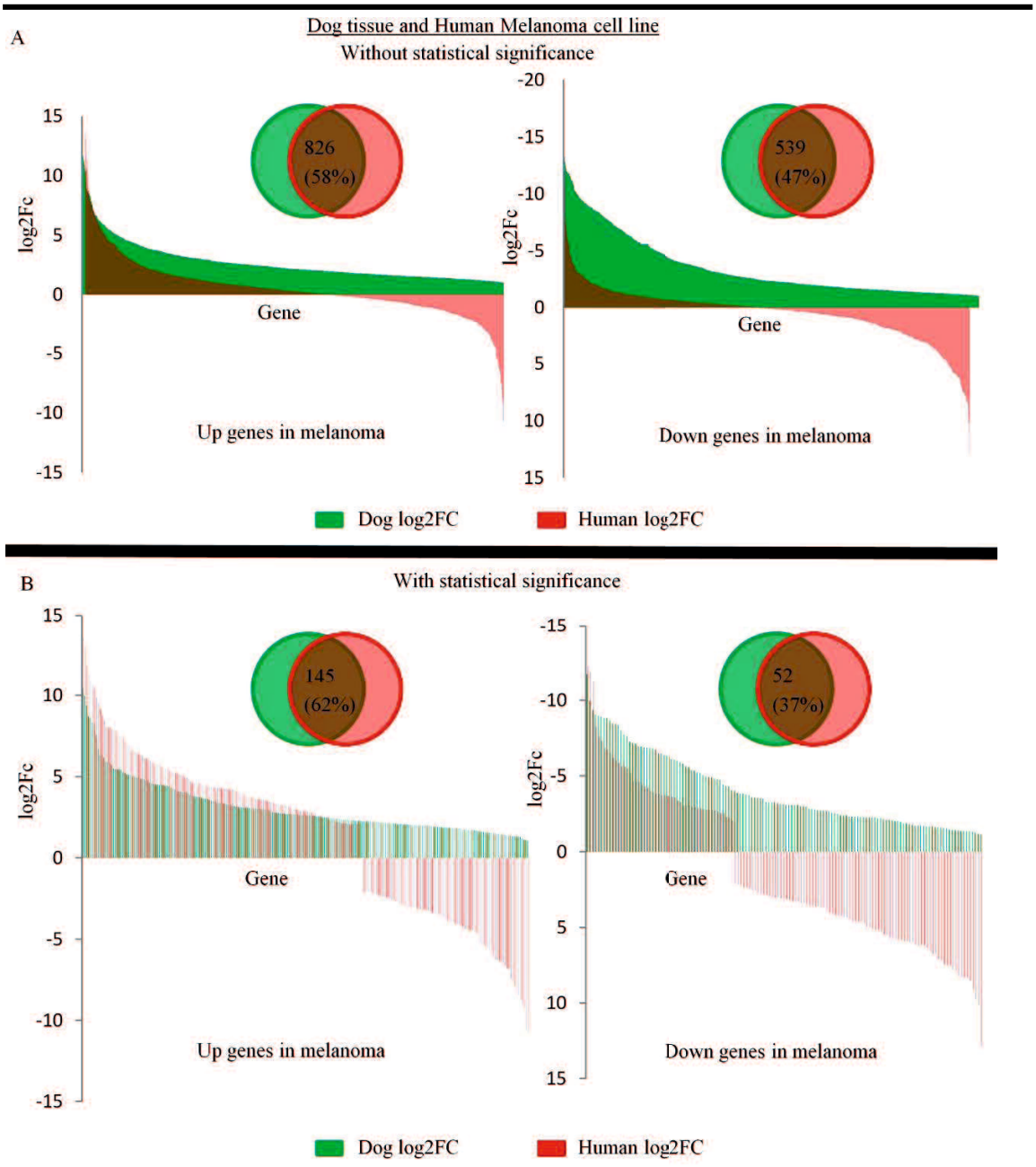

Appendix 3-20. Differentially expressed genes between human melanoma cell lines and dog melanoma. (A) Similarities of up- and downregulated genes with similar fold change between the species without considering statistical significance from cell lines. (B) Similarities of up and downregulated genes with similar fold change between the species

considering statistical significance. The x-axis indicates the number of genes and the y-axis indicates the fold change (FC).

Appendix 3-21. Common significant altered genes between human tissue and dog melanoma.

Available: https://www.spandidos-publications.com/10.3892/or.2019.7391 (Supplementary_Data 2_Table SX)

Appendix 3-22. Common significant altered genes between dog and human cell lines.

Available: https://www.spandidos-publications.com/10.3892/or.2019.7391 (Supplementary_Data 2_Table SXII)

Appendix 3-23. Melanoma signature genes and genes reported in MGDB

Available: https://www.spandidos-publications.com/10.3892/or.2019.7391 (Supplementary_Data 2_Table SXIV)

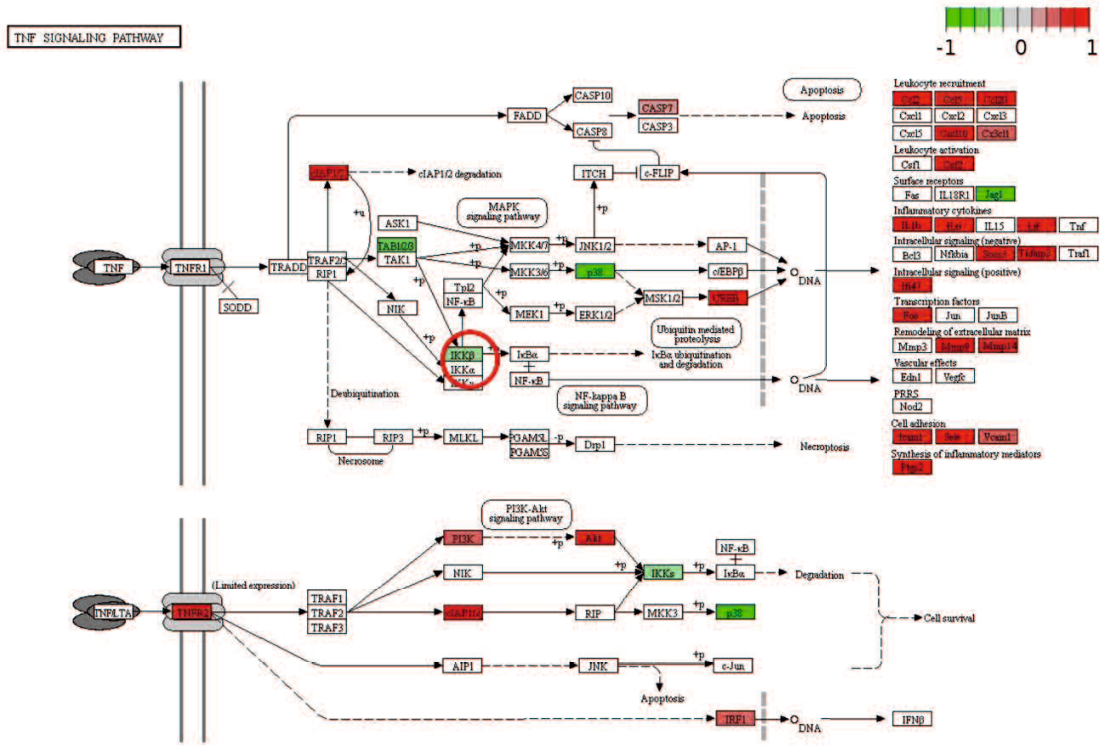

Appendix 3-24. TNF signaling pathway. Gene expression is indicated by the color gradient; red indicates upregulated and green indicates downregulated in melanoma. For example, IKKß (encircled in red) is shown in green to represent its down-regulation in canine oral melanoma. Data on KEGG graph rendered by Pathview.

Appendix 3-25. Significantly upregulated NF-kB or STAT3 shared target genes

Dog Ensembel gene Id	Dog log2Fc	Human log2Fc	Human Ensembel gene Id
ENSCAFG00000015205	11.74117065	6.147727722	ENSG00000173432
ENSCAFG00000002733	10.85176402	3.788697646	ENSG00000136244
ENSCAFG00000003029	8.318634019	3.706461398	ENSG00000169429
ENSCAFG00000018349	6.954792344	2.306089365	ENSG00000108691
ENSCAFG00000015054	6.766954348		ENSG00000196611
ENSCAFG00000009905	6.728881362	11.93250094	ENSG00000100985
ENSCAFG00000013762	5.792667258	1.722175318	ENSG00000073756
ENSCAFG00000005306	5.265940518	5.852970103	ENSG00000184557
ENSCAFG00000013973	5.109736831		ENSG00000131095
ENSCAFG00000015155	4.687783993	1.363270096	ENSG00000102265
ENSCAFG00000025567	4.338114778		ENSG00000175899
ENSCAFG00000001711	3.857528725	1.217652705	ENSG00000100292
ENSCAFG00000009421	3.647513919		ENSG00000087245
ENSCAFG00000011197	2.420410341	0.356342293	ENSG00000157227
ENSCAFG00000000280	2.401717671	0.859553955	ENSG00000135446
ENSCAFG00000001938	2.122546889	3.714252105	ENSG00000112715
ENSCAFG00000031460	1.993356536	2.268718109	ENSG00000090339
ENSCAFG00000005302	1.685674443	0.623320797	ENSG00000089685
ENSCAFG00000014463	1.621550065	7.445565895	ENSG00000111679
ENSCAFG00000000851	1.38162827	2.60012	ENSG00000125347
ENSCAFG00000005014	1.047362106	1.237842317	ENSG00000105329

Fc, fold change

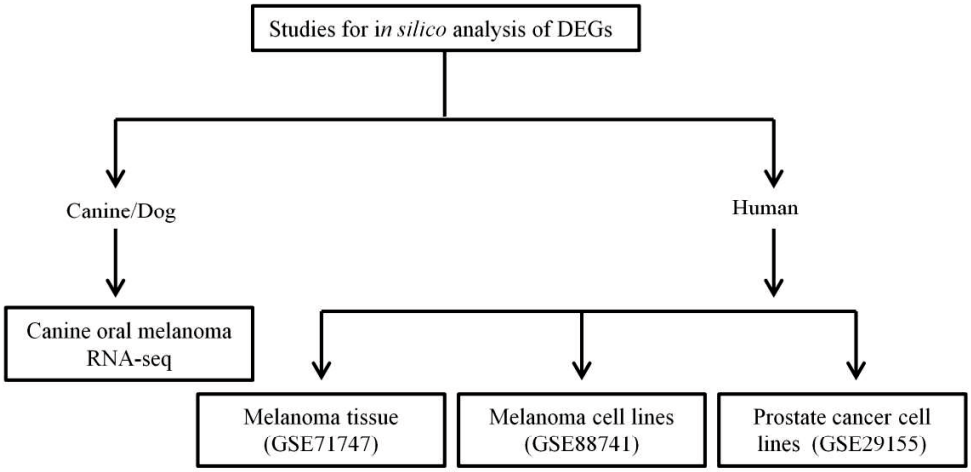

Appendix 3-26. Melanoma experiments used for the *in silico* cross species analysis of differentially expressed genes (DEGs).

References

1. Okechukwu IB. Introductory Chapter: Animal Models for Human Diseases, a Major Contributor to Modern Medicine. In: Experimental Animal Models of Human Diseases - An Effective Therapeutic Strategy. 2018. p. 23:1.
2. Hajar R. Animal testing and medicine. Heart Views. 2011;12(1):42.
3. Conn PM. Animal Models for the Study of Human Disease. 2007 Jun 2. Animal Models for the Study of Human Disease. Academic Press; 2013.
4. Ibeh BO, Furuta Y, Habu JB, Ogbadu L. Humanized mouse as an appropriate model for accelerated global HIV research and vaccine development: current trend. Immunopharmacol Immunotoxicol. 2016;38(6):395–407.
5. Swearengen JR. Choosing the right animal model for infectious disease research. Anim Model Exp Med. 2018;1(2):100–8.
6. Curry SH. Why have so many drugs with stellar results in laboratory stroke models failed in clinical trials? A theory based on allometric relationships. Ann N Y Acad Sci. 2003;993(1):69–74.
7. Mak IWY, Evaniew N, Ghert M. Lost in translation: Animal models and clinical trials in cancer treatment. Am J Transl Res. 2014;6(2):114.
8. Bart van der Worp H, Howells DW, Sena ES, Porritt MJ, Rewell S, O'Collins V, et al. Can animal models of disease reliably inform human studies? PLoS Med. 2010;30(7):e1000245.
9. Akhtar A. The Flaws and Human Harms of Animal Experimentation. Cambridge Q Healthc Ethics. 2015;24(4):407–19.
10. Conn PM. Source book of models for biomedical research. Source Book of Models for Biomedical Research. Springer Science & Business Media; 2008.
11. Leiter EH. The NOD Mouse: A Model for Insulin-Dependent Diabetes Mellitus. In: Current Protocols in Immunology. 2001. p. 15–9.
12. Fransén-Pettersson N, Duarte N, Nilsson J, Lundholm M, Mayans S, Larefalk Å, et al. A new mouse model that spontaneously develops chronic liver inflammation and fibrosis. PLoS One. 2016;11(7):e0159850.
13. Hytönen MK, Lohi H. Canine models of human rare disorders. Rare Dis. 2016;4(1):e1006037.
14. Pinho SS, Carvalho S, Cabral J, Reis CA, Gärtner F. Canine tumors: A spontaneous

animal model of human carcinogenesis. Transl Res. 2012;159(3):165–72.

15. Morey DF. Dogs: Domestication and the development of a social bond. Cambridge University Press; 2010.

16. Freedman AH, Lohmueller KE, Wayne RK. Evolutionary history, slective sweeps, and deleterious variation in the dog. Annu Rev Ecol Evol Syst. 2016;47(Nov 1):73–96.

17. Frantz LAF, Mullin VE, Pionnier-Capitan M, Lebrasseur O, Ollivier M, Perri A, et al. Genomic and archaeological evidence suggests a dual origin of domestic dogs. Science (80-). 2016;352(6290):1228–31.

18. Botigué LR, Song S, Scheu A, Gopalan S, Pendleton AL, Oetjens M, et al. Ancient European dog genomes reveal continuity since the Early Neolithic. Nat Commun. 2017;8:1682.

19. Wayne RK, Ostrander EA. Lessons learned from the dog genome. Trends Genet. 2007;23(11):557–67.

20. Parker HG, Ostrander EA. Canine genomics and genetics: Running with the pack. PLoS Genet. 2005;1(5):e58.

21. Patterson DF. Companion animal medicine in the age of medical genetics. J Vet Intern Med. 2000;14(1):1–9.

22. Karlsson EK, Lindblad-Toh K. Leader of the pack: Gene mapping in dogs and other model organisms. Nat Rev Genet. 2008;9(9):713.

23. Switonski M. Dog as a model in studies on human hereditary diseases and their gene therapy. Reprod Biol. 2014;14(1):44–50.

24. Tsai KL, Clark LA, Murphy KE. Understanding hereditary diseases using the dog and human as companion model systems. Mamm Genome. 2007;18(6–7):444–51.

25. Schütt T, Helboe L, Pedersen LØ, Waldemar G, Berendt M, Pedersen JT. Dogs with cognitive dysfunction as a spontaneous model for early alzheimer's disease: a translational study of neuropathological and inflammatory markers. J Alzheimer's Dis. 2016;52(2):433–49.

26. Nødtvedt A, Berke O, Bonnett BN, Brønden L. Current status of canine cancer registration - report from an international workshop. Vet Comp Oncol. 2012;10(2):95–101.

27. Baioni E, Scanziani E, Vincenti MC, Leschiera M, Bozzetta E, Pezzolato M, et al. Estimating canine cancer incidence: Findings from a population-based tumour registry in northwestern Italy. BMC Vet Res. 2017;13(1):203.

28. Boo G, Leyk S, Fabrikant SI, Graf R, Pospischil A. Exploring uncertainty in canine cancer data sources through dasymetric refinement. Front Vet Sci. 2019;(6):45.

29. Schiffman JD, Breen M. Comparative oncology: What dogs and other species can teach us about humans with cancer. Philos Trans R Soc B Biol Sci. 2015;370(1673):20140231.

30. Lindblad-Toh K, Wade CM, Mikkelsen TS, Karlsson EK, Jaffe DB, Kamal M, et al. Genome sequence, comparative analysis and haplotype structure of the domestic dog. Nature. 2005;438(8):803–19.

31. Valli VE, Myint M, Barthel A, Bienzle D, Caswell J, Colbatzky F, et al. Classification of canine malignant lymphomas according to the world health organization criteria. Vet Pathol. 2011;48(1):198–211.

32. Lunn KF, Page RL. Withrow and MacEwen's Small Animal Clinical Oncology. Withrow and MacEwen's Small Animal Clinical Oncology, 5/e. 2013.

33. Parkin DM. The evolution of the population-based cancer registry. Nat Rev Cancer. 2006;6(8):603.

34. Brønden LB, Flagstad A, Kristensen AT. Veterinary cancer registries in companion animal cancer: A review. Vet Comp Oncol. 2007;5(3):133–44.

35. Fenger JM, London CA, Kisseberth WC. Canine osteosarcoma: A naturally occurring disease to inform pediatric oncology. ILAR J. 2014;55(1):69–85.

36. Merlo DF, Rossi L, Pellegrino C, Ceppi M, Cardellino U, Capurro C, et al. Cancer incidence in pet dogs: Findings of the animal tumor registry of Genoa, Italy. J Vet Intern Med. 2008;22(4):976–84.

37. Hortobagyi GN, Connolly JL, D'Orsi CJ, Edge SB, Mittendorf EA, Rugo HS, et al. AJCC Cancer Staging Manual: Breast. AJCC Cancer Staging Manual. 2017.

38. Hallett RM, Dvorkin-Gheva A, Bane A, Hassell JA. A gene signature for predicting outcome in patients with basal-like breast cancer. Sci Rep. 2012;17(2):227.

39. Perou CM, Sørile T, Eisen MB, Van De Rijn M, Jeffrey SS, Ress CA, et al. Molecular portraits of human breast tumours. Nature. 2000;406(6797):747–52.

40. Santos AA, Lopes CC, Ribeiro JR, Martins LR, Santos JC, Amorim IF, et al. Identification of prognostic factors in canine mammary malignant tumours: A multivariable survival study. BMC Vet Res. 2013;9(1):1.

41. Li G, Guo X, Tang L, Chen M, Luo X, Peng L, et al. Analysis of BRCA1/2 mutation spectrum and prevalence in unselected Chinese breast cancer patients by next-generation sequencing. J Cancer Res Clin Oncol. 2017;143(10):2011–24.

42. Rivera PJ, Melin M, Biagi T, Fall T, Häggström J, Lindblad-Toh K, et al. Mammary tumor development in dogs is associated with BRCA1 and BRCA2. Cancer Res. 2009;69(22):8770–4.

43. Uva P, Aurisicchio L, Watters J, Loboda A, Kulkarni A, Castle J, et al. Comparative expression pathway analysis of human and canine mammary tumors. BMC Genomics. 2009;10(1):135.

44. Gama A, Alves A, Schmitt F. Identification of molecular phenotypes in canine mammary carcinomas with clinical implications: Application of the human classification. Virchows Arch. 2008;453(2):123–32.

45. Hsu WL, Huang HM, Liao JW, Wong ML, Chang SC. Increased survival in dogs with malignant mammary tumours overexpressing HER-2 protein and detection of a silent single nucleotide polymorphism in the canine HER-2 gene. Vet J. 2009;180(1):116–23.

46. Martín De Las Mulas J, Ordás J, Millán Y, Fernández-Soria V, Ramón Y Cajal S. Oncogene HER-2 in canine mammary gland carcinomas: An immunohistochemical and chromogenic in situ hybridization study. Breast Cancer Res Treat. 2003;80(3):363–7.

47. Rowell JL, McCarthy DO, Alvarez CE. Dog models of naturally occurring cancer. Trends Mol Med. 2011;17(7):380–8.

48. Sargan DR, Milne BS, Aguirre Hernandez J, O'Brien PCM, Ferguson-Smith MA, Hoather T, et al. Chromosome rearrangements in canine fibrosarcomas. J Hered. 2005;96(7):766–73.

49. Dirix LY, Van Oosterom AT. Soft tissue sarcoma in adults. Curr Opin Oncol. 1999;9(4):348–59.

50. Mandahl N, Mertens F. Soft tissue tumors. In: Cancer Cytogenetics: Fourth Edition. John Wiley & Sons; 2015.

51. Aguirre-Hernández J, Milne BS, Queen C, O'Brien PCM, Hoather T, Haugland S, et al. Disruption of chromosome 11 in canine fibrosarcomas highlights an unusual variability of CDKN2B in dogs. BMC Vet Res. 2009;5(1):27.

52. Orlow I, Drobnjak M, Zhang ZF, Lewis J, Woodruff JM, Brennan MF, et al. Alterations of INK4A and INK4B genes in adult soft tissue sarcomas: Effect on survival. J Natl Cancer Inst. 1999;91(1):73–9.

53. Hirota S, Isozaki K, Moriyama Y, Hashimoto K, Nishida T, Ishiguro S, et al. Gain-of-function mutations of c-kit in human gastrointestinal stromal tumors. Science (80-). 1998;279(5350):577–80.

54. Gregory-Bryson E, Bartlett E, Kiupel M, Hayes S, Yuzbasiyan-Gurkan V. Canine and human gastrointestinal stromal tumors display similar mutations in c-KIT exon 11. BMC Cancer. 2010;10(1):559.

55. Stojadinovic A, Leung DHY, Allen P, Lewis JJ, Jaques DP, Brennan MF. Primary adult soft tissue sarcoma: Time-dependent influence of prognostic variables. J Clin Oncol. 2002;20(21):4344–52.

56. Kirpensteijn J, Kik M, Teske E, Rutteman GR. TP53 gene mutations in canine osteosarcoma. Vet Surg. 2008;37(5):454–60.

57. Van Leeuwen IS, Cornelisse CJ, Misdorp W, Goedegebuure SA, Kirpensteijn J, Rutteman GR. P53 gene mutations in osteosarcomas in the dog. Cancer Lett. 1997;111:173–8.

58. Mendoza S, Konishi T, Dernell WS, Withrow SJ, Miller CW. Status of the p53, Rb and Mdm2 genes in canine osteosarcoma. Anticancer Res. 1998;18(6A):4449–53.

59. Gokgoz N, Wunder JS, Mousses S, Eskandarian S, Bell RS, Andrulis IL. Comparison of p53 mutations in patients with localized osteosarcoma and metastatic osteosarcoma. Cancer. 2001;92(8):2181–9.

60. Weichselbaum RR, Yandell DW, Little JB, Hen-era GE, Yandell DW. Mutation spectrum of the p53 gene in bone and soft tissue sarcomas. Cancer Res. 1992;52(22):6194–9.

61. Gardner HL, Sivaprakasam K, Briones N, Zismann V, Perdigones N, Drenner K, et al. Canine osteosarcoma genome sequencing identifies recurrent mutations in DMD and the histone methyltransferase gene SETD2. Commun Biol. 2019;July19(2):266.

62. Thomas R, Wang HJ, Tsai PC, Langford CF, Fosmire SP, Jubala CM, et al. Influence of genetic background on tumor karyotypes: Evidence for breed-associated cytogenetic aberrations in canine appendicular osteosarcoma. Chromosom Res. 2009;17(3):365–77.

63. Karlsson EK, Sigurdsson S, Ivansson E, Thomas R, Elvers I, Wright J, et al. Genome-wide analyses implicate 33 loci in heritable dog osteosarcoma, including regulatory variants near CDKN2A/B. Genome Biol. 2013;14(12):R132.

64. Scott MC, Sarver AL, Gavin KJ, Thayanithy V, Getzy DM, Newman RA, et al. Molecular subtypes of osteosarcoma identified by reducing tumor heterogeneity through an interspecies comparative approach. Bone. 2011;49(3):356–67.

65. Buettner R, Mora LB, Jove R. Activated STAT signaling in human tumors provides novel molecular targets for therapeutic intervention. Clin Cancer Res. 2002;8(4):945–54.

66. Chen CL, Loy A, Cen L, Chan C, Hsieh FC, Cheng G, et al. Signal transducer and activator of transcription 3 is involved in cell growth and survival of human rhabdomyosarcoma and osteosarcoma cells. BMC Cancer. 2007;7(1):111.

67. Fossey SL, Bear MD, Kisseberth WC, Pennell M, London CA. Oncostatin M promotes STAT3 activation, VEGF production, and invasion in osteosarcoma cell lines. BMC Cancer. 2011;11(1):125.

68. Seelig DM, Avery AC, Ehrhart EJ, Linden MA. The comparative diagnostic features of canine and human lymphoma. Vet Sci. 2016;3(2):11.

69. Shiels MS, Engels EA, Linet MS, Clarke CA, Li J, Hall HI, et al. The epidemic of non-Hodgkin lymphoma in the United States: Disentangling the effect of HIV, 1992-2009. Cancer Epidemiol Biomarkers Prev. 2013;22(6):1069–78.

70. Breen M, Modiano JF. Evolutionarily conserved cytogenetic changes in hematological malignancies of dogs and humans - Man and his best friend share more than companionship. Chromosom Res. 2008;16(1):145–54.

71. Thomas R, Seiser EL, Motsinger-Reif A, Borst L, Valli VE, Kelley K, et al. Refining tumor-associated aneuploidy through "genomic recoding" of recurrent DNA copy number aberrations in 150 canine non-Hodgkin lymphomas. Leuk Lymphoma. 2011;52(7):1321–35.

72. Habineza Ndikuyeze G, Gaurnier-Hausser A, Patel R, Baldwin AS, May MJ, Flood P, et al. A phase I clinical trial of systemically delivered NEMO binding domain peptide in dogs with spontaneous activated B-cell like diffuse large B-cell lymphoma. PLoS One. 2014;9(5):e95404.

73. Richards KL, Motsinger-Reif AA, Chen HW, Fedoriw Y, Fan C, Nielsen DM, et al. Gene profiling of canine B-Cell lymphoma reveals germinal center and postgerminal center subtypes with different survival times, modeling human DLBCL. Cancer Res. 2013;73(16):5029–39.

74. Mudaliar MAV, Haggart RD, Miele G, Sellar G, Tan KAL, Goodlad JR, et al. Comparative gene expression profiling identifies common molecular signatures of nf-κb activation in canine and human diffuse large B cell lymphoma (DLBCL). PLoS One. 2013;8(9):e72591.

75. Gaurnier-Hausser A, Patel R, Baldwin AS, May MJ, Mason NJ. NEMO-binding domain peptide inhibits constitutive NF-κB activity and reduces tumor burden in a canine model of relapsed, refractory diffuse large B-cell lymphoma. Clin Cancer Res. 2011;17(14):4661–71.

76. Bushell KR, Kim Y, Chan FC, Ben-Neriah S, Jenks A, Alcaide M, et al. Genetic inactivation of TRAF3 in canine and human B-cell lymphoma. Blood.

2015;125(6):999–1005.

77. Tasca S, Carli E, Caldin M, Menegazzo L, Furlanello T, Gallego LS. Hematologic abnormalities and flow cytometric immunophenotyping results in dogs with hematopoietic neoplasia: 210 cases (2002-2006). Vet Clin Pathol. 2009;38(1):2–12.

78. Carulli G, Cannizzo E, Zucca A, Buda G, Orciuolo E, Marini A, et al. CD45 expression in low-grade B-cell non-Hodgkin's lymphomas. Leuk Res. 2008;32(2):263–7.

79. Deininger M, Buchdunger E, Druker BJ. The development of imatinib as a therapeutic agent for chronic myeloid leukemia. Blood. 2005;105(7):2640–53.

80. Suter SE, Small GW, Seiser EL, Thomas R, Breen M, Richards KL. FLT3 mutations in canine acute lymphocytic leukemia. BMC Cancer. 2011;11(1):38.

81. Gary Gilliland D, Griffin JD. The roles of FLT3 in hematopoiesis and leukemia. Blood. 2002;100(5):1532–42.

82. Gardner HL, Fenger JM, London CA. Dogs as a model for cancer. Annu Rev Anim Biosci. 2016;4:199–222.

83. Sommer BC, Dhawan D, Ratliff TL, Knapp DW. Naturally-occurring canine invasive urothelial carcinoma: a model for emerging therapies. Bl Cancer. 2018;4(2):149–59.

84. Knapp DW, Ramos-Vara JA, Moore GE, Dhawan D, Bonney PL, Young KE. Urinary bladder cancer in dogs, a naturally occurring model for cancer biology and drug development. ILAR J. 2014;55(1):100–18.

85. Dhawan D, Craig BA, Cheng L, Snyder PW, Mohammed SI, Stewart JC, et al. Effects of short-term celecoxib treatment in patients with invasive transitional cell carcinoma of the urinary bladder. Mol Cancer Ther. 2010;9(5):1371–7.

86. Modelska A, Quattrone A, Re A. Molecular portraits: The evolution of the concept of transcriptome-based cancer signatures. Brief Bioinform. 2015;16(6):1000–7.

87. Adams MD, Kelley JM, Gocayne JD, Dubnick MAK, Polymeropoulos MH, Xiao H, et al. Complementary DNA sequencing: Expressed sequence tags and human genome project. Science (80-). 1991;252(5013):1651–6.

88. Hudson TJ, Anderson W, Aretz A, Barker AD, Bell C, Bernabé RR, et al. International network of cancer genome projects. Nature. 2010;464(7291):993–8.

89. Roychowdhury S, Iyer MK, Robinson DR, Lonigro RJ, Wu YM, Cao X, et al. Personalized oncology through integrative high-throughput sequencing: A pilot study. Sci Transl Med. 2011;3(111):111–21.

90. Brenner S, Johnson M, Bridgham J, Golda G, Lloyd DH, Johnson D, et al. Gene expression analysis by massively parallel signature sequencing (MPSS) on microbead arrays. Nat Biotechnol. 2000;2000(18):630–4.

91. Bainbridge MN, Warren RL, Hirst M, Romanuik T, Zeng T, Go A, et al. Analysis of the prostate cancer cell line LNCaP transcriptome using a sequencing-by-synthesis approach. BMC Genomics. 2006;2007(7):246.

92. Lappalainen T, Sammeth M, Friedländer MR, 'T Hoen PAC, Monlong J, Rivas MA, et al. Transcriptome and genome sequencing uncovers functional variation in humans. Nature. 2013;501(7468):506–11.

93. Ozsolak F, Milos PM. RNA sequencing: Advances, challenges and opportunities. Nat Rev Genet. 2011;12(2):87–98.

94. Mortazavi A, Williams BA, McCue K, Schaeffer L, Wold B. Mapping and quantifying mammalian transcriptomes by RNA-Seq. Nat Methods. 2008;5(7):621–8.

95. Wilhelm BT, Marguerat S, Watt S, Schubert F, Wood V, Goodhead I, et al. Dynamic repertoire of a eukaryotic transcriptome surveyed at single-nucleotide resolution. Nature. 2008;453(7199):1239–43.

96. Taking pan-cancer analysis global. Nat Genet. 2013;45:1263.

97. Leinonen R, Sugawara H, Shumway M. The sequence read archive. Nucleic Acids Res. 2011;39:D19–21.

98. Petryszak R, Keays M, Tang YA, Fonseca NA, Barrera E, Burdett T, et al. Expression Atlas update - An integrated database of gene and protein expression in humans, animals and plants. Nucleic Acids Res. 2016;44(D1):D746-752.

99. Gerstein MB, Rozowsky J, Yan KK, Wang D, Cheng C, Brown JB, et al. Comparative analysis of the transcriptome across distant species. Nature. 2014;512:445–8.

100. Breschi A, Gingeras TR, Guigó R. Comparative transcriptomics in human and mouse. Nat Rev Genet. 2017;18(7):425–40.

101. Lee KH, Park HM, Son KH, Shin TJ, Cho JY. Transcriptome signatures of canine mammary gland tumors and its comparison to human breast cancers. Cancers (Basel). 2018;10(9):317.

102. Amini P, Nassiri S, Ettlin J, Malbon A, Markkanen E. Next-generation RNA sequencing of FFPE subsections reveals highly conserved stromal reprogramming between canine and human mammary carcinoma. Dis Model Mech. 2019;12(8):dmm040444.

103. Scott MC, Temiz NA, Sarver AE, LaRue RS, Rathe SK, Varshney J, et al. Comparative transcriptome analysis quantifies immune cell transcript levels, metastatic progression, and survival in osteosarcoma. Cancer Res. 2018;78(2):326–37.

104. Weinstein JN, Akbani R, Broom BM, Wang W, Verhaak RGW, McConkey D, et al. Comprehensive molecular characterization of urothelial bladder carcinoma. Nature. 2014;507(7492):315–22.

105. Maeda S, Tomiyasu H, Tsuboi M, Inoue A, Ishihara G, Uchikai T, et al. Comprehensive gene expression analysis of canine invasive urothelial bladder carcinoma by RNA-Seq. BMC Cancer. 2018;18(1):472.

106. Ramsey SA, Xu T, Goodall C, Rhodes AC, Kashyap A, He J, et al. Cross-species analysis of the canine and human bladder cancer transcriptome and exome. Genes Chromosom Cancer. 2017;56(4):328–43.

107. Macewen EG, Patnaik AK, Harvey HJ, Hayes AA, Matus R. Canine oral melanoma: Comparison of surgery versus surgery plus corynebacterium parvum. Cancer Invest. 1986;4(5):397–402.

108. Weiden PL, Storb R, Lerner KG, Kao GF, Graham TC, Thomas ED. Treatment of canine malignancies by 1200 R total body irradiation and autologous marrow grafts. Exp Hematol. 1975;3(2):124–34.

109. Tsoi MS, Weiden PL, Storb R. Lymphocyte reactivity to autochthonous tumor cells in dogs with spontaneous malignancies. Cell Immunol. 1974;13(3):431–9.

110. Storb R, Epstein RB, Ragde H, Bryant J, Thomas ED. Marrow engraftment by allogeneic leukocytes in lethally irradiated dogs. Blood. 1967;30(6):805–11.

111. Crow SE, Theilen GH, Benjamini E, Torten M, Henness AM, Buhles WC. Chemoimmunotherapy for canine lymphosarcoma. Cancer. 1977;40(5):2102–8.

112. Benjamini E, Theilen GH, Torten M, Fong S, Crow S, Henness AM. Tumor vaccines for immunotherapy of canine lymphosarcoma. Ann N Y Acad Sci. 1976;277(1):305–12.

113. Siegel RL, Miller KD, Jemal A. Cancer Statistics, 2018. CA Cancer J Clin. 2018;67(1):7–30.

114. Akbani R, Akdemir KC, Aksoy BA, Albert M, Ally A, Amin SB, et al. Genomic classification of cutaneous melanoma. Cell. 2015;161(7):1681–96.

115. Hayward NK, Wilmott JS, Waddell N, Johansson PA, Field MA, Nones K, et al. Whole-genome landscapes of major melanoma subtypes. Nature. 2017;545(7653):175–80.

116. Ascierto PA, Kirkwood JM, Grob JJ, Simeone E, Grimaldi AM, Maio M, et al. The role of BRAF V600 mutation in melanoma. J Transl Med. 2012;10(1):85.

117. Hodis E, Watson IR, Kryukov G V., Arold ST, Imielinski M, Theurillat JP, et al. A landscape of driver mutations in melanoma. Cell. 2012;150(2):251–63.

118. van 't Veer LJ, Burgering BM, Versteeg R, Boot AJ, Ruiter DJ, Osanto S, et al. N-ras mutations in human cutaneous melanoma from sun-exposed body sites. Mol Cell Biol. 1989;9(7):3114–6.

119. Hernandez B, Adissu HA, Wei BR, Michael HT, Merlino G, Mark Simpson R. Naturally occurring canine melanoma as a predictive comparative oncology model for human mucosal and other triple wild-type melanomas. Int J Mol Sci. 2018;19(2):394.

120. van der Weyden L, Patton EE, Wood GA, Foote AK, Brenn T, Arends MJ, et al. Cross-species models of human melanoma. J Pathol. 2016;238(2):152–65.

121. Kaufman CK, Mosimann C, Fan ZP, Yang S, Thomas AJ, Ablain J, et al. A zebrafish melanoma model reveals emergence of neural crest identity during melanoma initiation. Science (80-). 2016;351(6272):aad2197.

122. Pérez-Guijarro E, Day C-P, Merlino G, Zaidi MR. Genetically engineered mouse models of melanoma. Cancer. 2017;123(S11):2089–103.

123. Gillard M, Cadieu E, De Brito C, Abadie J, Vergier B, Devauchelle P, et al. Naturally occurring melanomas in dogs as models for non-UV pathways of human melanomas. Pigment Cell Melanoma Res. 2014;27(1):90–102.

124. Simpson RM, Bastian BC, Michael HT, Webster JD, Prasad ML, Conway CM, et al. Sporadic naturally occurring melanoma in dogs as a preclinical model for human melanoma. Pigment Cell Melanoma Res. 2014;27(1):37–47.

125. Mochizuki H, Kennedy K, Shapiro SG, Breen MB. BRAF mutations in canine cancers. PLoS One. 2015;10(6):e0129534.

126. Chu PY, Pan SL, Liu CH, Lee J, Yeh LS, Liao AT. KIT gene exon 11 mutations in canine malignant melanoma. Vet J. 2013;196(2):226–30.

127. Rupaimoole R, Slack FJ. MicroRNA therapeutics: towards a new era for the management of cancer and other diseases. Nat Rev Drug Discov. 2017;16(3):203–22.

128. Noguchi S, Mori T, Hoshino Y, Yamada N, Maruo K, Akao Y. MicroRNAs as tumour suppressors in canine and human melanoma cells and as a prognostic factor in canine melanomas. Vet Comp Oncol. 2013;11(2):113–23.

129. Noguchi S, MORI T, Hoshino Y, Nami Y, Nakagawa T, Sasaki N, et al. Comparative study of anti-oncogenic microRNA-145 in canine and human malignant melanoma. J Vet Med Sci. 2012;74(1):1–8.

130. Islam F, Gopalan V, Vider J, Wahab R, Ebrahimi F, Lu C tai, et al. MicroRNA-186-5p overexpression modulates colon cancer growth by repressing the expression of the FAM134B tumour inhibitor. Exp Cell Res. 2017;357(2):260–70.

131. Friedrich M, Pracht K, Mashreghi MF, Jäck HM, Radbruch A, Seliger B. The role of the miR-148/-152 family in physiology and disease. Eur J Immunol. 2017;47(12):2026–38.

132. Wang J, Li Y, Ding M, Zhang H, Xu X, Tang J. Molecular mechanisms and clinical applications of MIR-22 in regulating malignant progression in human cancer (Review). Int J Oncol. 2017;50(2):345–55.

133. Ushio N, Rahman MM, Maemura T, Lai YC, Iwanaga T, Kawaguchi H, et al. Identification of dysregulated microRNAs in canine malignant melanoma. Oncol Lett. 2019 Jan 1;17(1):1080–8.

134. Sun MM, Li JMFM, Guo LL, Xiao HT, Dong L, Wang F, et al. TGF-β1 suppression of microRNA-450b-5p expression: a novel mechanism for blocking myogenic differentiation of rhabdomyosarcoma. Oncogene. 2013;33(October 2012):1–12.

135. Guo YJ, Liu JX, Guan YW. Hypoxia induced upregulation of miR-301a/b contributes to increased cell autophagy and viability of prostate cancer cells by targeting NDRG2. Eur Rev Med Pharmacol Sci. 2016;20(1):101–8.

136. Yang L, Li Y, Wang X, Mu X, Qin D, Huang W, et al. Overexpression of miR-223 tips the balance of pro- and anti-hypertrophic signaling cascades toward physiologic cardiac hypertrophy. J Biol Chem. 2016;291(30):15700–13.

137. Zhou J, Gao Y, Lan Y, Jia S, Jiang R. Pax9 regulates a molecular network involving Bmp4, Fgf10, Shh signaling and the Osr2 transcription factor to control palate morphogenesis. Development. 2013;140(23):4709–18.

138. Laulan NB, St-Pierre Y. Bone morphogenetic protein 4 (BMP-4) and epidermal growth factor (EGF) inhibit metalloproteinase-9 (MMP-9) expression in cancer cells. Oncoscience. 2015;2(3):309–16.

139. Inoue K, Ohashi E, Kadosawa T, Hong S-H, Matsunaga S, Mochizuki M, et al. Establishment and characterization of four canine melanoma cell Lines. J Vet Med Sci. 2004;66(11):1437–40.

140. Cui L, Li Y, Lv X, Li J, Wang X, Lei Z, et al. Expression of microRNA-301a and its functional roles in malignant melanoma. Cell Physiol Biochem. 2016;40(1–2):230–44.

141. Larsen AC, Mikkelsen LH, Borup R, Kiss K, Toft PB, Von Buchwald C, et al. MicroRNA expression profile in conjunctival melanoma. Investig Ophthalmol Vis Sci. 2016;57(10):4205–12.

142. Mirzaei HHRH, Gholamin S, Shahidsales S, Sahebkar A, Jafaari MR, Mirzaei HHRH, et al. MicroRNAs as potential diagnostic and prognostic biomarkers in melanoma. Eur J Cancer. 2016;53:25–32.

143. Xu Y, Brenn T, Brown ERS, Doherty V, Melton DW. Differential expression of microRNAs during melanoma progression: MiR-200c, miR-205 and miR-211 are downregulated in melanoma and act as tumour suppressors. Br J Cancer. 2012;106:553–61.

144. Fattore L, Costantini S, Malpicci D, Ruggiero CF, Ascierto PA, Croce CM, et al. MicroRNAs in melanoma development and resistance to target therapy. Oncotarget. 2015;8(13):22262–78.

145. Bai X, Fisher DE, Flaherty KT. Cell-state dynamics and therapeutic resistance in melanoma from the perspective of MITF and IFNγ pathways. Nat Rev Clin Oncol. 2019;16(9):549–62.

146. Garraway LA, Widlund HR, Rubin MA, Getz G, Berger AJ, Ramaswamy S, et al. Integrative genomic analyses identify MITF as a lineage survival oncogene amplified in malignant melanoma. Nature. 2005;436(7047):117–22.

147. Laganà A, Russo F, Sismeiro C, Giugno R, Pulvirenti A, Ferro A. Variability in the incidence of miRNAs and genes in fragile sites and the role of repeats and CpG islands in the distribution of genetic material. PLoS One. 2010;5(6):1–8.

148. Calin GA, Sevignani C, Dumitru CD, Hyslop T, Noch E, Yendamuri S, et al. Human microRNA genes are frequently located at fragile sites and genomic regions involved in cancers. Proc Natl Acad Sci USA. 2004;101(9):2999–3004.

149. Calin GA, Dumitru CD, Shimizu M, Bichi R, Zupo S, Noch E, et al. Frequent deletions and down-regulation of micro-RNA genes miR15 and miR16 at 13q14 in chronic lymphocytic leukemia. Proc Natl Acad Sci USA. 2002;99(24):15524–9.

150. Dambal S, Shah M, Mihelich B, Nonn L. The microRNA-183 cluster: The family that plays together stays together. Nucleic Acids Res. 2015;43(15):7173–88.

151. Kim A, Yang Y, Lee MS, Yoo Y Do, Lee HG, Lim JS. NDRG2 gene expression in B16F10 melanoma cells restrains melanogenesis via inhibition of Mitf expression. Pigment Cell Melanoma Res. 2008;21(6):653–64.

152. Hata S, Hamada J-I, Maeda K, Murai T, Tada M, Furukawa H, et al. PAX4 has the potential to function as a tumor suppressor in human melanoma. Int J Oncol. 2008;33(5):1065–71.

153. Sand M, Skrygan M, Sand D, Georgas D, Gambichler T, Hahn SA, et al. Comparative microarray analysis of microRNA expression profiles in primary cutaneous malignant melanoma, cutaneous malignant melanoma metastases, and benign melanocytic nevi. Cell Tissue Res. 2013;351(1):85–98.

154. Shon SK, Kim A, Kim JY, Kim K Il, Yang Y, Lim JS. Bone morphogenetic protein-4 induced by NDRG2 expression inhibits MMP-9 activity in breast cancer cells. Biochem Biophys Res Commun. 2009;385(2):198–203.

155. Brachelente C, Cappelli K, Capomaccio S, Porcellato I, Silvestri S, Bongiovanni L, et al. Transcriptome analysis of canine cutaneous melanoma and melanocytoma reveals a modulation of genes regulating extracellular matrix metabolism and cell cycle. Sci Rep. 2017;7(1):6386.

156. Dong Y, Fu C, Guan H, Zhang Z, Zhou T, Li BS. Prognostic significance of miR-126 in various cancers: A meta-analysis. Onco Targets Ther. 2016;9:2547–55.

157. Liu F, Zhang F, Li X, Liu Q, Liu W, Song P, et al. Prognostic role of miR-17-92 family in human cancers: evaluation of multiple prognostic outcomes. Oncotarget. 2017;8(40):69125–38.

158. Scoggins CR, Ross MI, Reintgen DS, Noyes RD, Goydos JS, Beitsch PD, et al. Gender-related differences in outcome for melanoma patients. Ann Surg. 2006;243(5):693–700.

159. Mihajlovic M, Vlajkovic S, Jovanovic P, Stefanovic V. Primary mucosal melanomas: A comprehensive review. Int J Clin Exp Pathol. 2012;5(8):739–53.

160. Muñoz-Rodríguez JL, Vrba L, Futscher BW, Hu C, Komenaka IK, Meza-Montenegro MM, et al. Differentially expressed microRNAs in postpartum breast cancer in Hispanic women. PLoS One. 2015;10(4):1–17.

161. Ghorai A, Ghosh U. miRNA gene counts in chromosomes vary widely in a species and biogenesis of miRNA largely depends on transcription or post-transcriptional processing of coding genes. Front Genet. 2014;5(APR):1–11.

162. Kozomara A, Griffiths-Jones S. MiRBase: Annotating high confidence microRNAs using deep sequencing data. Nucleic Acids Res. 2014;42(D1):D68–73.

163. Robinson MD, Smyth GK. Small-sample estimation of negative binomial dispersion, with applications to SAGE data. Biostatistics. 2008;9(2):321–32.

164. Schmittgen TD, Livak KJ. Analyzing real-time PCR data by the comparative CT method. Nat Protoc. 2008;3:1103–8.

165. Huang DW, Sherman BT, Tan Q, Kir J, Liu D, Bryant D, et al. DAVID Bioinformatics Resources: Expanded annotation database and novel algorithms to

better extract biology from large gene lists. Nucleic Acids Res. 2007;35:169–75.

166. Lewis BP, Burge CB, Bartel DP. Conserved seed pairing, often flanked by adenosines, indicates that thousands of human genes are microRNA targets. Cell. 2005;120(1):15–20.

167. Wong N, Wang X. miRDB: An online resource for microRNA target prediction and functional annotations. Nucleic Acids Res. 2015;43:146–52.

168. Lopes CT, Franz M, Kazi F, Donaldson SL, Morris Q, Bader GD, et al. Cytoscape Web: An interactive web-based network browser. Bioinformatics. 2011;27(13):2347–8.

169. Szklarczyk D, Franceschini A, Wyder S, Forslund K, Heller D, Huerta-Cepas J, et al. STRING v10: Protein-protein interaction networks, integrated over the tree of life. Nucleic Acids Res. 2015;43(D1):D447–52.

170. Scardoni G, Petterlini M, Laudanna C. Analyzing biological network parameters with CentiScaPe. Bioinformatics. 2009;25(21):2857–9.

171. Carolina N, Hill C. Eulogy for junk DNA. Genomics. 2012;9(37):1159–61.

172. Anastasiadou E, Jacob LS, Slack FJ. Non-coding RNA networks in cancer. Nat Rev Cancer. 2017;18(1):5–18.

173. Chen JE, Glover GH. Small RNAs with big implications: New insights into H/ACA snoRNA function and their role in human disease. Wiley Interdiscip Rev RNA. 2016;25(3):289–313.

174. Bellodi C, McMahon M, Contreras A, Juliano D, Kopmar N, Nakamura T, et al. H/ACA small RNA dysfunctions in disease reveal key roles for noncoding RNA modifications in hematopoietic stem cell differentiation. Cell Rep. 2013;3(5):1493–502.

175. Sanabria-salas C, Garay J, Serrano-go SJ, Mejı JC, Garcı O, Baddoo C, et al. Ancestry as a potential modifier of gene expression in breast tumors from colombian women. PLoS One. 2017;2:1–21.

176. Gong J, Li Y, Liu C jie, Xiang Y, Li C, Ye Y, et al. A Pan-cancer analysis of the expression and clinical relevance of small nucleolar RNAs in human cancer. Cell Rep. 2017;21(7):1968–81.

177. López-Corral L, Mateos MV, Corchete LA, Sarasquete ME, de la Rubia J, de Arriba F, et al. Genomic analysis of high-risk smoldering multiple myeloma. Haematologica. 2012;97(9):1439–43.

178. Patterson DG, Roberts JT, King VM, Houserova D, Barnhill EC, Crucello A, et al.

Human snoRNA-93 is processed into a microRNA-like RNA that promotes breast cancer cell invasion. npj Breast Cancer. 2017;3(1):1–12.

179. Köhler J, Schuler M, Gauler TC, Nöpel-Dünnebacke S, Ahrens M, Hoffmann AC, et al. Circulating U2 small nuclear RNA fragments as a diagnostic and prognostic biomarker in lung cancer patients. J Cancer Res Clin Oncol. 2016;142(4):795–805.

180. Baraniskin A, Zaslavska E, Nöpel-Dünnebacke S, Ahle G, Seidel S, Schlegel U, et al. Circulating U2 small nuclear RNA fragments as a novel diagnostic biomarker for primary central nervous system lymphoma. Neuro Oncol. 2016;18(3):361–7.

181. Kuhlmann JD, Baraniskin A, Hahn SA, Mosel F, Bredemeier M, Wimberger P, et al. Circulating U2 small nuclear RNA fragments as a novel diagnostic tool for patients with epithelial ovarian cancer. Clin Chem. 2014;60(1):206–13.

182. Kuhlmann JD, Wimberger P, Wilsch K, Fluck M, Suter L, Brunner G. Increased level of circulating U2 small nuclear RNA fragments indicates metastasis in melanoma patients. Clin Chem Lab Med. 2015;53(4):605–11.

183. P. Kumar, C. Kuscu, Anindya D. Biogenesis and function of transfer RNA related fragments (tRFs). Trends Biochem Sci. 2016;41(8):679–89.

184. Sun C, Fu Z, Wang S, Li J, Li Y, Zhang Y, et al. Roles of tRNA-derived fragments in human cancers. Cancer Lett. 2018;414:16–25.

185. Huang SQ, Sun B, Xiong ZP, Shu Y, Zhou HH, Zhang W, et al. The dysregulation of tRNAs and tRNA derivatives in cancer. J Exp Clin Cancer Res. 2018;37(1):1–11.

186. Balatti V, Nigita G, Veneziano D, Drusco A, Stein GS, Messier TL, et al. tsRNA signatures in cancer. Proc Natl Acad Sci USA. 2017;114(30):8071–6.

187. Grafanaki K, Anastasakis D, Kyriakopoulos G, Skeparnias I, Georgiou S, Stathopoulos C. Translation regulation in skin cancer from a tRNA point of view. Epigenomics. 2019;11(2):215–45.

188. Pekarsky Y, Balatti V, Palamarchuk A, Rizzotto L, Veneziano D, Nigita G, et al. Dysregulation of a family of short noncoding RNAs, tsRNAs, in human cancer. Proc Natl Acad Sci USA. 2016;113(18):5071–6.

189. Wang L, Chen ZJ, Zhang YK, Le HB. The role of mitochondrial tRNA mutations in lung cancer. Int J Clin Exp Med. 2015;8(8):13341–6.

190. He ZF, Zheng LC, Xie DY, Yu SS, Zhao J. Mutational analysis of mitochondrial tRNA genes in patients with lung cancer. Balk J Med Genet. 2016;19(2):45–50.

191. Goodarzi H, Liu X, Nguyen HCBB, Zhang S, Fish L, Tavazoie SF, et al. Endogenous tRNA-derived fragments suppress breast cancer progression via YBX1

displacement. Cell. 2015;161(4):790–802.

192. Ku HY, Lin H. PIWI proteins and their interactors in piRNA biogenesis, germline development and gene expression. Natl Sci Rev. 2014;1(2):205–18.

193. Fu A, Jacobs DI, Hoffman AE, Zheng T, Zhu Y. PIWI-interacting RNA 021285 is involved in breast tumorigenesis possibly by remodeling the cancer epigenome. Carcinogenesis. 2015;36(10):1094–102.

194. Qu A, Du L, Wang Y, Wang C. A serum piRNA signature as promising non-invasive diagnostic and prognostic biomarkers for colorectal cancer. Cancer Manag Res. 2019;29(11):3703–20.

195. Weng W, Liu N, Toiyama Y, Kusunoki M, Nagasaka T, Fujiwara T, et al. Novel evidence for a PIWI-interacting RNA (piRNA) as an oncogenic mediator of disease progression, and a potential prognostic biomarker in colorectal cancer. Mol Cancer. 2018;17(1):16.

196. Lin X, Xia Y, Hu D, Mao Q, Yu Z, Zhang H, et al. Transcriptome-wide piRNA profiling in human gastric cancer. Oncol Rep. 2019;41(5):3089–99.

197. Mitra S, Ganguli S, Chakrabarti J. Chapter 1 – Introduction. In: Cancer and Noncoding RNAs. 1st ed. USA: Academic Press; 2018. p. 1–23.

198. Wagner S, Willenbrock S, Nolte I, Escobar HM. Comparison of non-coding RNAs in human and canine cancer. Front Genet. 2013;4(April):1–9.

199. Kiss AM, Jady BE, Bertrand E, Kiss T. Human box H/ACA pseudouridylation guide RNA machinery. Mol Cell Biol. 2004;24(13):5797–807.

200. Deogharia M, Majumder M. Guide snoRNAs: Drivers or passengers in human disease? Biology (Basel). 2018;8(1):1.

201. Penzo M, Montanaro L. Turning uridines around: Role of rRNA pseudouridylation in ribosome biogenesis and ribosomal function. Biomolecules. 2018;8(2):1–10.

202. Kierzek E, Malgowska M, Lisowiec J, Turner DH, Gdaniec Z, Kierzek R. The contribution of pseudouridine to stabilities and structure of RNAs. Nucleic Acids Res. 2014;42(5):3492–501.

203. Krogh N, Jansson MD, Häfner SJ, Tehler D, Birkedal U, Christensen-Dalsgaard M, et al. Profiling of 2′-O-Me in human rRNA reveals a subset of fractionally modified positions and provides evidence for ribosome heterogeneity. Nucleic Acids Res. 2016;44(16):7884–95.

204. Taoka M, Nobe Y, Yamaki Y, Sato K, Ishikawa H, Izumikawa K, et al. Landscape of the complete RNA chemical modifications in the human 80S ribosome. Nucleic

Acids Res. 2018;46(18):9289–98.

205. Stepanov GA, Filippova JA, Komissarov AB, Kuligina E V., Richter VA, Semenov D V. Regulatory role of small nucleolar RNAs in human diseases. Biomed Res Int. 2015;2015:1–10.

206. Williams GT, Farzaneh F. Are snoRNAs and snoRNA host genes new players in cancer? Nat Rev Cancer. 2012;12(2):84–8.

207. Falaleeva M, Pages A, Matuszek Z, Hidmi S, Agranat-Tamir L, Korotkov K, et al. Dual function of C/D box small nucleolar RNAs in rRNA modification and alternative pre-mRNA splicing. Proc Natl Acad Sci USA. 2016;113(12):E1625–34.

208. Cheng Z, Sun Y, Niu X, Shang Y, Ruan J, Chen Z, et al. Gene expression profiling reveals U1 snRNA regulates cancer gene expression. Oncotarget. 2017;8(68):112867–74.

209. Borja-Cacho D, Matthews J. U1 snRNA Rewrites the "Script." Cell. 2012;150(1):9–11.

210. Dvinge H, Guenthoer J, Porter PL, Bradley RK. RNA components of the spliceosome regulate tissue- and cancer-specific alternative splicing. Genome Res. 2019;29(10):1591–604.

211. Anczukow O, Krainer AR. Splicing-factor alterations in cancers. RNA. 2016;22(9):1285–301.

212. Weng W, Li H, Goel A. Piwi-interacting RNAs (piRNAs) and cancer: Emerging biological concepts and potential clinical implications. Biochim Biophys Acta - Rev Cancer. 2019;1871(1):160–9.

213. Ng KW, Anderson C, Marshall EA, Minatel BC, Enfield KSS, Saprunoff HL, et al. Piwi-interacting RNAs in cancer: Emerging functions and clinical utility. Mol Cancer. 2016;15(5):1–13.

214. Ossio R, Roldán-Marín R, Martínez-Said H, Adams DJ, Robles-Espinoza CD. Melanoma: A global perspective. Nat Rev Cancer. 2017;17(7):393–4.

215. Kong Y, Si L, Zhu Y, Xu X, Corless CL, Flaherty KT, et al. Large-scale analysis of KIT aberrations in Chinese patients with melanoma. Clin Cancer Res. 2011;17(7):1684–91.

216. Smith SH, Goldschmidt MH, McManus P. A Comparative review of melanocytic neoplasms. Vet Pathol. 2002;39:651–78.

217. Treggiari, Elisabetta Grant, Jessica Pauline North SM. A retrospective review of outcome and survival following surgery and adjuvant xenogeneic DNA vaccination

in 32 dogs with oral malignant melanoma. J Vet Med Sci. 2016;78(5):845–50.

218. Prouteau, André. Canine Melanomas as Models for Human Melanomas: Clinical, Histological, and Genetic Comparison. Genes (Basel). 2019;10(7):501.

219. Li RW, Schroeder SG. Cytoskeleton remodeling and alterations in smooth muscle contractility in the bovine jejunum during nematode infection. Funct Integr Genomics. 2012;12(1):35–44.

220. Mi H, Muruganujan A, Casagrande JT, Thomas PD. Large-scale gene function analysis with the panther classification system. Nat Protoc. 2013;8(8):1551–66.

221. Bhattacharya S, Dunn P, Thomas CG, Smith B, Schaefer H, Chen J, et al. ImmPort, toward repurposing of open access immunological assay data for translational and clinical research. Sci Data. 2018;5:1–9.

222. Spangler WL, Kass PH. The histologic and epidemiologic bases for prognostic considerations in canine melanocytic neoplasia. Vet Pathol. 2006;43(2):136–49.

223. Miskolczi Z, Smith MP, Rowling EJ, Ferguson J, Barriuso J, Wellbrock C. Collagen abundance controls melanoma phenotypes through lineage-specific microenvironment sensing. Oncogene. 2018;37(23):3166–82.

224. Han MJ, Wang H, Beer LA, Tang HY, Herlyn M, Speicher DW. A systems biology analysis of metastatic melanoma using in-depth three-dimensional protein profiling. Proteomics. 2010;10(24):4450–62.

225. Tichet M, Prodhomme V, Fenouille N, Ambrosetti D, Mallavialle A, Cerezo M, et al. Tumour-derived SPARC drives vascular permeability and extravasation through endothelial VCAM1 signalling to promote metastasis. Nat Commun. 2015;6:6993.

226. Wurth L, Papasaikas P, Olmeda D, Bley N, Calvo GT, Guerrero S, et al. UNR/CSDE1 Drives a Post-transcriptional Program to Promote Melanoma Invasion and Metastasis. Cancer Cell. 2016;30(5):694–707.

227. Naganuma K, Hatta M, Ikebe T, Yamazaki J. Epigenetic alterations of the keratin 13 gene in oral squamous cell carcinoma. BMC Cancer. 2014;14:988.

228. Khammanivong A, Sorenson BS, Ross KF, Dickerson EB, Hasina R, Lingen MW, et al. Involvement of calprotectin (S100A8/A9) pathways associated with HNSCC in molecular pathways associated with HNCC. Oncotarget. 2016;7(12):14029–47.

229. Kim JH, Frantz AM, Anderson KL, Graef AJ, Scott MC, Robinson S, et al. Interleukin-8 promotes canine hemangiosarcoma growth by regulating the tumor microenvironment. Exp Cell Res. 2014;323(1):155–64.

230. Andrlová H, Mastroianni J, Madl J, Kern JS, Melchinger W, Dierbach H, et al.

Biglycan expression in the melanoma microenvironment promotes invasiveness via increased tissue stiffness inducing integrin-β1 expression. Oncotarget. 2017;8(26):42901–16.

231. Nagarsheth N, Wicha MS, Zou W. Chemokines in the cancer microenvironment and their relevance in cancer immunotherapy. Nat Rev Immunol. 2017;17(9):559–72.

232. Labidi-Galy SI, Clauss A, Ng V, Duraisamy S, Elias KM, Piao HY, et al. Elafin drives poor outcome in high-grade serous ovarian cancers and basal-like breast tumors. Oncogene. 2015;34(3):299–309.

233. Smedley D, Sidhar S, Birdsall S, Bennett D, Herlyn M, Cooper C, et al. Characterization of chromosome 1 abnormalities in malignant melanomas. Genes Chromosom Cancer. 2000;28:121–5.

234. Dracopoli NC, Harnett P, Bale SJ, Stanger BZ, Tucker MA, Housman DE, et al. Loss of alleles from the distal short arm of chromosome 1 occurs late in melanoma tumor progression. Proc Natl Acad Sci. 1989;86(12):4614–8.

235. Kuo PT, Zeng Z, Salim N, Mattarollo S, Wells JW, Leggatt GR. The role of CXCR3 and its chemokine ligands in skin disease and cancer. Front Med. 2018;5(September):1–10.

236. Payne AS, Cornelius LA. The role of chemokines in melanoma tumor growth and metastasis. J Invest Dermatol. 2002;118(6):915–22.

237. Jacquelot N, Duong CPM, Belz GT, Zitvogel L. Targeting chemokines and chemokine receptors in melanoma and other cancers. Front Immunol. 2018;9(October):2480.

238. Lappano R, Maggiolini M. G protein-coupled receptors: Novel targets for drug discovery in cancer. Nat Rev Drug Discov. 2011;10(1):47–60.

239. Cohen S, Levi-Montalcini R, Hamburger V. A nerve growth-stimulating factor isolated from sarcom as 37 and 180. Proc Natl Acad Sci. 1954;40(10):1014–8.

240. Witsch E, Sela M, Yarden Y. Roles for growth factors in cancer progression. Physiology. 2010;25(2):85–101.

241. Afratis N, Gialeli C, Nikitovic D, Tsegenidis T, Karousou E, Theocharis AD, et al. Glycosaminoglycans: Key players in cancer cell biology and treatment. FEBS J. 2012;279(7):1177–97.

242. Wang Y, van Boxel-Dezaire AHH, Cheon H, Yang J, Stark GR. STAT3 activation in response to IL-6 is prolonged by the binding of IL-6 receptor to EGF receptor. Proc Natl Acad Sci. 2013;110(42):16975–80.

243. Han C. Dan, Matthew J. Cooper, Patricia C. Cogswell JAD, an, Jenny P.-Y. Ting and ASB. regulation of NF-{kappa}B is controlled by mTOR and Raptor in association with IKK. Genes Dev. 2008;22:1490–500.

244. Gentry JJ, Casaccia-Bonnefil P, Carter BD. Nerve growth factor activation of nuclear factor κB through its p75 receptor is an anti-apoptotic signal in RN22 schwannoma cells. J Biol Chem. 2000;275(11):7558–65.

245. Ng YP, Cheung ZH, Ip NY, Yu PN, Cheung ZH, Ip NY. STAT3 as a downstream mediator of Trk signaling and functions. J Biol Chem. 2006 Jun 9;281(23):15636–44.

246. Hendricks WPD, Zismann V, Sivaprakasam K, Legendre C, Poorman K, Tembe W, et al. Somatic inactivating PTPRJ mutations and dysregulated pathways identified in canine malignant melanoma by integrated comparative genomic analysis. PLoS Genet. 2018;14(9):1–30.

247. Zhang D, Zhu R, Zhang H, Zheng CH, Xia J. MGDB: A comprehensive database of genes involved in melanoma. Database. 2015;2015:1–7.

248. Bushell KR, Kim Y, Chan FC, Ben-Neriah S, Jenks A, Alcaide M, et al. Genetic inactivation of TRAF3 in canine and human B-cell lymphoma. Blood. 2015;125(6):999–1005.

249. Ulvé R, Rault M, Bahin M, Lagoutte L, Abadie J, De Brito C, et al. Discovery of human-similar gene fusions in canine cancers. Cancer Res. 2017;77(21):5721–7.

250. Li Z, Ivanov AA, Su R, Gonzalez-Pecchi V, Qi Q, Liu S, et al. The OncoPPi network of cancer-focused protein-protein interactions to inform biological insights and therapeutic strategies. Nat Commun. 2017;8:15350.

251. Hamidi H, Pietilä M, Ivaska J. The complexity of integrins in cancer and new scopes for therapeutic targeting. Br J Cancer. 2016;115(9):1017–23.

252. Chen P, Cescon M, Bonaldo P. Collagen VI in cancer and its biological mechanisms. Trends Mol Med. 2013;19(7):410–7.

253. Bednarski R, Grimm K, Harvey R, Lukasik VM, Penn WS, Sargent B, et al. AAHA anesthesia guidelines for dogs and cats. J Am Anim Hosp Assoc. 2011;47(6):377–85.

254. Hoeppner MP, Lundquist A, Pirun M, Meadows JRS, Zamani N, Johnson J, et al. An improved canine genome and a comprehensive catalogue of coding genes and non-coding transcripts. PLoS One. 2014;9(3):e91172.

255. Kinsella RJ, Kähäri A, Haider S, Zamora J, Proctor G, Spudich G, et al. Ensembl BioMarts: A hub for data retrieval across taxonomic space. Database. 2011;2011:1–

9.

256. Wang J, Vasaikar S, Shi Z, Greer M, Zhang B. WebGestalt 2017: A more comprehensive, powerful, flexible and interactive gene set enrichment analysis toolkit. Nucleic Acids Res. 2017;45(W1):W130–7.

257. Luo W, Pant G, Bhavnasi YK, Blanchard SG, Brouwer C. Pathview Web: User friendly pathway visualization and data integration. Nucleic Acids Res. 2017;45(W1):W501–8.

258. Livak KJ, Schmittgen TD. Analysis of relative gene expression data using real-time quantitative PCR and the 2-ΔΔCT method. Methods. 2001;25(4):402–8.